LOW VALENT TECHNETIUM NITROSYL COMPLEXES

Low Valent Technetium Nitrosyl Complexes

by

DAVID EDWARD GREEN

A Thesis

Submitted to the School of Graduate Studies

In Partial Fulfillment of the Requirements

for the Degree

Masters of Science

McMaster University

MASTERS OF SCIENCE (1997)
(Chemistry)

McMASTER
UNIVERSITY
Hamilton, Ontario

TITLE:	Low Valent Technetium Nitrosyl Complexes
AUTHOR:	David Edward Green, Hons. BSc. (Brock University)
SUPERVISORS:	Professor Russell Arthur Bell Professor John Richard Thornback Professor Colin James Lyne Lock
NUMBER OF PAGES:	xiii, 98

ABSTRACT

This thesis describes reactions involving low valent technetium nitrosyl complexes. O-Substituted hydroxylamines were reacted with $[TcOCl_4]^-$ in methanol producing $[Tc(NO)Cl_4]^-$. NMR studies have shown that two species are present besides the starting material during this reaction. One of these species was confirmed by NMR to be the corresponding alcohol of the O-substituted hydroxylamine. The other species is believed to be a hydroxylamine intermediate that is in equilibrium with the final product, $[Tc(NO)Cl_4]^-$. A plausible mechanism for this reaction was proposed that included an oxo group attack of the α-carbon of the O-substituted hydroxylamine which would lead to the formation of the corresponding alcohol. In an attempt to confirm the mechanism, O-18 labeled $[TcOCl_4]^-$ was synthesized, however, there is no conclusive evidence that the label is transferred to the corresponding alcohol at the present time.

Substitution reactions of $[Tc(NO)Cl_4]^-$ with phenanthroline and bipyridyl ligands were also investigated. Reactions with these ligands produced $[Tc^{(II)}(NO)Cl_3phen]$ (**4a**) and $[Tc^{(II)}(NO)Cl_3bipy]$ (**5**), respectively. The crystal structures of these complexes showed that the meridonial isomer is produced with one nitrogen atom of the bidentate ligand *trans* to the nitrosyl moiety. EPR spectra of these compounds confirm the Tc(II) oxidation state of the metal. All of the chloride ligands of **4a** and **5** can be displaced using $AgBF_4$ in acetonitrile solvent, which, in the case of bipyridyl, produces $[Tc^{(I)}(NO)(bipy)_2(MeCN)]^{2+}$ (**6**). Other technetium nitrosyl containing complexes are formed in these reactions and are currently awaiting x-ray structure determination.

ACKNOWLEDGEMENTS

I wish to express my thanks to the following people for their helpful contributions to this work:

Dr. Russell Bell for his patience, guidance, and expertise that have helped me through this project.

Dr. John Thornback for his enthusiasm, motivation, and encouragement, especially at the start of this project when chaos seemed to loom.

Dr. Lijuan Li for all her help regarding EPR and other inorganic problems, as well as Dr. Gary Schrobilgen for his discussions and advice.

Dr. Alan Guest for all his help in the lab over the last few years.

Drs. Ernest Wong and Theresa Fauconnier for their comments, suggestions, and other help during this project.

Dr. Daren Leblanc for his friendship and guidance through most of my stay at McMaster and Dr. John Valliant for his comments and suggestions during this project.

Extra special thanks are owed to Samantha Bennett and Chris McCrory for their freindship and all their help throughout this thesis which made time in the lab much more enjoyable.

Drs. Jim Britten, Richard Smith, and Don Hughes are irreplaceable. Thanks to George Timmins for all his laborious help and conversations about the country, Brian Sayer for his numerous NMR hints, and Mike Malott for our computer needs.

Thanks to the polymer boys (aka Fabio's) for dragging me out the lab every now and then for a few beers.

Nic and Michael's stimulating inorganic chats were very helpful. The visits to the gym with my "Arnold-like" work-out partner (Nic) really helped to vent my frustrations when I needed it most.

Thanks to Jerome for all your computer related expertise and Kelly for all your help and support throughout this thesis.

Mom and Dad - thanks for everything, all your help over the years and encouragement have made this possible.

Last, but not least, Dr. Lock's jolly personality and vast knowledge of inorganic chemistry will be deeply missed.

TABLE OF CONTENTS

LIST OF TABLES

LIST OF FIGURES

LIST OF ABBREVIATIONS AND SYMBOLS

Å	angstrom(s)
bipy	2, 2'-bipyridyl
Bn	benzyl
CCD	charge coupled device
cm^{-1}	wavenumbers
EI	electron ionization
EPR	electron paramagnetic resonance
ESMS	electrospray mass spectrometry
Et	Ethyl
FID	free induction decay
I	nuclear spin
IR	infrared spectroscopy
K	degrees Kelvin
m/z	mass to charge ratio
M	molarity
Me	methyl
MS	mass spectrometry
NMR	nuclear magnetic resonance
Ph	phenyl
phen	1, 10-phenanthroline
TBA	tetrabutylammonium cation, $[n\text{-}Bu_4N]^+$

CHAPTER 1

INTRODUCTION

1.1.1 Discovery of Technetium

The last transition metal (3d-5d) to be discovered was element 43. Mendeleev had predicted the existence of ekamanganese in 1869[1] but it was not until 1925 when Noddack, Tacke, and Berg reported the discovery of two new elements named masurium and rhenium.[2] Indeed, rhenium, the last stable element, was characterized but experiments failed to characterize masurium.[3] It was not until 1937 when Perrier and Segré correctly identified the radiations of element 43 from a molybdenum plate that had been bombarded with deuterons in a cyclotron.[4] This element was renamed technetium which was derived from the Greek adjective for artificial, signifying it as being the first artificially produced element.

1.1.2 Occurrence in Nature

There is no stable isotope of technetium. The half life of the longest lived isotope of technetium is 4.2 million years for ^{98}Tc and explains why primordial technetium no longer exists on earth. Trace quantities do exist in nature as a result of the spontaneous fission of ^{238}U to ^{99}Tc. The first isolation of an appreciable quantity of natural technetium was reported in 1961 when 1 ng was isolated from 5.3 kg of pitchblende ($UO_{2\text{-}2.25}$) mined in the Congo.[5] There are reports that technetium is also present in the atmosphere of certain stars.[6]

1.1.3 The Production and Properties of ^{99}Tc

There are twenty-one radioisotopes of technetium, ranging from mass number 90-110 and several metastable isomers are known.[7] Of all the isotopes and their nuclear isomers, to date only ^{99}Tc and ^{99m}Tc have widespread use. Most chemical studies of technetium are performed using the long-lived ^{99}Tc ($t_{1/2}$ = 2.111(12) x 10^5 y; β^- decay energy = 293.6 keV),[8] primarily because it is the only technetium isotope with a reasonably long half-life that is available in macroscopic quantities and it does not pose a considerable radiation hazard. The first gram of artificially produced ^{99}Tc was isolated in 1952.[9] This isotope is produced in 6% yield from the neutron-induced fission of ^{235}U and is now isolated in kilogram quantities from spent nuclear fuel.[10]

1.2.1 ^{99m}Tc in Nuclear Medicine

The short-lived metastable isomer of ^{99}Tc, ^{99m}Tc ($t_{1/2}$ = 6.01 h; γ decay energy = 140 keV),[1] is the other commonly used form of technetium which has found applications in diagnostic nuclear medicine.[11] Having the ideal properties of a short half-life of 6.01 h and the absence of α or β^- particle emission, ^{99m}Tc can be injected as a radiopharmaceutical in humans with activities of up to 1.11 GBq,[12] (corresponding to 6.0 ng of ^{99m}Tc or 11.3 ng of $Na^{99m}TcO_4$) with low radiation dose to the patient. The availability of ^{99m}Tc is made possible via a $^{99}Mo/^{99m}Tc$ generator based on the decay scheme shown in Figure 1.1.[12] Typically, fission-produced $^{99}MoO_4^{2-}$ is loaded onto an alumina column and decays to $^{99m}TcO_4^-$, which is eluted from the column in 0.15 M NaCl (physiological saline concentration) while $^{99}MoO_4^{2-}$ is retained.[11] ^{99}Mo decays with a 87% probability to ^{99m}Tc (13% to ^{99}Tc; 4 x 10^{-3} % to ^{99}Ru), which then almost quantitatively

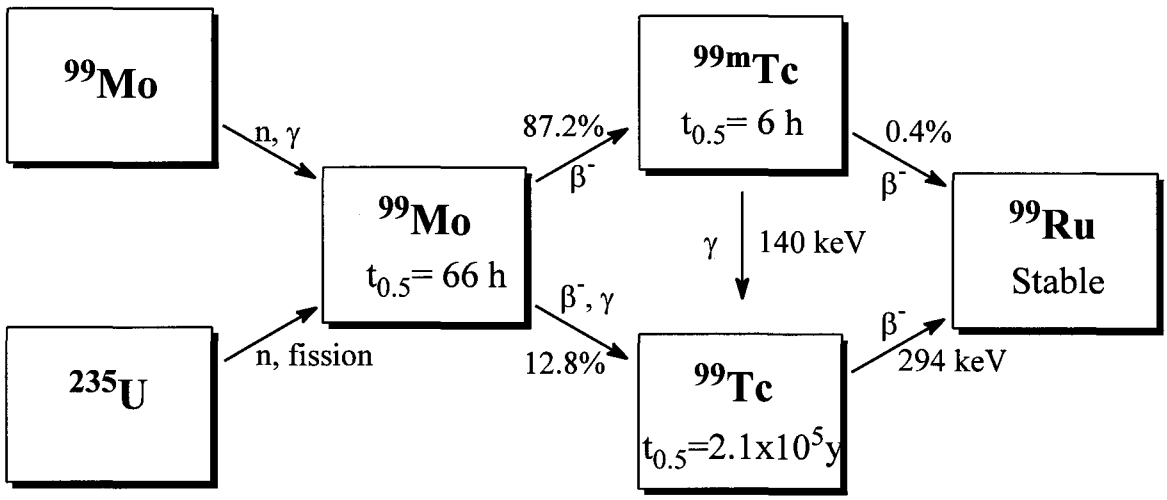

Figure 1.1: Formation and Decay of ^{99m}Tc and ^{99}Tc

converts to ^{99}Tc. The eluent from the column does contain a small portion of $^{99}TcO_4^-$ mixed with $^{99m}TcO_4^-$ and this mixture is referred to as "no carrier added" since no ^{99}Tc is physically added, and is simply denoted as $^{99m}TcO_4^-$. Radiopharmaceuticals are typically prepared by reducing the $^{99m}TcO_4^-$ (often with a stannous salt) in the presence of a ligand, which forms a ^{99m}Tc complex that having a specific physiological behaviour. The radiopharmaceutical is then injected into the patient and the *in vivo* distribution is monitored by the use of a conventional gamma camera or by single photon emission computed tomography (SPECT).

1.2.2 SPECT Imaging

Gamma rays are electromagnetic radiation which have a shorter wavelength (higher frequency) than those of x-rays. For ^{99m}Tc, the β^- decay from ^{99}Mo is followed by the emission of γ rays which results from ^{99m}Tc relaxing from its excited state to its ground state, ^{99}Tc. The *gamma* rays are detected by a scintillation camera.[13] These

photons are of sufficient energy to penetrate from deeply seated tissues or organs of the body. On the other hand, photons of this energy are not exceedingly penetrative, which allows them to be collimated with relatively low wall thickness lead collimators. The collimator is used to localize the radiation on the detector as the radiation is randomly emitted from the patient. The detector consists of a thallium doped sodium iodide crystal that emits a flash of light when struck by a *gamma* ray. The light flashes are amplified using photomultipliers and are counted as electrical pulses. A three-dimensional image is obtained by mounting the scintillation camera on a rotating gantry, recording multiple images at different angles of the patient and reconstructing the activity distribution.

1.3 Technetium Radiopharmaceuticals

A number of different technetium radiopharmaceuticals exist that are able to image the brain, heart, kidneys, thyroid, skeleton, etc. These are divided into two main types. The first type is classed as *Tc-tagged* compounds which are large biomolecules that have been derivatized with ^{99m}Tc. An example of this would be ^{99m}Tc labeled macroaggregated human serum albumin (MAA) that is injected for lung imaging.[12] The second type is classed as *Tc-essential* radiopharmaceuticals and these are simple technetium compounds whose biodistribution is determined because of the physical or metabolic properties of its coordinated ligands. These radiopharmaceuticals encompass technetium in a variety of different oxidation states from Tc(VII) for pertechnetate, to Tc(I) for the hexakisisonitrile Tc(I) cation (Tc-HEXAMIBI).[14] Examples of these radiopharmaceuticals are shown in Figure 1.2. While a number of these compounds involve the Tc(V) oxidation state, other possibilities exist for the inclusion of low valent

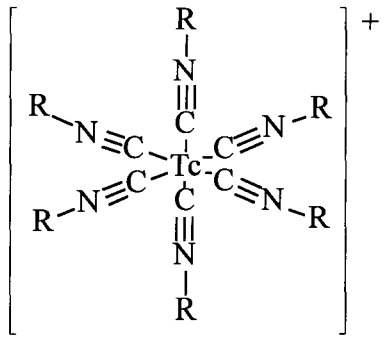

Tc-HEXAMIBI (Cardiolite®),
R = C≡NCH$_2$C(OCH$_3$)(CH$_3$)$_2$
(Tc(I), heart imaging)

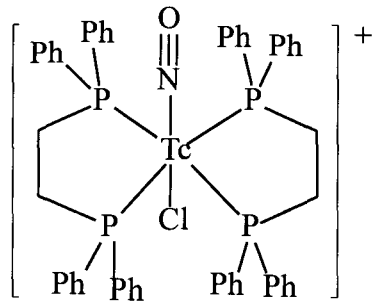

[Tc(NO)(dppe)$_2$Cl]$^+$
(Tc(I), heart imaging)

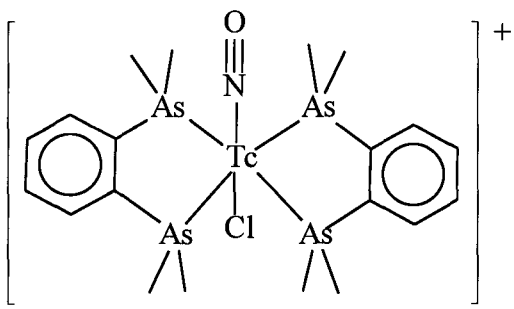

[Tc(NO)(diars)$_2$Cl]$^+$
(Tc(I), heart imaging)

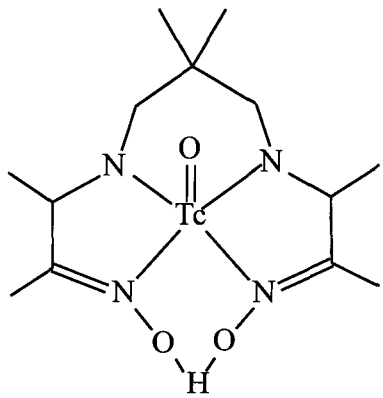

TcO-d,l-HMPAO
(Tc(V), brain flow imaging)

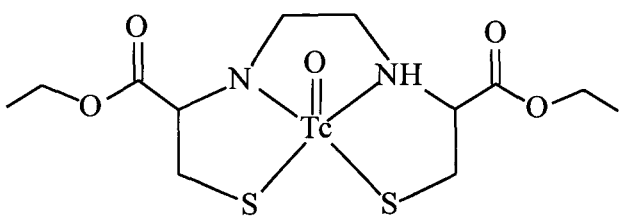

TcO-L,L-ECD
(Tc(V), brain flow imaging)

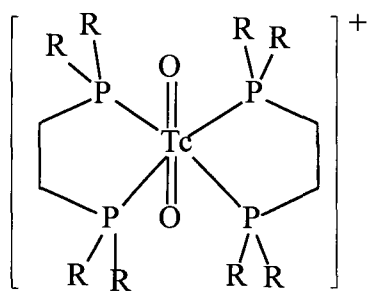

Myoview®, R = CH$_2$CH$_2$OEt
(Tc(V), heart imaging)

Figure 1.2: Some Tc-essential radiopharmaceuticals with oxidation state shown.

complexes in nuclear medicine. Nitrosyls are commonly used to stabilize low valent metal complexes and the Tc-nitrosyl containing cations of $[Tc(NO)(dppe)_2Cl]^+$ and $[Tc(NO)(diars)_2Cl]^+$ (Figure 1.2) have significant heart uptake in animals.[15]

This work is primarily concerned with the synthesis and characterization of low valent technetium nitrosyl complexes which may have the possibility of being used for radiopharmaceutical purposes.

1.4.1 Technetium Chemistry

Technetium has a very diverse chemistry with complexes ranging from -I (d^8) to +VII (d^0) and coordination numbers from four to nine.[1] The π donating nitrido (N^{3-}) and oxo (O^{2-}) ligands tend to stabilize higher oxidation states of technetium whereas the π accepting ligands such as nitric oxide (NO^+ when linear) tend to stabilize lower oxidation states of the metal. Because the present work is concerned with low valent technetium nitrosyl complexes the ensuing review of technetium's chemistry will be confined to this area. A brief description of the metal-nitrosyl bonding is first needed to better understand these systems.

1.4.2 Bonding of Metal-Nitrosyl Compounds

The nitrosyl group can bond to metals in different ways resulting in different geometries about the N atom. One method used to describe the bonding of nitrosyl compounds (the method used in this thesis) is to assign formal oxidation states to the metal and the nitrosyl ligand.[16] With this assignment, the linear M-NO unit possesses a bound $(NO)^+$ ligand (isoelectronic with CO, N_2) and a bent M-NO unit possesses a bound $(NO)^-$ ligand as shown in Figure 1.3.[17] Coordination of nitric oxide as $(NO)^+$ involves a net donation of

three electrons from NO to the metal, whereas coordination as $(NO)^-$ involves a net donation of one electron to the metal.

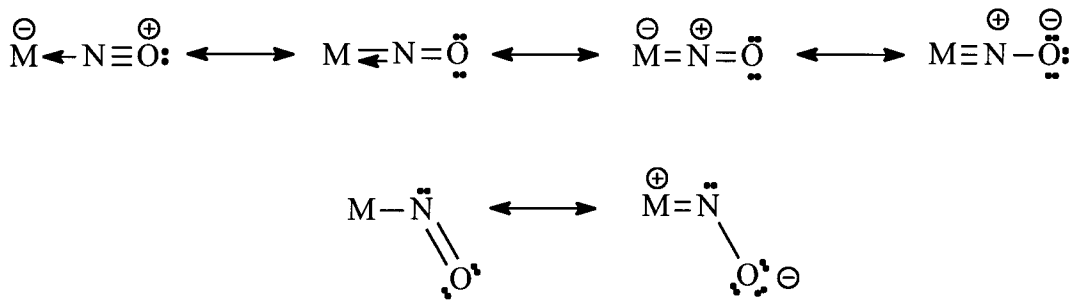

Figure 1.3: Linear and bent metal nitrosyl bonding

Although the formalism described above can be useful in designating formal charges to the metal nitrosyl system and for general electron counting purposes, the overall bonding of the system is more accurately described using a molecular orbital approach. With molecular orbitals, the bonding in transition metal nitrosyl complexes is generally regarded as having a synergic interaction involving two bonding components. There is a σ component, which arises from the donation of an unshared electron pair on the nitrogen atom, and a concerted backbonding π component, which arises from a donation of electron density from the occupied metal d-orbitals into the π^* antibonding orbitals of the nitrosyl ligand. These bonding interactions are indicated in Figure 1.4.[17] In general, NO is considered to be a weak σ-donor and a strong π-acceptor. The end result is that the M-N bond is strengthened by the backdonation while the addition of electron density to the antibonding π^* orbital weakens or lengthens the NO bond.

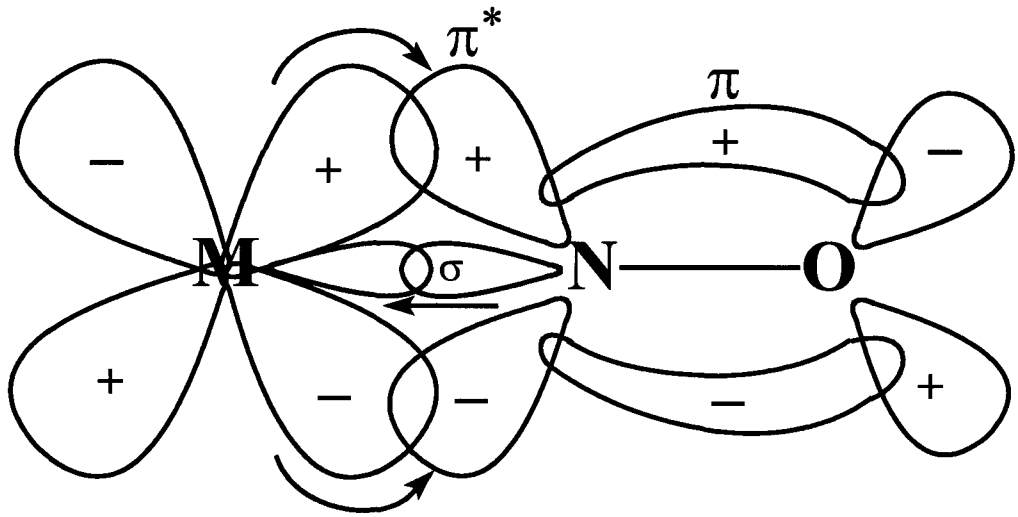

Figure 1.4: Metal nitrosyl σ and π backbonding with arrows indicating electron density flow.

1.4.3 Low Valent Tc Nitrosyl Compounds

$[Tc(NO)X_4]^-$ type species:

Early work by the Russians on technetium nitrosyl complexes led to the preparation of $Tc(NO)Br(py)_3$ by reacting $[Tc(NO)Br_4]^-$ in neat pyridine.[18] Following this work, a more convenient preparation of $[Tc(NO)Br_4]^-$ was achieved by reacting nitric oxide with freshly precipitated TcO_2 in 4M HBr at 75 °C and isolating the product as the tetrabutylammonium salt.[19] The chloro analogue was prepared by simple halide substitution on this material. Similarly, the iodo analogue, $[Tc(NO)I_4]^-$, was prepared by halide substitution of $[Tc(NO)Br_4]^-$ with HI in acetone.[20] The EPR spectrum $[Tc(NO)I_4]^-$ was subsequently reported[21] and a comparison to the other halide analogues shows a considerable increase in covalency for the equatorial ligand bonds proceeding to the heavier halide donors. EPR was also used to characterize the mixed ligand halide

complexes such as $[Tc(NO)Br_3I]^-$, $[Tc(NO)Br_2I_2]^-$, etc., when the corresponding haloacid was added.[22]

Nitrogen donor ligands:

Related nitrosyl complexes involving nitrogen donor ligands include *trans*-$[Tc^{(I)}(NO)(NH_3)_4(H_2O)]Cl_2$ (*vide infra*).[23] This complex is made by addition of $[NH_4]_2[TcCl_6]$ to a solution of hydroxylamine followed by neutralization with ammonia solution. The one electron oxidation product, *trans*-$[Tc^{(II)}(NO)(NH_3)_4(H_2O)]Cl_3$, is EPR active and its spectrum has been observed.[24] By altering the oxidation state from Tc(I) to Tc(II) the ammine ligands become more labile as is shown by the ability of $[Tc^{(II)}(NO)(NH_3)_4(H_2O)]^{2+}$ to form $[Tc^{(II)}(NO)Cl_5]^{2-}$ in concentrated hydrochloric acid whereas the Tc(I) complex is indefinitely stable in acid. When Armstrong and Taube used phenanthroline in place of neutralizing ammonia three species formed.[23] The main component was the red coloured $[Tc^{(I)}(NO)(phen)_2(NH_3)]^{2+}$ and a minor component was the green coloured $[Tc^{(I)}(NO)(phen)(NH_3)_2(H_2O)]^{2+}$ (characterized by elemental analysis and IR). The crystal structure of *cis*-$[Tc^{(I)}(NO)(phen)_2(NH_3)][PF_6]_2$ was eventually determined as was the related complex *cis*-$[Tc^{(I)}(NS)(phen)_2(Cl)][PF_6]\cdot Me_2CO$ that was synthesized by sulfur atom transfer to *cis*-$[Tc^{(V)}(N)(phen)_2(Cl)][PF_6]$ with S_2Cl_2 in chloroform.[25]

A number of pyridine and alkyl pyridine complexes have been synthesized as well. $Tc^{(I)}(NO)Cl_2(PPh_3)_2Y$, $Tc^{(I)}(NO)Cl_2(PPh_3)Y_2$, $Tc^{(I)}(NO)Cl_2Y_3$ (Y = pyridine, 3,5-lutidine) can synthesized from $Tc^{(I)}(NO)Cl_2(PPh_3)(NCCH_3)$ with varying conditions involving pyridine or lutidine.[26] The crystal structure of $Tc^{(I)}(NO)Cl_2py_3$ shows this complex to be the *mer* isomer. $Tc^{(I)}(NO)Cl_2py_3$ can also be prepared from $[Tc(NO)Cl_4]^-$ in

a 52% yield. Reaction of the methanol adduct $Tc^{(I)}(NO)Cl_2(PPh_3)(HOCH_3)$ with bipyridyl in chloroform or terpyridyl in dichloromethane produces $Tc^{(I)}(NO)Cl_2(PPh_3)$(bipy) and from $Tc^{(I)}(NO)Cl_2$(terpy), respectively.

Another N ligand donor is the thiocyanate ion. Addition of excess NCS^- to $[Tc(NO)Br_4]^-$ produces $[Tc^{(II)}(NO)(NCS)_5]^{2-}$ which can be electrochemically reduced to $[Tc^{(I)}(NO)(NCS)_5]^{3-}$.[19] These complexes were characterized by elemental analysis, IR and conductivity measurements. The Tc(II) complex was also characterized by EPR spectroscopy.[27]

Phosphorus and Arsenic donor ligands:

The $Tc^{(I)}(NO)Cl_2(PPh_3)_2(NCCH_3)$ complex described above can be prepared from $[Tc(NO)Cl_4]^-$ with excess triphenylphosphine in refluxing acetonitrile.[26] Other substitution reactions of the acetonitrile ligand can occur with carbon monoxide for instance, forming $Tc^{(I)}(NO)(CO)Cl_2(PPh_3)_2$.[28]

$Tc^{(II)}(NO)Cl_3(PMe_2Ph)_2$ was prepared by bubbling NO gas through a refluxing benzene solution containing $Tc^{(III)}Cl_3(PMe_2Ph)_3$ and was characterized with EPR spectroscopy.[29] $Tc^{(I)}(NO)Cl_3(PPh_3)_2$ was prepared with similar conditions from $Tc^{(I)}Cl_3(PPh_3)_2(NCCH_3)$.[30]

$[Tc(NO)(dppe)_2Cl]^+$ and $[Tc(NO)(diars)_2Cl]^+$ compounds can be prepared from $[Tc(NO)Cl_4]^-$ by adding excess of their respective ligands.[15]

Oxygen and Sulfur donor ligands:

$[Tc^{(II)}(NO)Cl_3(acac)]^-$ is formed when acetylacetone is added to $[Tc(NO)Cl_4]^-$ and has been characterized by x-ray crystallography[31] and EPR.[32]

Reaction of $[Tc(NO)Cl_4]^-$ with tetramethylbenzenethiol (tmbt) produces a trigonal bypyramidal structure of $Tc^{(III)}(NO)Cl(tmbt)_3$ where the nitrosyl and chloro ligands occupy the axial positions.[33] A number of seven-coordinate dithiocarbamato complexes of the type $[Tc(NO)(S_2CNR_2)_3]^+$ can be prepared by substitution of $[Tc(CO)(S_2CNR_2)_3]$ with $NOBF_4$.[1]

1.5.1 Synthesis of Tc-Nitrosyl Compounds

The typical way to make a metal-nitrosyl complex has been to bubble nitric oxide into a solution containing a metal complex which then binds the nitrosyl either with,[34] or without,[35] substitution of another ligand. This is an inconvenient procedure from a radiopharmaceutical perspective since nitric oxide is a corrosive gas that would have to be generated *in situ* or transferred directly from an outside source. As an alternative approach, hydroxylamine can be used to generate metal-nitrosyl complexes.[37] This is a convenient method because hydroxylamine is a stable salt, available as $[NH_3OH][Cl]$ for instance, and is non-corrosive and can be stored for long periods of time.

1.5.2 History of Tc-Hydroxylamine Reactions

The first reaction of hydroxylamine with a Tc compound was reported by Eakins *et al.* and used $[NH_4]_2[TcCl_6]$, where the product of the reaction was neutralized with a solution of ammonia.[38] The authors misformulated the final product as an hydroxylamine bound species, $[Tc(NH_2OH)_2(NH_3)_3]^{2+}$, which was corrected 12 years later with Armstrong and Taube's formulation[23] and eventual crystal structure[39] of trans-$[Tc(NO)(NH_3)_4(H_2O)]^{2+}$. This compound is inert to substitution so has little utility as a precursor to other low valent technetium nitrosyl compounds. Hydroxylamine can be used to synthesize other nitrosyl compounds such as $[TBA][Tc(NO)Cl_4]$, which

crystallizes in methanol as [TBA][Tc(NO)Cl_4(MeOH)].[40] This can be easily prepared in high yields from $[TcO_4]^-$, $[TcCl_6]^{2-}$, or $[TcOCl_4]^-$ depending on the reaction conditions.[32, 41] The chlorides of $[Tc(NO)Cl_4]^-$ are easily substituted by ligands such as isonitriles, thiocyanates, pyridines, phosphines and arsines, making this a much more versatile starting material for low valent technetium nitrosyl compounds.

1.6 Objectives

One objective of this thesis has been to study the reactions of O-substituted hydroxylamines with $[TcOCl_4]^-$. These reactions proceed in a similar fashion as the reaction of hydroxylamine and $[TcOCl_4]^-$, producing a dark brown-red coloured intermediate that is believed to be a Tc-hydroxylamine bound species, that eventually converts to $[Tc(NO)Cl_4]^-$. A related aim of this work has been to gain a better understanding of the mechanism of nitrosylation of $[TcOCl_4]^-$ with O-substituted hydroxylamines.

The second objective of this thesis was to investigate substitution reactions of $[Tc(NO)Cl_4]^-$ with a variety of nitrogen donor ligands. This work involved the synthesis and structural characterization of these complexes. The results of these studies are presented herein.

CHAPTER 2

REACTIONS OF O-SUBSTITUTED HYDROXYLAMINES WITH TETRACHLOROOXOTECHNETATE(V)

2.1 Introduction

It has been known for some time that reactions of certain metal compounds with hydroxylamine salts can be used in the synthesis of a metal-nitrosyl bond.[37] More intimately related to the present work, was the fact that hydroxylamine hydrochloride (or other salts) react with $[TcOCl_4]^-$ in methanol to form the technetium-nitrosyl complex $[Tc(NO)Cl_4(MeOH)]^-$.[40] The introduction of this versatile starting material has resulted in a variety of new technetium-nitrosyl complexes, some of which show potential as useful imaging agents in diagnostic nuclear medicine.[15] At the outset of the present work, it was thought that investigations with O-substituted hydroxylamines might lead to a new series of complexes with a $Tc\text{-}NH_2OR$ core having a different chemistry than that of the Tc-NO complexes and that they might have potential to be used as imaging agents.

2.2 Characterization of the Reaction Product

The addition of $[NH_3OH][Cl]$ or $[NH_3OR][Cl]$ (R = Me, Et, Bn) to a methanol solution of $[TcOCl_4]^-$ immediately changed the green solution to a dark brown-red colour. After a period of approximately 24-72 hours at room temperature, a gradual colour change from brown-red to green took place. Infrared spectroscopy showed a very strong

absorption for this green product at 1785-1790 cm^{-1}, depending on the reaction, which is characteristic of the nitrosyl stretching frequency for $[Tc(NO)Cl_4]^-$.[41] Negative ion electrospray mass spectrometry was used to confirm the presence of the $[Tc(NO)Cl_4]^-$ ion which also had the proper chlorine distribution for this complex as shown in Figure 2.1.

2.3 Proposed Mechanism of the Reaction

Given that $[Tc(NO)Cl_4]^-$ was the final product, the O-substituted hydroxylamine, NH_2OR, was the most likely source of nitrosyl which indicates that the R-ONH_2 bond must have been broken. This was interesting because a C-O bond is fairly strong and requires 355 $kJ \cdot mol^{-1}$ of energy to break.[42] For this reason it was decided to investigate the mechanism of this reaction to determine how the C-O bond was broken and formation of the nitrosyl occurs. ^1H NMR was used to follow the reaction course and demonstrated that there were three species present in each reaction. Some of the excess starting material was present (1.1 equivalents of the hydroxylamine was used), as well as what was thought to be the hydroxylamine bound intermediate, and the corresponding alcohol of the hydroxylamine formed after time (i.e. MeOH formed with the reaction involving $[NH_3OMe][Cl]$). Since the corresponding alcohol was produced in this reaction, it was proposed that it originated from the Tc-NH_2OR intermediate. Taking this into consideration, a mechanism was proposed for the reaction and this is shown in Figure 2.2. The initial attack of hydroxylamine was followed by the oxo group attack of the α-carbon of the O-alkyl substituent forming Tc-OR which was then cleaved as ROH. The linear nitrosyl group was formally considered as NO^+ which corresponds to a net three electron

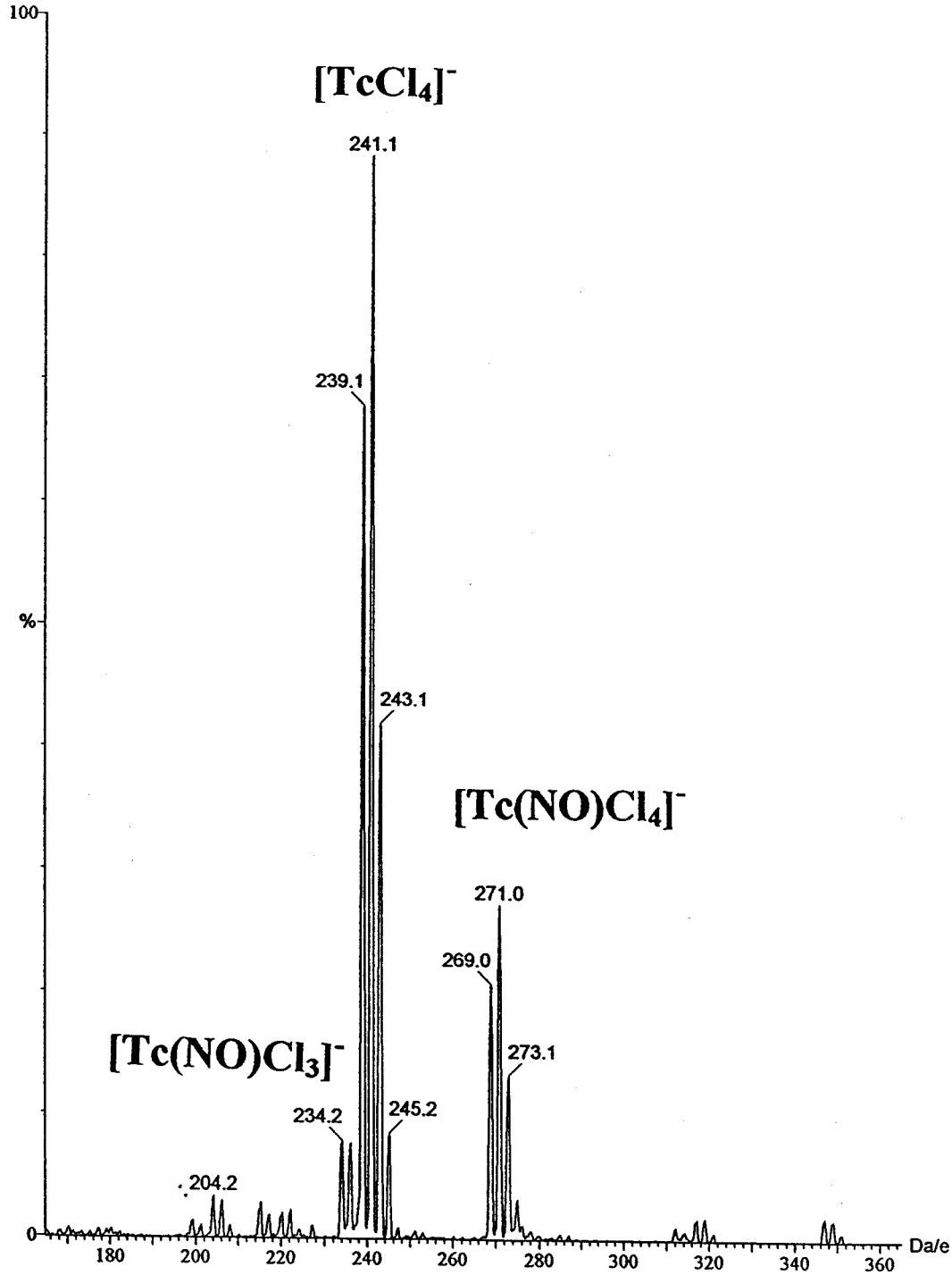

Figure 2.1: Negative ion ESMS for the reaction of [TBA][TcOCl$_4$] + [NH$_3$OMe][Cl] after the reaction was completed (green coloured crystals formed). The sample was injected in 50/50 MeCN/H$_2$O with no base added.

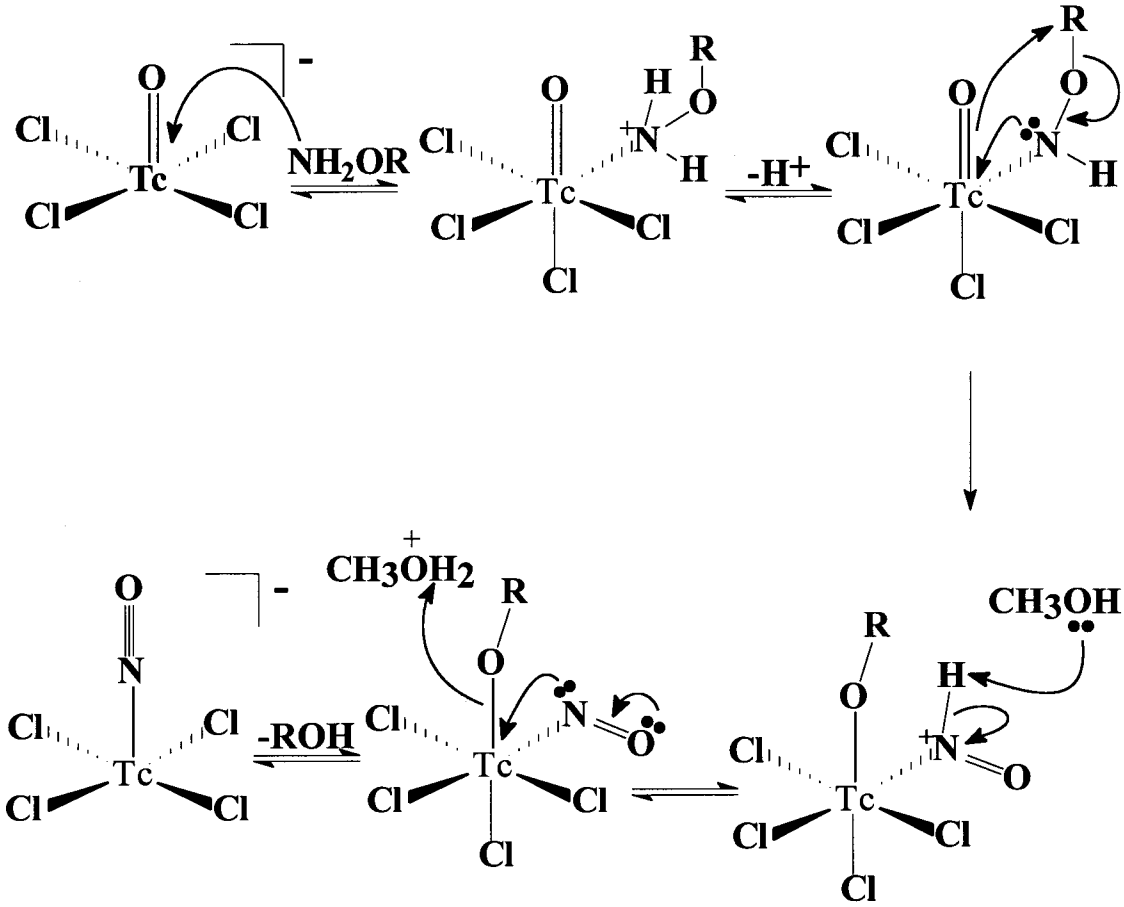

Figure 2.2: Proposed mechanism of nitrosylation with oxo group attack.

donation to the metal reducing it from the Tc(V) complex in $[TcOCl_4]^-$ to the Tc(II) complex in $[Tc(NO)Cl_4]^-$. The only flaw in this mechanism is that an extra proton is produced for which there is no evident counterion.

There was precedence in the literature for an oxo group attack of an intermediate complexed to $[TcOCl_4]^-$. Abram *et al.*[43] have proposed a similar mechanism for the reaction of $[TcOCl_4]^-$ and $PhCN(Me_3Si)N(Me_3Si)_2$ that produces $[TcNCl_4]^-$ as shown in Figure 2.3. With this proposed mechanism, the oxo group attacks a silicon atom of $SiMe_3$

to form a Tc-OSi bond that then attacks another $SiMe_3$ substituent to form $(SiMe_3)_2O$. Although $[TcOCl_4]^-$ was converted to $[TcNCl_4]^-$, there was no experimental evidence of these intermediates.

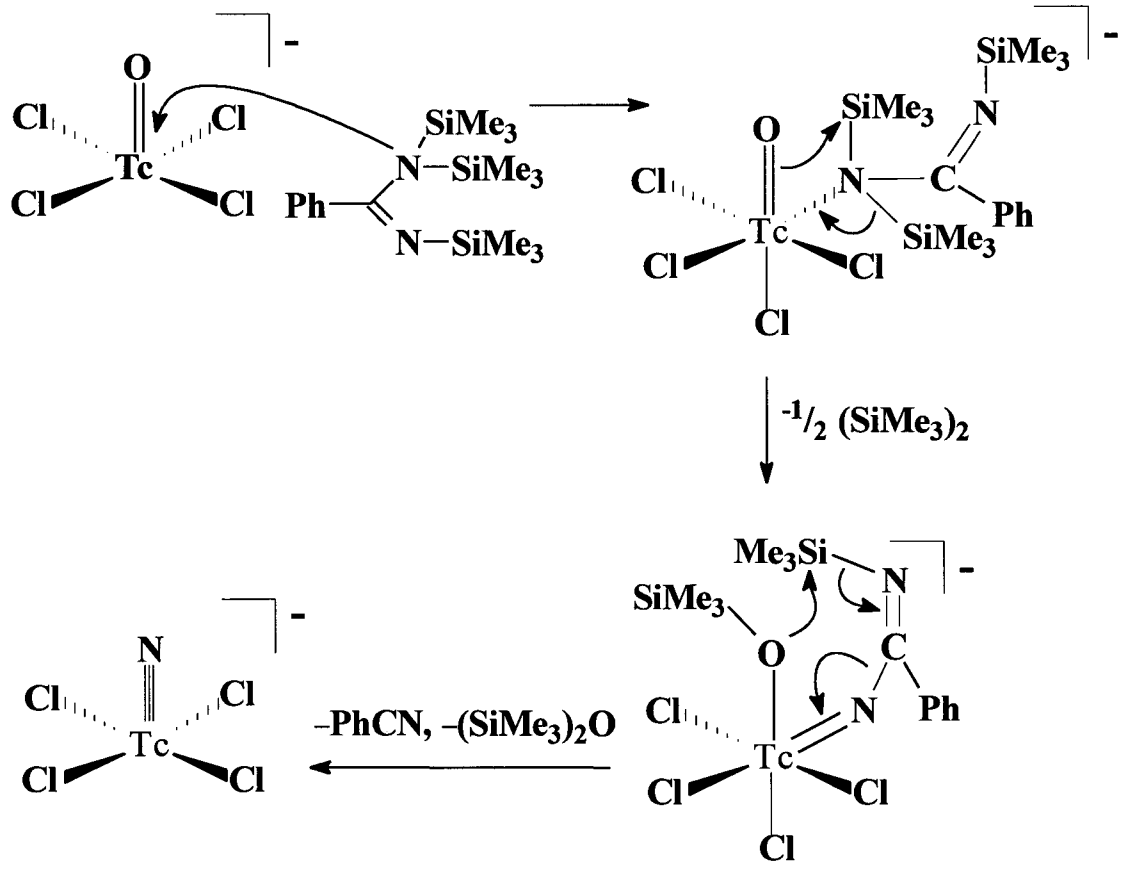

Figure 2.3: Proposed mechanism for the formation of $[TcNCl_4]^-$ by Abram *et al.*[43]

2.4 Characterization of the Intermediate

To gain more insight into this mechanism, attempts were made to crystallize the brown-red intermediate at low temperatures. Unfortunately, these attempts failed to produce any crystalline material. Simultaneous efforts by use of ESMS, NMR and IR

spectroscopies were also employed to follow the progress of the reaction. Although low temperature NMR would have been preferred in the detection of any intermediates, the insolubility of $[TcOCl_4]^-$ at low temperature made this approach difficult. Since the intermediates appeared stable at room temperature for many hours or even days, room temperature NMR was therefore used to follow the reaction progress.

Both the O-methyl and O-benzyl hydroxylamines seem to produce the corresponding alcohols approximately 4-12 hours after the start of the reaction whereas for O-ethyl hydroxylamine, ethanol was formed almost immediately. Proton NMR spectra of the reaction mixture for O-methyl and O-ethyl hydroxylamine are shown in Figures 2.4 and 2.5 respectively. The unlabeled peak(s) in these spectra might correspond to the hydroxylamine bound intermediate or possibly the corresponding chloroalkane (*vide infra*). The O-methyl starting material definitely decreased during the interval from 5 to 15 minutes after mixing reagents, while the unlabeled peak did not change dramatically in intensity. For the O-ethyl starting material, all the peaks appeared after 5 minutes and the starting material only decreased slightly in intensity after 15 minutes.

Consistent with all these reactions was that eventually the initial starting material was no longer present after lengthy periods of time (> 1 week). Another commonality in all the reactions was that even after the solution had turned green and formed $[Tc(NO)Cl_4]^-$, the unlabeled peak(s) still remained at relatively the same intensity. The signals for these reactions were typically broad which was likely indicative of paramagnetic technetium species present in solution or possibly chemical exchange

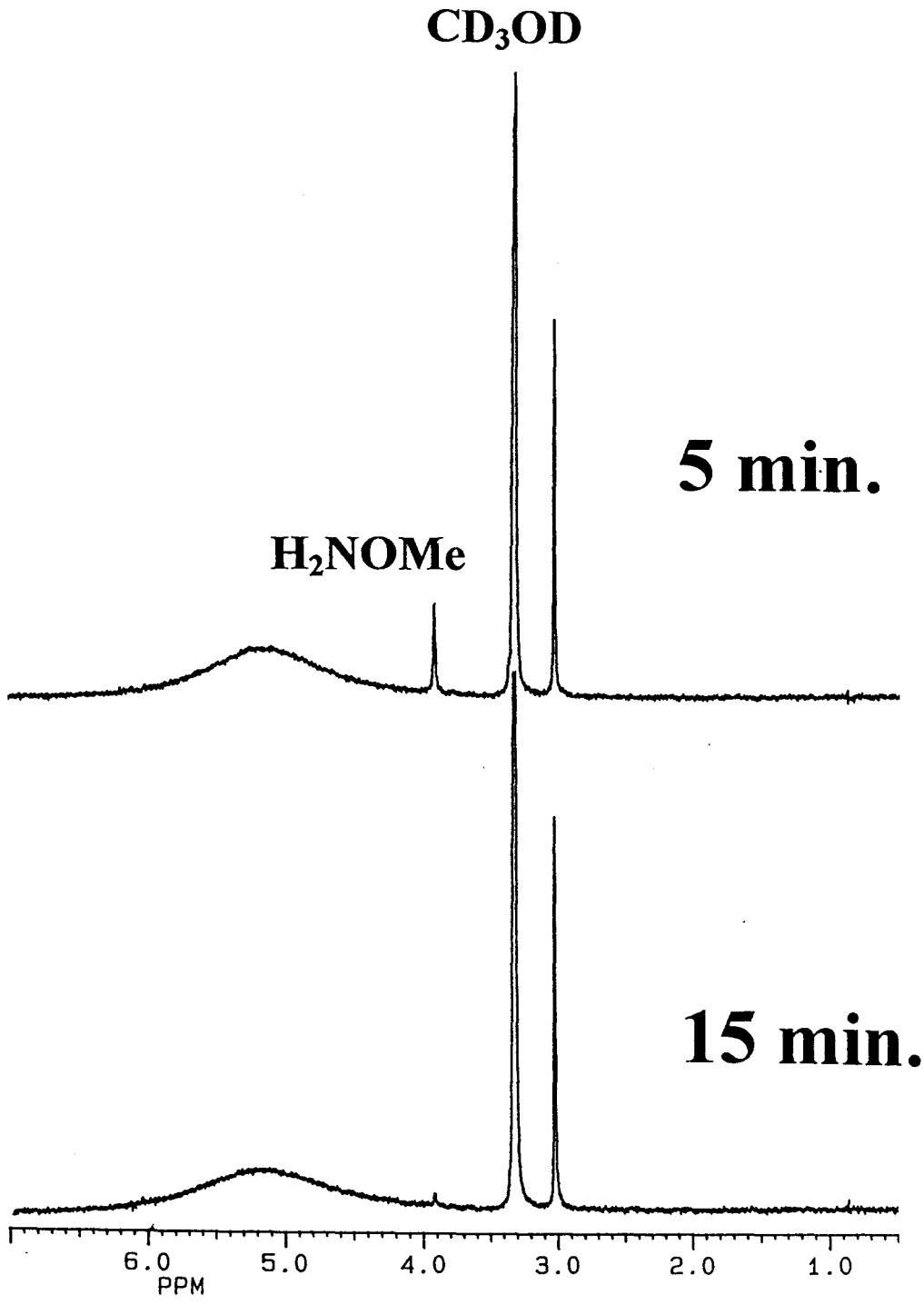

Figure 2.4: ^{1}H NMR spectra for the reaction of $[NH_3OMe][Cl]$ and $[K][TcOCl4]$ in CD_3OD after 5 and 15 minutes.

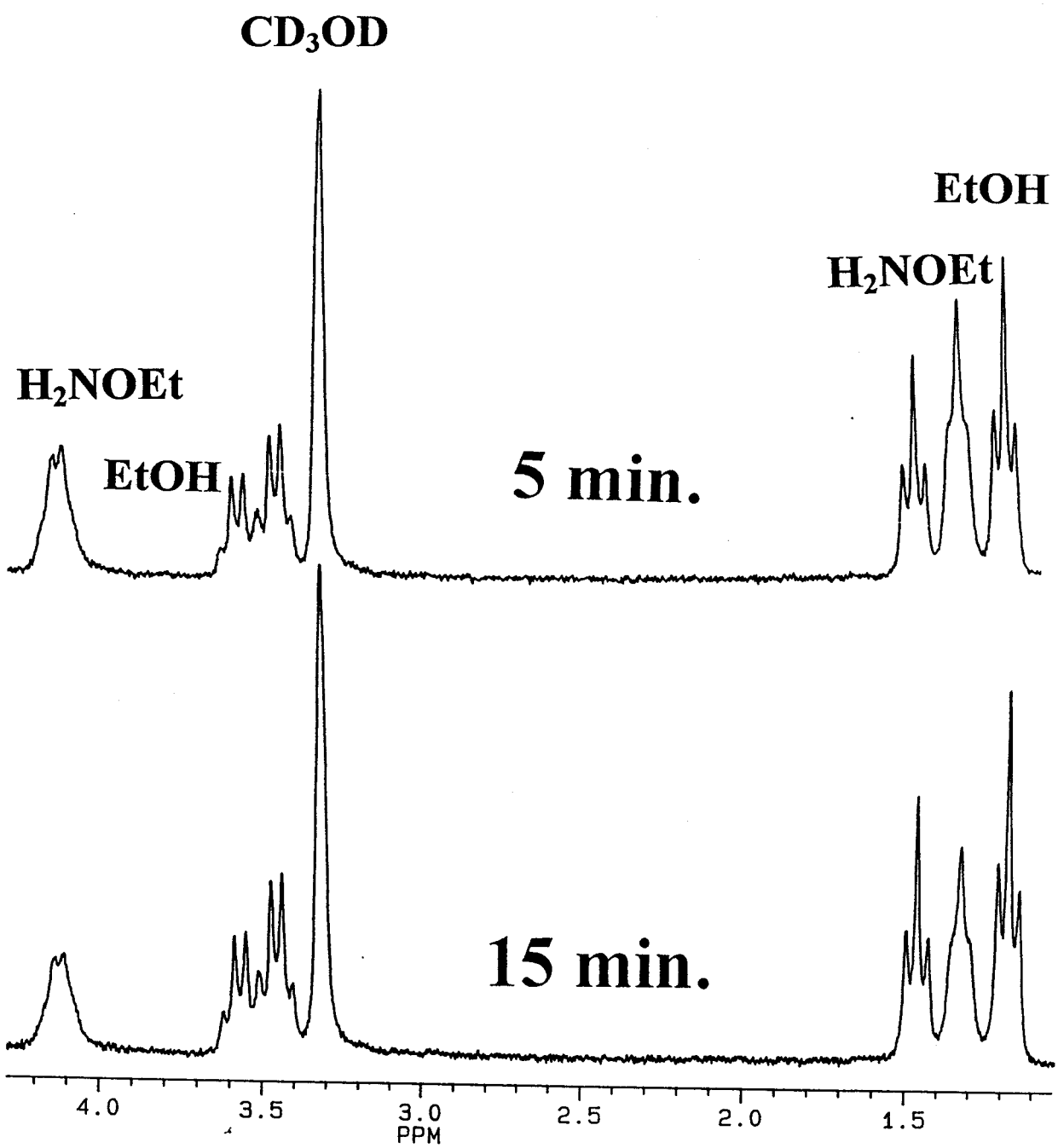

Figure 2.5: ^{1}H NMR spectra for the reaction of $[NH_3OEt][Cl]$ and $[K][TcOCl4]$ in CD_3OD after 5 and 15 minutes.

processes occurring. An EPR spectrum of the O-ethyl hydroxylamine reaction was recorded while it was a brown-red colour, but it was very complex and could not be interpreted.

Portions of each of the solutions containing the brown-red intermediates were evaporated producing brownish oils that were ground with KBr and made into pellets for recording the infrared spectra. Very strong nitrosyl stretching frequencies were present ranging from 1785-1803 depending on the reaction. This frequency is characteristic of $[Tc(NO)Cl_4]^-$. The N-O stretching frequency for NH_2OH gas[44] is 895 cm^{-1} compared to a range of 910-1035 for bound M-NH_2OH complexes.[45] No literature values for M-NH_2OR complexes are known to have been reported and the N-O stretches from the present infrared spectra were not sufficiently clear to be able to draw any definitive conclusions.

Electrospray mass spectrometry was used to characterize $[Tc(NO)Cl_4]^-$ and in attempts to detect and characterize the brown-red intermediates. The samples were injected into the instrument soon after the brown-red colour was generated. The O-methyl and O-ethyl hydroxylamine spectra are shown in Figures 2.6 and 2.7, respectively, and the solution of the completed reaction mixture ($[Tc(NO)Cl_4]^-$ has formed) for O-ethyl hydroxylamine reaction was shown in Figure 2.8. These spectra are difficult to interpret. It was hoped there would be a pattern for a O-methyl and O-ethyl (MW increase of 14) bound species for the brown-red coloured intermediate but this was not observed. All of the spectra of the brown-red intermediates (for NH_2OH, NH_2OMe, NH_2OEt, and NH_2OBn) closely resembled these spectra in Figure 2.6 and 2.7. In Figure 2.6, the largest m/z species was 347, 349, 351, 353 which corresponds to a three chlorine pattern. Nitrosyl and chlorine are also fragmented from this high m/z species. Therefore the

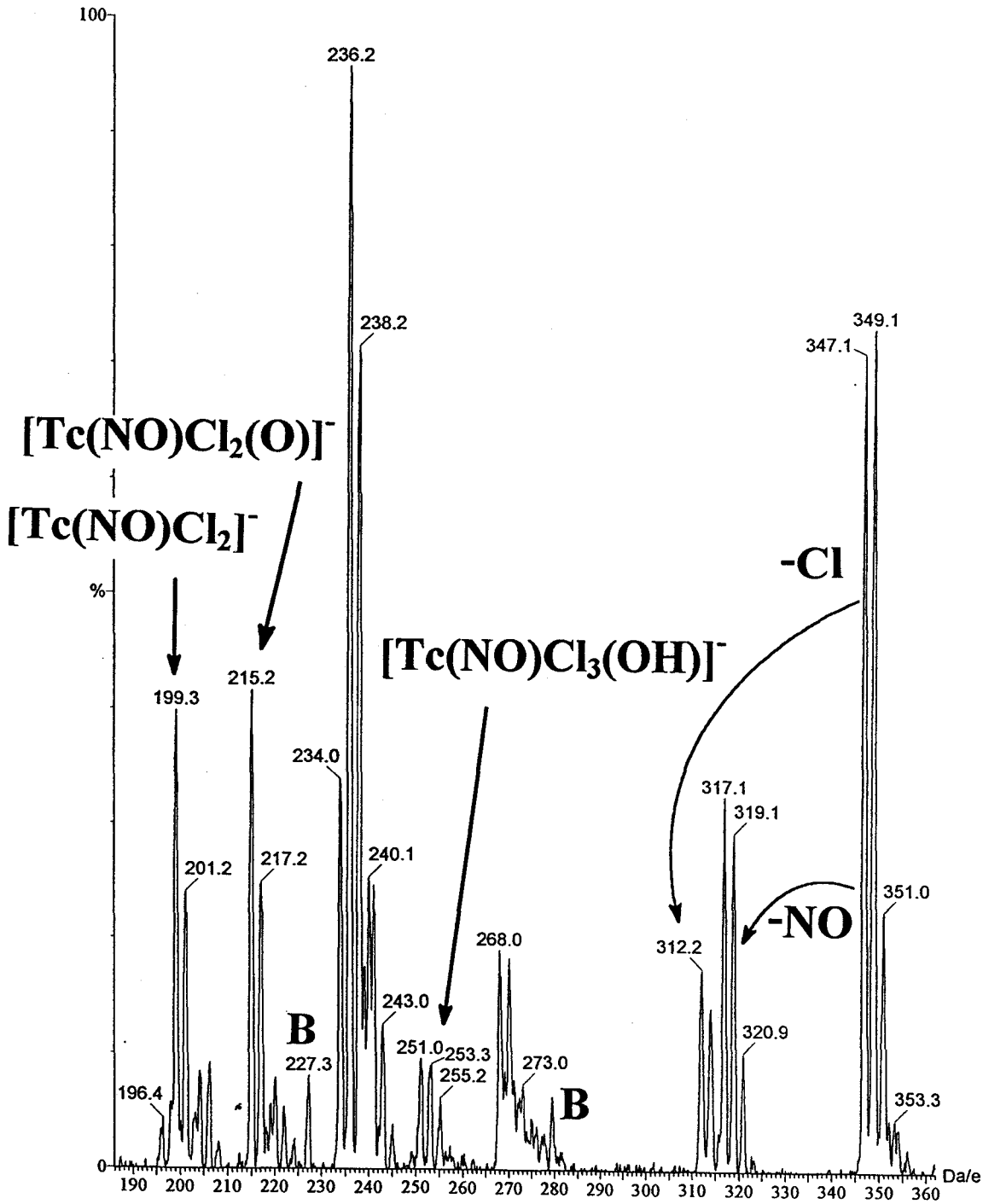

Figure 2.6: Negative ion ESMS for the brown-red intermediate generated from the reaction of [TBA][$TcOCl_4$] + [NH_3OMe][Cl] in CD_3OD. The sample was injected in 50/50 MeCN/H_2O with no base added. B indicates background ions.

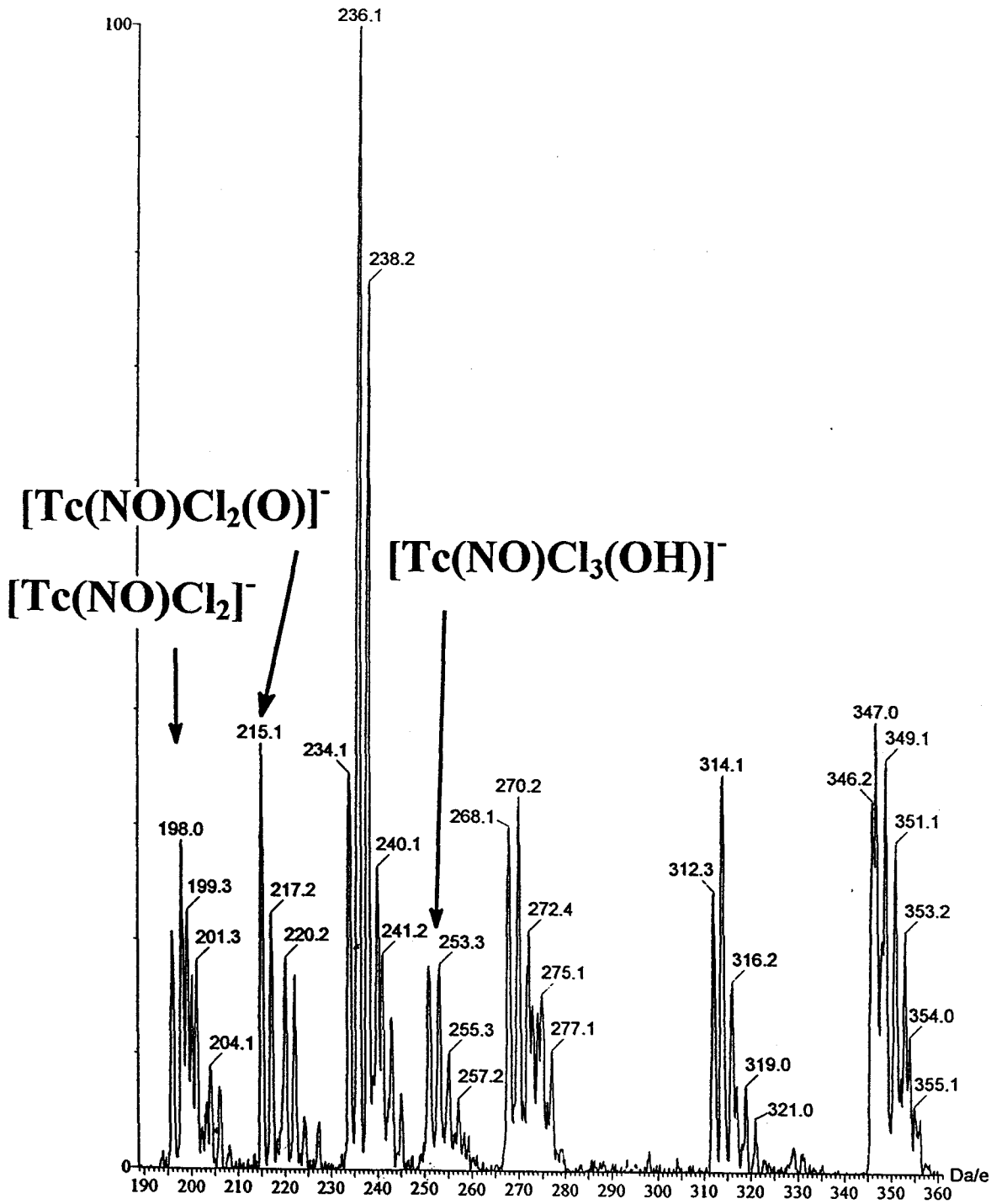

Figure 2.7: Negative ion ESMS for the brown-red intermediate generated from the reaction of [TBA][$TcOCl_4$] + [NH_3OEt][Cl] in CD_3OD. The sample was injected in 50/50 MeCN/H_2O with no base added.

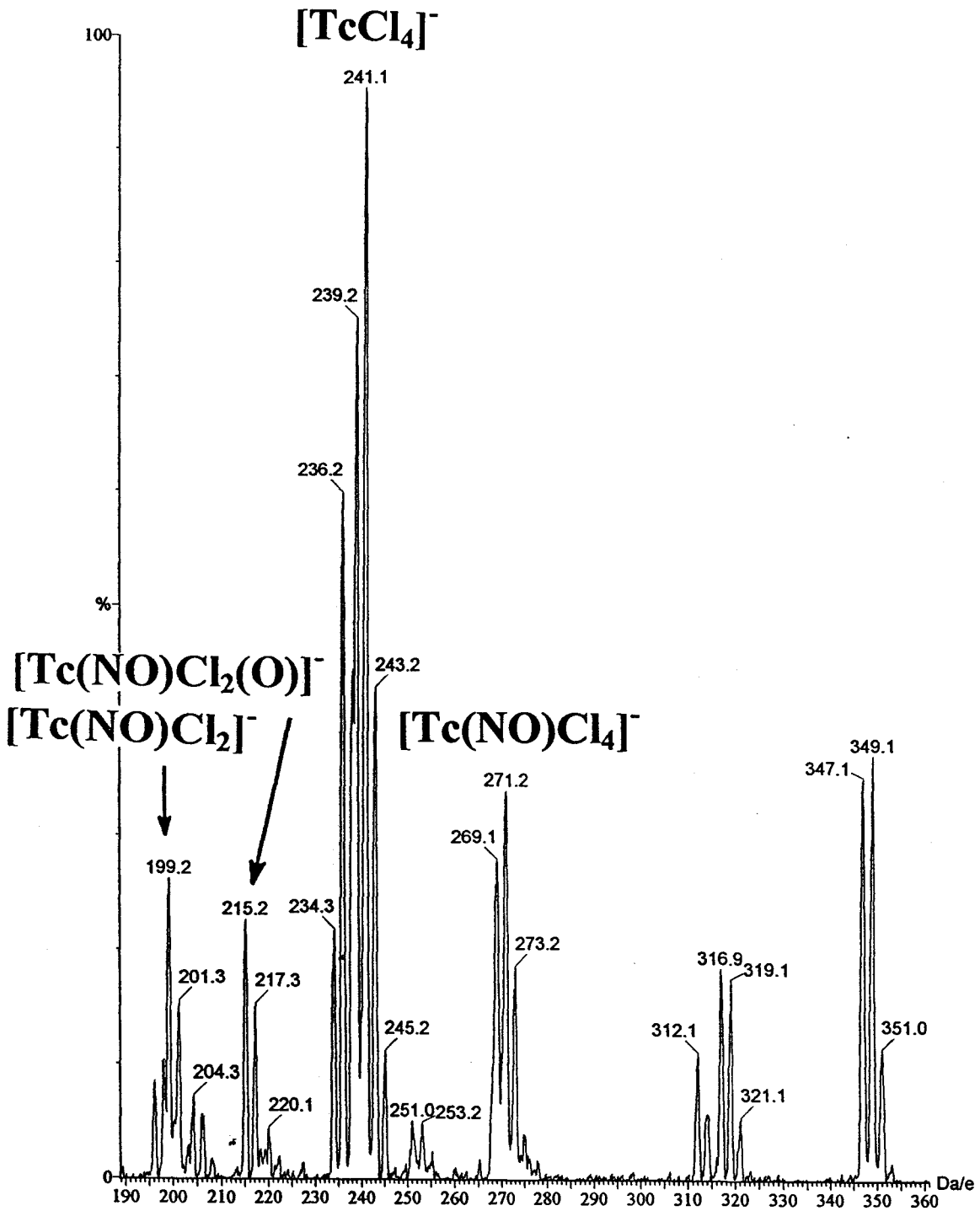

Figure 2.8: Negative ion ESMS of an aliquot from the reaction of [TBA][$TcOCl_4$] + [NH_3OEt][Cl] in CD_3OD after completion of the reaction (green coloured [$Tc(NO)Cl_4$]$^-$ has formed). The sample was injected in 50/50 MeCN/H_2O with no base added.

species probably contains a $Tc(NO)Cl_3$ unit which has a molecular weight of 234. Subtracting 234 from 347 results in 113 mass units that are unaccounted for in the spectrum. Trifluoroacetic acid was commonly used in the mass spectrometer for recording the spectra and was always present as a background ion with a m/z ratio of 113. Similarly, a species with a smaller intensity and a m/z ratio of 227 can often be observed and this corresponds to $\{[H][CF_3COO]_2\}^-$ as is noted in Figure 2.6 (denoted as a background ion B). Therefore it was considered that the largest m/z species was most likely $[Tc(NO)Cl_3(CF_3CO_2)]^-$ and this was produced in the mass spectrometer.

A chlorine patterned species was present in a m/z ratio of 268-277 which closely resembled a three chlorine pattern for a m/z ratio of 268, 270, and 272. It was unclear what these species may be since crystals of $[Tc(NO)Cl_4]^-$ have a m/z of 269, 271, 273, and 275 as shown in Figure 2.1. The species $[Tc(NO)Cl_3(OH)]^-$ and $[Tc(NO)Cl_2(O)]^-$ are observed and it was believed that these are either formed from $[Tc(NO)Cl_4]^-$ and water or are hydrolysis products from other species present in the reaction mixture since these ions are not observed in the ESMS for crystals of $[Tc(NO)Cl_4]^-$ in Figure 2.1. The ESMS for the O-18 reaction shown in Figure 2.11 (*vide infra*) provides evidence that no O-18 from the oxo group of $[Tc^{18}OCl_4]^-$ is incorporated into $[Tc(NO)Cl_3(^{18}OH)]^-$ or $[Tc(NO)Cl_2(^{18}O)]^-$. This is a strong indication that the oxygen atoms incorporated in these species originate from the solvent system of the instrument. Figure 2.6 also shows a chlorine distribution pattern for species with a m/z ratio of 234-243. The chloride distribution is not correct for a $[Tc(NO)Cl_3]^-$ species with a m/z ratio of 234, 236, and 238. The 234 and 236 peaks should have approximately the same intensity and if this amount is subtracted from the 236 peak, there is a species with a correct three chlorine

pattern distribution with a m/z ratio of 236, 238, and 240. If this species contains a $TcCl_3$ unit, there are 32 mass units that are unaccounted for. The reactions were done in CD_3OD and then diluted into a 1:1 MeCN:H_2O mixture. Possibly the 32 mass units are a N-OD, ND-O, NH-OH, or NH_2O bound species that results from the cleavage of the R group in the reaction or in the mass spectrometer. If this is the case, the molecular ion with one more chlorine should be present at a m/z ratio of 271, 273, 275, and 277 and may explain why this region of the spectrum is complicated. The region is resolved better in Figure 2.7 and there does appear to be peaks with a m/z ratio at 273, 275, and 277, possibly up to 278 or 279 (a background peak may overlap with this). The region might also consist of a mixture of $[Tc(NH_2OH)Cl_4]^-$ or a $[Tc(NDHOH)Cl_4]^-$ species (m/z = 272, 274, 276, 278). It would be worthwhile to try these reactions in non-deuterated methanol for a comparison. The peaks with a m/z ratio of 268, 270, and 272 with a three chlorine pattern however are still unexplained.

Figure 2.8 is a completed reaction and the major change in this spectrum is that $[Tc(NO)Cl_4]^-$ is present with a m/z ratio of 269, 271, 273, and 275 without the complexity of peaks shown in Figures 2.6 and 2.7.

2.5 Attempts to verify the mechanism:

In an attempt to confirm that the O-substituted hydroxylamine reaction was actually proceeding according to the proposed mechanism, O-18 labeled $[TBA][TcOCl_4]$ was synthesized. Concentrated hydrochloric acid was prepared by dissolving HCl gas into $H_2{}^{18}O$ and adding this to $[NH_4][TcO_4]$ dissolved in labeled water (Section 2.6). This preparation yielded 69% of $[TBA][Tc^{18}OCl_4]$. The ratio of the intensities for the

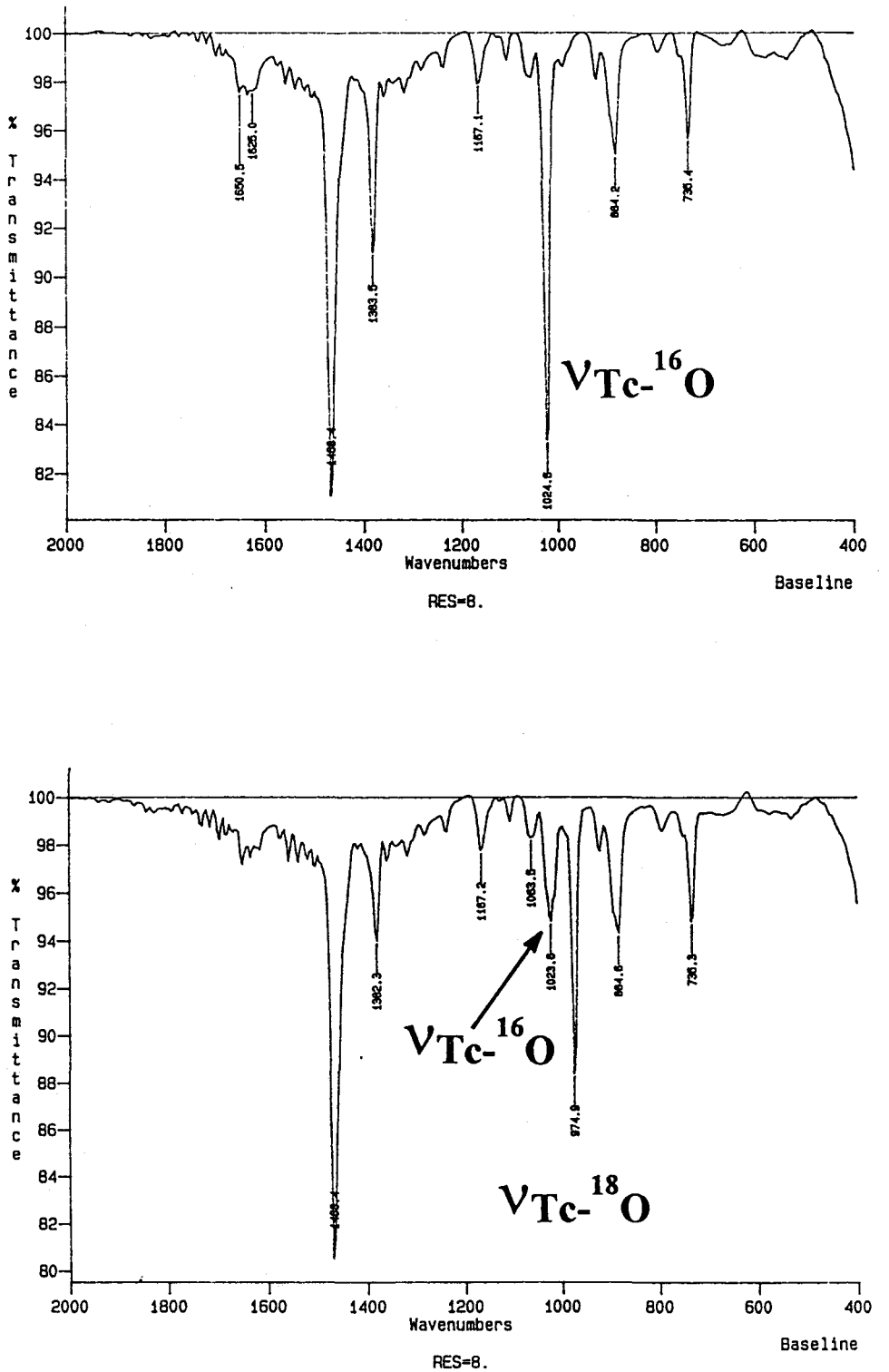

Figure 2.9: Infrared spectrum (KBr) of O-18 labeled [TBA][$TcOCl_4$] (bottom) and unlabeled [TBA][$TcOCl_4$] (top). The ratio of $\nu_{Tc-^{18}O}$: $\nu_{Tc-^{16}O}$ is approximately 70:30.

Tc-^{18}O:Tc-^{16}O stretch was measured to be 70:30 from the infrared spectrum shown in Figure 2.9.

If the proposed mechanism was correct, the O-18 label would eventually be incorporated into the alcohol that originated from the O-substituted hydroxylamine. O-benzylhydroxylamine was chosen for the reaction with $[Tc^{18}OCl_4]^-$ because it produces labeled benzyl alcohol, which has a higher molecular weight (for simpler detection by the mass spectrometer) and a relatively high boiling point (205 °C)[44] that might be needed if distillation from methanol solvent was required.

Carbon-13 NMR spectroscopy can also be used for mechanistic studies involving O-18.[47, 48] There is a small chemical shift difference observed between ^{13}C-^{16}O and ^{13}C-^{18}O systems. For labeled benzyl alcohol, this difference was approximately 2 Hz (400 MHz instrument) in non-polar solvents but the two signals tend to coalesce in polar solvents such as water and methanol.[49] The labeled $[TcOCl_4]^-$ reaction was first attempted in methanol but only one signal at 65.0 ppm was observed (at 500 MHz) for the benzylic carbon as shown in Figure 2.10. The position of the benzylic carbon at 65.0 ppm was confirmed by recording the spectrum of an authentic sample of benzyl alcohol in CD_3OD and also by adding one drop to the NMR tube containing in the unlabeled O-benzyl hydroxylamine reaction and observing the difference. The reaction was then attempted in a less polar solvent, dichloromethane, but the reagents did not react. When a 1:1 mixture of methanol:dichloromethane was used, a darker colour formed after a few minutes and changed to green after 24 hours, however, no signal for the benzylic carbon at 65 ppm could be detected in this sample.

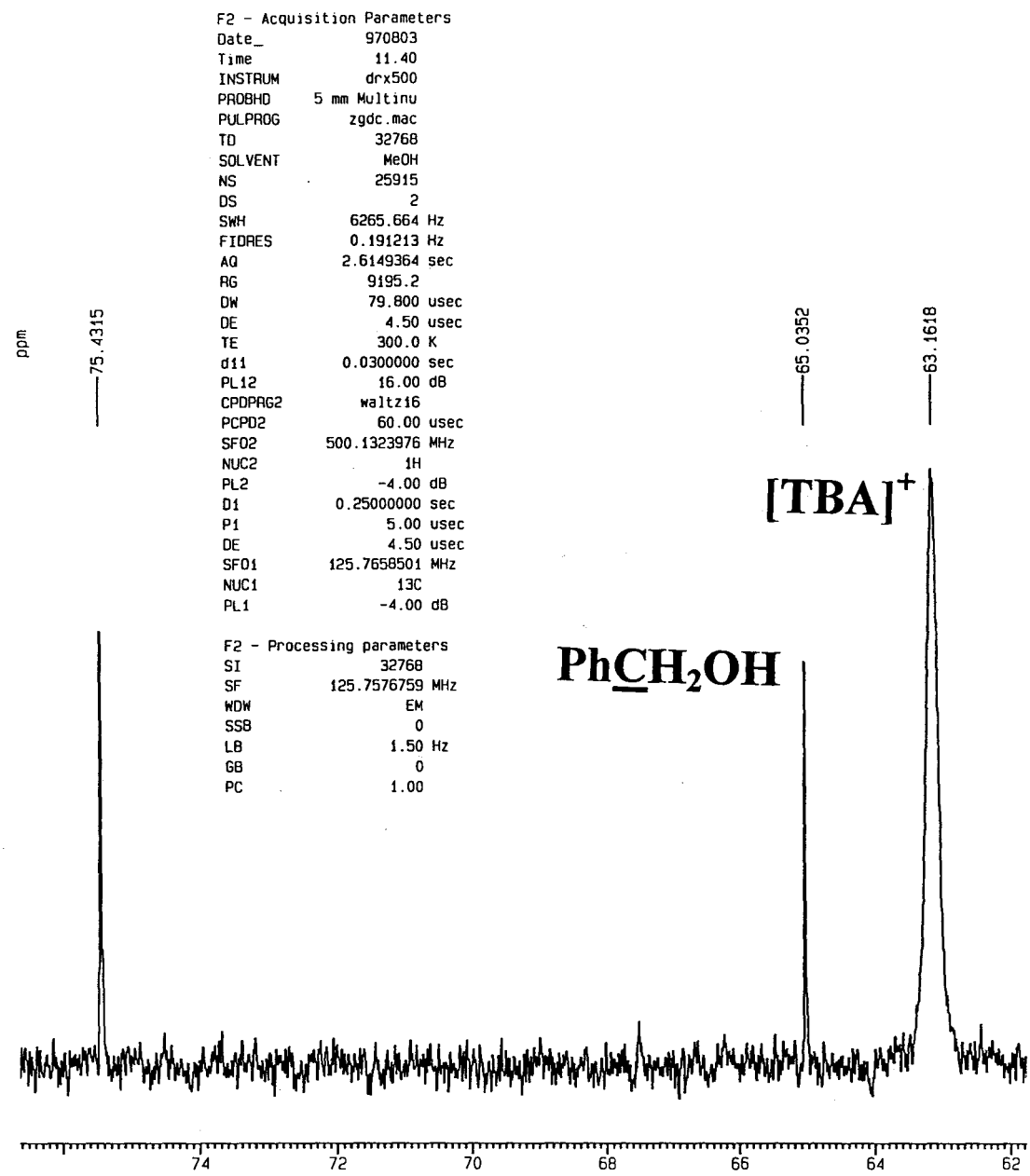

Figure 2.10: ^{13}C NMR spectrum (125 MHz) showing a single benzylic carbon of benzyl alcohol at 65.0 ppm.

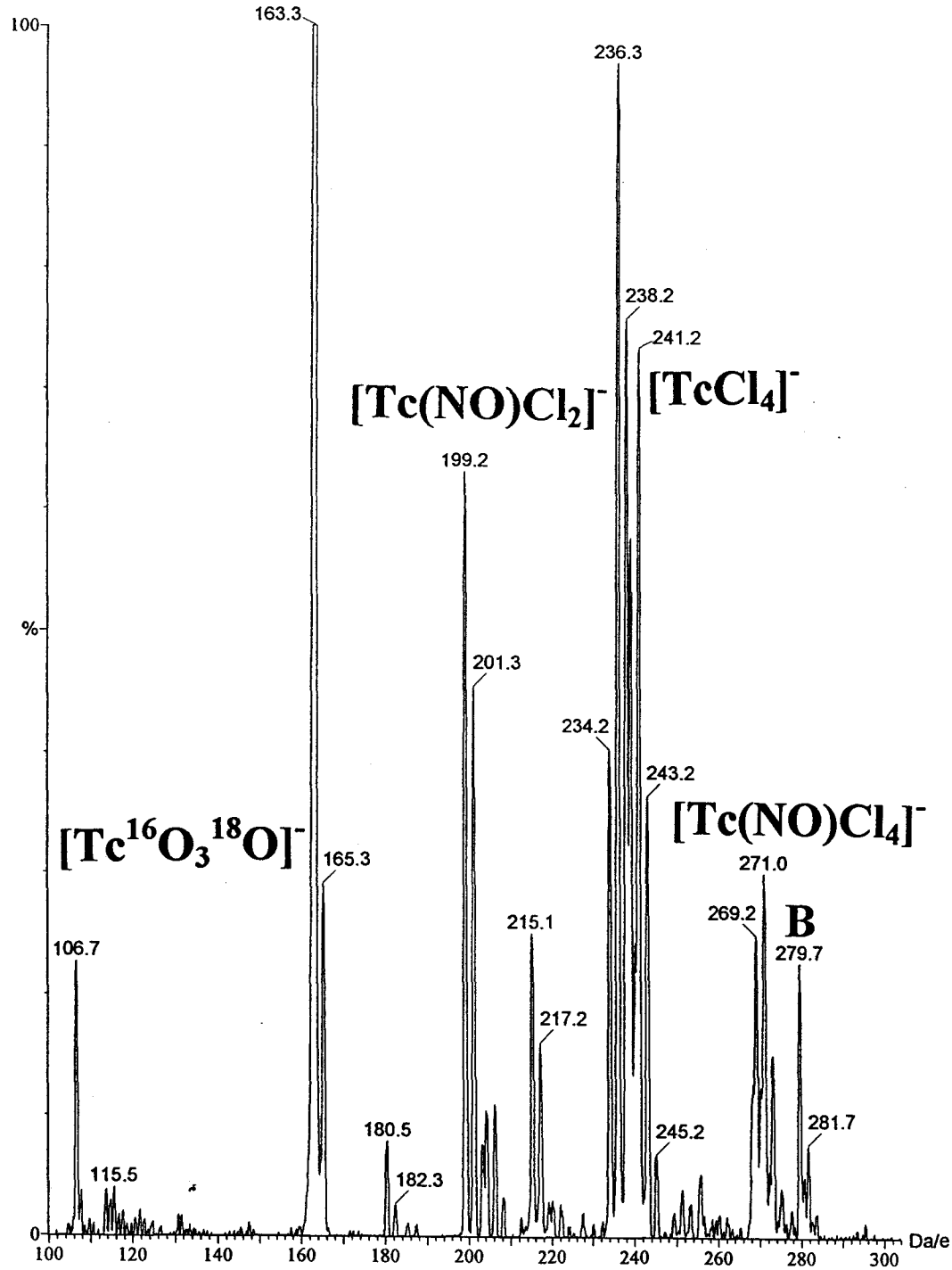

Figure 2.11: Negative ion ESMS for the completed reaction of [TBA][$Tc^{18}OCl_4$] + [NH_3OBn][Cl] in CD_3OD. The sample was injected in 50/50 MeCN/H_2O with no base added. B indicates background ions.

Negative ion ESMS of the completed reaction between [TBA][$Tc^{18}OCl_4$] and [NH_3OBn][Cl] in deuterated methanol is shown in Figure 2.11. The completed reaction mixture did not show any ions for labeled (m/z = 110) or unlabeled benzyl alcohol (m/z = 108) for ESMS, but peaks indicative of [$Tc(NO)Cl_4$]$^-$ were present. This revealed the O-18 label was not incorporated into the nitrosyl of [$Tc(NO)Cl_4$]$^-$ since the 269, 271, 273, and 275 peaks with a proper chlorine distribution were present. The only presence of O-18 was in the form of [$Tc^{16}O_3{}^{18}O$]$^-$ that had a m/z ratio of 165. There is often a small amount of unreacted [TBA][TcO_4] that carries through in the synthesis of [TBA][$TcOCl_4$] that can be observed in the infrared spectrum and ESMS. Whether this has been carried through or is a decomposition product of the reaction is not known. The ratios of intensities of [$Tc^{16}O_4$]$^-$ and [$Tc^{16}O_3{}^{18}O$]$^-$ are meaningless since some [$Tc^{16}O_4$]$^-$ is almost always present as a background ion in the instrument and water from the mobile phase is continually exchanging and diluting the amount of the [$Tc^{16}O_3{}^{18}O$]$^-$.

At this point, there is no direct evidence for the presence of labeled benzyl alcohol in the reaction mixture. If the reaction does not proceed following the proposed mechanism in Figure 2.2, another plausible mechanism is shown in Figure 2.12. In this case a chloride ion attacks the α-carbon of the hydroxylamine forming the corresponding alkyl chloride. The O-18 then would be incorporated into a labeled water molecule and this also accounts for the loss of the extra proton that could not be explained by the earlier proposal. An explanation for the alcohol formation might be that the excess hydroxylamine was cleaved to form ammonia and alcohol after time, although this is a reductive process and some Tc must concommitantly revert to a higher oxidation state.

Another problem with this mechanism is that water readily reacts with $[TcOCl_4]^-$ forming TcO_2 and $[TcO_4]^-$ according to the equation in Figure 2.13.[50] No TcO_2 was precipitated from the reaction mixture so it could be that there was not much water present or the release of water was the rate determining step and all of the $[TcOCl_4]^-$ has been consumed at that point.

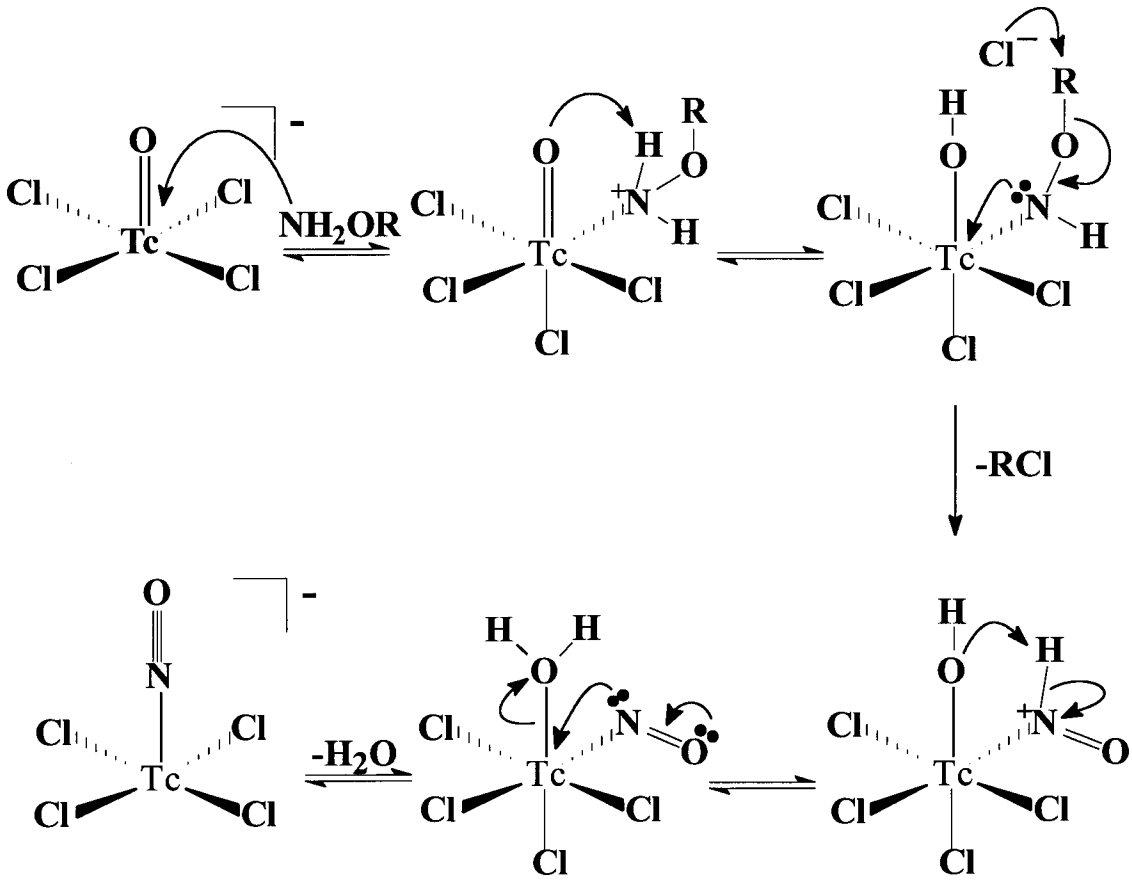

Figure 2.12: Alternative mechanism of nitrosyl formation with chloride attack

$$3\ [TcOCl_4]^- + 15\ H_2O \rightarrow [TcO_4]^- + 2\ TcO_2 + 10\ H_3O^+ + 12\ Cl^-$$

Figure 2.13: Equation for the hydrolysis of $[TcOCl_4]^-$

The proton NMR of the benzylic protons of benzyl chloride (in CD_3OD) have a chemical shift (4.4 ppm) that is in the region of the supposed intermediate (4.4 ppm) which shifts to 4.5 ppm with addition of O-benzyl hydroxylamine hydrochloride. The benzylic carbon of benzyl chloride has a chemical shift of 46 ppm which is not in the correct region for the intermediate (75 ppm) and is not at all present in any of the O-benzyl hydroxylamine reactions. Physical evidence such as this strongly suggests this is not the mechanism of the reaction.

To summarize the proposed mechanisms to this point, the chloride attack seems unlikely since the corresponding chloroalkanes are not present in the reaction mixtures. The oxo group attack seems to be the most plausible mechanism, however, there is only one ^{13}C NMR signal for benzyl alcohol which may be ascribed to the coalescing of the labeled and unlabeled signals in a polar solvents (even though it is a sharp signal). The intermediates appear to be the unlabeled peaks in the NMR figures described above. These are present after the reaction has reached completion and are possibly in equilibrium with the final product, $[Tc(NO)Cl_4]^-$.

2.6 Experimental Section

Preparation of ammonium pertechnetate:

A procedure similar to that described by Peacock[51] and Keller[52] was followed. Black TcO_2 (400 mg, 3.0 mmol) was dissolved in 5 mL of 30 % hydrogen peroxide in an open 100 mL beaker to form a yellow-peach coloured solution. To this solution was added ~40 mL of concentrated aqueous ammonia which caused the whole solution to become a dark purple colour. Heating at 90 °C for ~15 minutes changed the purple coloration to colourless ($[NH_4][TcO_4]$) and the volume was reduced to 10 mL by slow

boiling to avoid splattering. Another 40 mL of concentrated aqueous ammonia was added and this was either boiled gently to dryness to form a colourless powder of $[NH_4][TcO_4]$ or a few mL of the solution was dried in a vacuum desiccator for 48 hours forming colourless crystals.

This compound showed:

IR (KBr pellet; cm^{-1}): ν_{Tc-O} = 898 (vs, vbr); literature value[53] ν_{Tc-O} = 840 (s), 900 (s), 925 (sh)

ESMS (negative ion): 163 (M^+)

Preparation of tetrabutylammonium and potassium tetrachlorooxotechnetate(V), 1a, 1b

For the tetrabutylammonium salt, the method of Davison *et al.* was followed.[54, 55] A modified procedure was used for the potassium salt. To a beaker containing a magnetic stir bar were added 116 mg (0.64 mmol) of ammonium pertechnetate in 2.0 mL of water (0.32 M). To this colourless solution was added 16 mL conc. HCl and the reaction turned yellow and then green. After stirring for 10 minutes, 53 mg (0.71 mmol, 1.1 equivalents) of potassium chloride were added and the solution was warmed to 40 °C to remove excess ammonia, as a stream of nitrogen reduced the volume. A dark green crystalline solid was deposited to give 147.7 mg (78 % yield) of **1b**.

Compound **1a** showed:

IR (KBr pellet; cm^{-1}): ν_{Tc-O} = 1024, literature value[55] ν_{Tc-O} = 1020 cm^{-1}

ESMS (negative ion): 163 $[TcO_4]^-$

Compound **1b** showed:

IR (KBr pellet, cm^{-1}): ν_{Tc-O}=984.

Preparation of ^{18}O labeled tetrabutylammonium tetrachloro-^{18}O-oxotechnetate, 2

A modified procedure for the synthesis of [TBA][$TcOCl_4$] was used.[53] Recycled $H_2{}^{18}O$ (2mL) was used.[56] The percentage of labeled water was determined to be 85+/-2% by EI-MS. A concentrated hydrochloric acid solution was made by passing dry HCl gas (Liquid Air™) through Tygon® tubing attached to a glass pipette that was carefully inserted into a septum and gently blown approximately 2 cm over 1.2 mL of O-18 labeled water in a disposable 10 mL weighed vial that was cooled in an ice bath. A syringe needle with Tygon® tubing outletted from this vial to another 10 mL disposable vial with a septum that was used as a trap, and the excess HCl gas was bubbled into a 400 mL slurry of NaOH. After fifteen minutes the gas was turned off and the disposable vial had a weight difference indicating the solution was greater than 12 M HCl. The volume of the solution had also increased to ~ 2 mL. This concentrated acid was then added to 0.6 mL of a 0.44 M (0.27 mmol, 48 mg) solution of ammonium pertechnetate in a 10 mL disposable vial equipped with magnetic stir bar and septum. The system was purged with nitrogen for 10 minutes with stirring beforehand, then the septum removed, the 2 mL acid solution quickly added with a disposable plastic tipped pipetter, and the septum reinserted. The solution turned immediately yellow and then green after a few seconds and darker green after a few minutes. The solution was stirred at room temperature with nitrogen flowing for thirty minutes with no further colour change. Dry [TBA][Cl] (120 mg, 0.431 mmol) was dissolved in 0.3 mL labeled water and added dropwise to the solution which immediately precipitated a green/grey solid. This was collected by

filtration with a fine porousity frit at water aspirator pressure, washed with 1.5 mL of isopropanol, and dried *in vacuo* to give 87 mg (69%) of the green-grey semi-crystalline $[TBA][Tc^{18}OCl_4]$.

The compound showed:

IR (KBr pellet, cm^{-1}) $\nu_{Tc-^{18}O}$=975, $\nu_{Tc-^{16}O}$=1024.

The ratio of the intensities for the Tc-^{18}O:Tc-^{16}O stretch was measured to be 70:30. ESMS experiments were attempted with injections in acetonitrile with a 50/50 acetonitrile/water mixture as the mobile phase but only the TcO_4^- ion was present (a decomposition product of $[TcOCl_4]^-$ and H_2O). There was a very small intensity peak at 165 which corresponds to $[Tc^{16}O_3{}^{18}O]^-$.

Preparation of the tetrachloronitrosyltechnetate(II) anion using O-substituted hydroxylamines:

A typical reaction that was followed in an NMR tube had ~5-20 mg of $[TBA][TcOCl_4]$ or $[K][TcOCl_4]$ dissolved in 0.3-0.5 mL of dry CD_3OD. The $[K][TcOCl_4]$ normally required ultrasonication for it to dissolve in the CD_3OD. The $[TcOCl_4]^-$ containing solution was transferred to a 5 mm NMR tube and NH_2OR (1.1 equivalent) was added as a solution in 0.3-0.5 mL CD_3OD and the green colour changed to a brown or brown-red colour. The NMR tube was inverted several times and the first spectrum could be obtained within 5 minutes. The specific details for each reaction are given below.

Reaction of [NH3OMe][Cl] with [K][TcOCl4]:

To a 5 mL disposable vial was added 15.3 mg (0.052 mmol) of [K][$TcOCl_4$] and 0.5 mL CD_3OD. After completely dissolving, this solution was pipetted into a 5 mm NMR tube. To a separate 5 mL disposable vial was added 4.8 mg (0.057 mmol)of dry [NH_3OMe][Cl] and 0.3 mL CD_3OD. Once dissolved this solution was added all at once to the NMR tube and inverted several times. The initial green colour immediately changed to brown-red.

This reaction showed:

^1H NMR (ppm): 3.903, s - CH_3 of [NH_3OMe][Cl] starting material; 3.010, s - possible intermediate; 3.346, s - CH_3 of CH_3OH

A larger scale reaction was done at low temperature in attempts to crystallize any intermediates. To a 20 mL disposable scintillation vial was added 57.3 mg (0.115 mmol) [TBA][$TcOCl_4$] and 1 mL of CD_3OD. To this solution was added 10.5 mg (0.126 mmol, 1.1 equivalents) of [NH_3OMe][Cl] that had been dissolved in 1 mL of CD_3OD. The reaction immediately turned brown-red. This was swirled for a few seconds, capped, and placed in a Dewar with dry ice for 5 days. The colour did not change over this period and the sample was left in the freezer (-10 °C) for 3 months with still no colour change or formation of solid.

Reaction of [NH3OEt][Cl] with [K][TcOCl4]:

To a 5 mL disposable vial was added 16.0 mg (0.054 mmol) of [K][$TcOCl_4$] and 0.5 mL CD_3OD. After completely dissolving, this solution was pipetted into a 5 mm NMR tube. To a separate 5 mL disposable vial was added 5.8 mg (0.059 mmol, 1.1 equivalents)of dry [NH_3OEt][Cl] and 0.3 mL CD_3OD. Once dissolved this solution was

added all at once to the NMR tube and inverted several times. The initial green colour immediately changed to brown-red.

This reaction showed:

^{1}H NMR (ppm): 4.106, q (broad); 1.307 t (broad) - Et of $[NH_3OEt][Cl]$ starting material; 3.553, q; 1.161, t - EtOH; 3.4375, q; 1.446, t - possible intermediate

A larger scale reaction was done at low temperature in attempts to crystallize any intermediates. To a 20 mL disposable scintillation vial was added 54.7 mg (0.110 mmol) $[TBA][TcOCl_4]$ and 1 mL of CD_3OD. To this solution was added 11.8 mg (0.121 mmol, 1.1 equivalents) of $[NH_3OMe][Cl]$ that had been dissolved in 1 mL of CD_3OD. The reaction immediately turned brown-red. This was swirled for a few seconds, capped, and placed in a Dewar with dry ice for 5 days. The colour did not change over this period and the sample was left in the freezer (-10 °C) for 3 months with still no colour change or formation of solid.

Reaction of $[NH_3OBn][Cl]$ with $[K][TcOCl_4]$:

To a 5 mL disposable vial was added 20.7 mg (0.041 mmol) of $[TBA][TcOCl_4]$ and 0.5 mL CD_3OD. After completely dissolving, this solution was pipetted into a 5 mm NMR tube. To a separate 5 mL disposable vial was added 7.9 mg (0.046 mmol, 1.1 equivalents)of dry $[NH_3OBn][Cl]$ and 0.3 mL CD_3OD. Once dissolved this solution was added all at once to the NMR tube and inverted several times. The initial green colour immediately changed to brown-red.

This reaction showed:

^{1}H NMR (ppm): 7.431, s (phenyl); 5.038, s (benzylic) - [NH_3OBn][Cl] starting material; 7.331, s (phenyl); 4.583, s (benzylic) - benzyl alcohol; 7.312, s (phenyl); 4.439, s (benzylic) - possible intermediate

^{13}C NMR: 127-135 ppm, phenyl carbons; 78.2, benzylic carbon [NH_3OBn][Cl] starting material; 75.5 - benzylic carbon - possible intermediate; 65.1 benzyl alcohol benzylic carbon.

Reaction of [NH_3OBn][Cl] with [TBA][$Tc^{18}OCl_4$] :

To a 5 mL disposable vial was added 22.7 mg of [TBA][$Tc^{18}OCl_4$] (0.045 mmol) that was dissolved in 0.5 mL CD_3OD. In a separate 5mL disposable vial was added 7.9 mg (0.049 mmol, 1.1 equiv.) of [NH_3OBn][Cl] that was dissolved in 0.3 mL of CD_3OD. The solution of [NH_3OBn][Cl] was added all at once to the solution of [TBA][$Tc^{18}OCl_4$] which was swirled for approximately 30 seconds with a stream of nitrogen flowing into the vial. Half of this volume was transferred via a pipette to a 5 mm NMR tube and the other half was sealed in the vial.

This reaction showed:

^{1}H NMR (ppm): 7.431, s (phenyl); 5.038, s (benzylic) - [NH_3OBn][Cl] starting material; 7.324, s (phenyl); 4.583, s (benzylic) - benzyl alcohol; 7.315, s (phenyl); 4.440, s (benzylic) - possible intermediate

^{13}C NMR: 127-135 ppm, phenyl carbons; 78.2, benzylic carbon [NH_3OBn][Cl] starting material; 75.4 - benzylic carbon - possible intermediate; 65.0 benzyl alcohol benzylic carbon. 13,14,16-18,21,25-26,28,31,32-39 13,14,16-18,21,25-26,28,31,32-39 13,14,16-18,21,25-26,28,31,32-3913,14,16-18 13,14,16-18,21,25-26,28,31,32-392312394593495

^{1}H NMR (ppm): 7.431, s (phenyl); 5.038, s (benzylic) - $[NH_3OBn][Cl]$ starting material; 7.331, s (phenyl); 4.583, s (benzylic) - benzyl alcohol; 7.312, s (phenyl); 4.439, s (benzylic) - possible intermediate

^{13}C NMR: 127-135 ppm, phenyl carbons; 78.2, benzylic carbon $[NH_3OBn][Cl]$ starting material; 75.5 - benzylic carbon - possible intermediate; 65.1 benzyl alcohol benzylic carbon.

Reaction of $[NH_3OBn][Cl]$ with $[TBA][Tc^{18}OCl_4]$:

To a 5 mL disposable vial was added 22.7 mg of $[TBA][Tc^{18}OCl_4]$ (0.045 mmol) that was dissolved in 0.5 mL CD_3OD. In a separate 5mL disposable vial was added 7.9 mg (0.049 mmol, 1.1 equiv.) of $[NH_3OBn][Cl]$ that was dissolved in 0.3 mL of CD_3OD. The solution of $[NH_3OBn][Cl]$ was added all at once to the solution of $[TBA][Tc^{18}OCl_4]$ which was swirled for approximately 30 seconds with a stream of nitrogen flowing into the vial. Half of this volume was transferred via a pipette to a 5 mm NMR tube and the other half was sealed in the vial.

This reaction showed:

^{1}H NMR (ppm): 7.431, s (phenyl); 5.038, s (benzylic) - $[NH_3OBn][Cl]$ starting material; 7.324, s (phenyl); 4.583, s (benzylic) - benzyl alcohol; 7.315, s (phenyl); 4.440, s (benzylic) - possible intermediate

^{13}C NMR: 127-135 ppm, phenyl carbons; 78.2, benzylic carbon $[NH_3OBn][Cl]$ starting material; 75.4 - benzylic carbon - possible intermediate; 65.0 benzyl alcohol benzylic carbon.

CHAPTER 3

SUBSTITUTION REACTIONS OF TETRACHLORONITROSYLTECHNETATE(II)

3.1 Introduction

There are not many well characterized technetium nitrosyl complexes containing only nitrogen and/or halide donor ligands. In the literature, there are x-ray structure determinations for *trans*-$[Tc^{(I)}(NO)(NH_3)_4(H_2O)]$, *cis*-$[Tc^{(I)}(NO)(phen)_2(NH_3)][PF_6]_2$, and *mer*-$Tc^{(I)}(NO)py_3Cl_2$. For these complexes the synthesis of the former two compounds involved the use of $[NH_4]_2[TcCl_6]$ in a hydroxylamine solution followed by addition of solutions of ammonia or phenanthroline. The pyridine compound was made by the substitution of chlorides on $[Tc(NO)Cl_4]^-$ in neat pyridine. In the present work, the bidentate ligands phenanthroline and bipyridyl were used to substitute chlorides on $[Tc(NO)Cl_4]^-$ in appropriate solvents. Complexes with one complexing phenanthroline or bipyridyl ligand have been synthesized and structurally characterized. A complex with two complexing bipyridyl ligands has also been synthesized and structurally characterized. This chapter describes the synthesis and x-ray structure determinations used to characterize these compounds.

3.2 X-ray Crystal Structure Determination of *mer*-trichloronitrosyl-1,10-phenanthrolinetechnetium(II) (4a) and *mer*-trichloronitrosyl-1,10-phenanthrolinetechnetium(II) · (phen)·(MeCN) (4b):

Compound **4a** was prepared by the addition of five equivalents of phenanthroline monohydrate to [TBA][Tc(NO)Cl_4] in methanol with recrystallization of the product from acetonitrile and petroleum ether (50-110 °C) (Section 3.7). Preparation from dichloromethane yields the same crystals but in lower yield. Compound **4b** was prepared by the addition of ten equivalents of anhydrous phenanthroline to [TBA][Tc(NO)Cl_4] in acetonitrile followed by recrystallization of the product via vapour diffusion of petroleum ether into the acetonitrile.

The x-ray crystallographic data, atomic positional parameters and important interatomic distances for **4a** are summarized in Tables 3.1 - 3.3. Those for **4b** are summarized in Tables 3.4 - 3.6. A perspective view of **4a** is shown in Figure 3.1 and a packing diagram is shown in Figure 3.2. Those for **4b** are shown in Figures 3.3 - 3.4.

The structural characterization of **4a** and **4b** demonstrated that the meridonial isomer was synthesized rather than the facial isomer. There were no disorder problems associated with the nitrosyl moiety for **4a**, however, **4b** had a very highly disordered nitrosyl and acetonitrile solvent which are the likely reason for the high residuals. As a result of the disordered nitrosyl of **4b**, accurate Tc-N-O bond lengths and angles could only be determined for **4a**. The Tc-N-O angle is 168.3(5)° indicating that it is a linearly bonded nitrosyl and is formally considered as a NO^+ ligand. The nitrosyl bond is 1.107(5) Å in length which is one of the shorter technetium nitrosyl bond lengths known while the

Table 3.1: Summary of the crystal data, collection and refinement conditions for **4a**.

Crystal Data		
Identification code	dg2	
Empirical formula	$C_{12}H_8Cl_3N_3OTc$	
Formula weight	414.56	
Temperature	300(2) K	
Wavelength	0.71073 A	
Crystal system	Monoclinic	
Space group	P2(1)/n	
Unit cell dimensions	a = 9.1143(2) A	α = 90 deg.
	b = 14.83440(10) A	β = 100.1530(10) deg.
	c = 10.9840(2) A	γ = 90 deg.
Volume, Z	1461.84(4) A^3, 3	
Density (calculated)	1.413 Mg/m^3	
Crystal colour, habit	dark green-black	
Absorption coefficient	1.147 mm^-1	
F(000)	609	
Crystal size	.03 x .15 x .25 mm	
Data Collection		
Theta range for data collection	2.33 to 26.39 deg.	
Limiting indices	-11<=h<=10, -18<=k<=18, -13<=l<=13	
Reflections collected	11774	
Independent reflections	2968 [R(int) = 0.0355]	
Absorption correction	None	
Refinement		
Refinement method	Full-matrix least-squares on F^2	
Data / restraints / parameters	2968 / 0 / 181	
Goodness-of-fit on F^2	1.120	
Final R indices [I>2sigma(I)]	R1 = 0.0400, wR2 = 0.0793	
R indices (all data)	R1 = 0.0603, wR2 = 0.0884	
Largest diff. peak and hole	0.388 and -0.566 e.A^-3	

Table 3.2: Atomic coordinates (x 10^4) and equivalent isotropic displacement parameters ($Å^2$ x 10^3) for **4a**. U(eq) is defined as one third of the trace of the orthogonalized Uij tensor.

	x	y	z	U(eq)
Tc(1)	1139(1)	1773(1)	6944(1)	45(1)
Cl(1)	3532(2)	2273(1)	7745(2)	79(1)
Cl(2)	143(1)	3229(1)	7157(1)	61(1)
Cl(3)	1894(2)	250(1)	6911(1)	64(1)
N(1)	723(4)	1488(2)	8786(3)	44(1)
C(2)	1663(5)	1553(3)	9860(4)	52(1)
C(3)	1242(6)	1372(3)	10984(4)	59(1)
C(4)	-178(6)	1116(3)	11028(4)	59(1)
C(5)	-2725(6)	746(4)	9850(5)	63(1)
C(6)	-3647(6)	671(4)	8757(6)	64(1)
C(7)	-4080(6)	809(4)	6442(5)	65(1)
C(8)	-3507(6)	1002(4)	5418(5)	66(2)
C(9)	-2016(5)	1257(3)	5526(4)	57(1)
N(10)	-1124(4)	1329(2)	6599(3)	45(1)
C(11)	-1681(5)	1132(3)	7654(4)	43(1)
C(12)	-707(5)	1222(3)	8814(4)	44(1)
C(13)	-3153(5)	860(3)	7613(5)	54(1)
C(14)	-1216(5)	1023(3)	9924(4)	50(1)
N(21)	1337(5)	1911(3)	5356(4)	59(1)
O(1)	1650(6)	1897(4)	4427(4)	102(2)

Table 3.3: Bond lengths (Å) and angles (°) for **4a**.

Tc(1)-N(21)	1.797(4)	Tc(1)-N(10)	2.135(3)
Tc(1)-N(1)	2.165(3)	Tc(1)-Cl(1)	2.325(2)
Tc(1)-Cl(3)	2.3639(14)	Tc(1)-Cl(2)	2.3710(13)
N(1)-C(2)	1.333(5)	N(1)-C(12)	1.367(5)
C(2)-C(3)	1.383(7)	C(3)-C(4)	1.358(7)
C(4)-C(14)	1.407(7)	C(5)-C(6)	1.342(7)
C(5)-C(14)	1.423(7)	C(6)-C(13)	1.435(7)
C(7)-C(8)	1.352(7)	C(7)-C(13)	1.411(7)
C(8)-C(9)	1.395(7)	C(9)-N(10)	1.313(6)
N(10)-C(11)	1.375(5)	C(11)-C(13)	1.395(6)
C(11)-C(12)	1.425(6)	C(12)-C(14)	1.410(6)
N(21)-O(1)	1.107(5)		
N(21)-Tc(1)-N(10)	97.0(2)	N(21)-Tc(1)-N(1)	173.6(2)
N(10)-Tc(1)-N(1)	77.44(13)	N(21)-Tc(1)-Cl(1)	94.76(14)
N(10)-Tc(1)-Cl(1)	168.06(10)	N(1)-Tc(1)-Cl(1)	90.91(10)
N(21)-Tc(1)-Cl(3)	90.83(14)	N(10)-Tc(1)-Cl(3)	88.68(10)
N(1)-Tc(1)-Cl(3)	85.82(10)	Cl(1)-Tc(1)-Cl(3)	93.13(5)
N(21)-Tc(1)-Cl(2)	95.60(14)	N(10)-Tc(1)-Cl(2)	85.64(10)
N(1)-Tc(1)-Cl(2)	87.29(10)	Cl(1)-Tc(1)-Cl(2)	91.26(5)
Cl(3)-Tc(1)-Cl(2)	171.89(5)	C(2)-N(1)-C(12)	117.9(4)
C(2)-N(1)-Tc(1)	128.4(3)	C(12)-N(1)-Tc(1)	113.7(3)
N(1)-C(2)-C(3)	122.6(4)	C(4)-C(3)-C(2)	120.1(5)
C(3)-C(4)-C(14)	119.8(4)	C(6)-C(5)-C(14)	121.4(5)
C(5)-C(6)-C(13)	121.5(5)	C(8)-C(7)-C(13)	119.4(5)
C(7)-C(8)-C(9)	120.0(5)	N(10)-C(9)-C(8)	122.5(5)
C(9)-N(10)-C(11)	118.5(4)	C(9)-N(10)-Tc(1)	127.6(3)
C(11)-N(10)-Tc(1)	113.8(3)	N(10)-C(11)-C(13)	122.0(4)
N(10)-C(11)-C(12)	118.0(4)	C(13)-C(11)-C(12)	120.0(4)
N(1)-C(12)-C(14)	122.7(4)		
N(1)-C(12)-C(11)	116.9(4)		
C(14)-C(12)-C(11)	120.4(4)		
C(11)-C(13)-C(7)	117.5(5)		
C(11)-C(13)-C(6)	118.5(5)		
C(7)-C(13)-C(6)	123.9(5)		
C(4)-C(14)-C(12)	116.8(4)		
C(4)-C(14)-C(5)	125.0(4)		
C(12)-C(14)-C(5)	118.2(5)		
O(1)-N(21)-Tc(1)	168.3(5)		

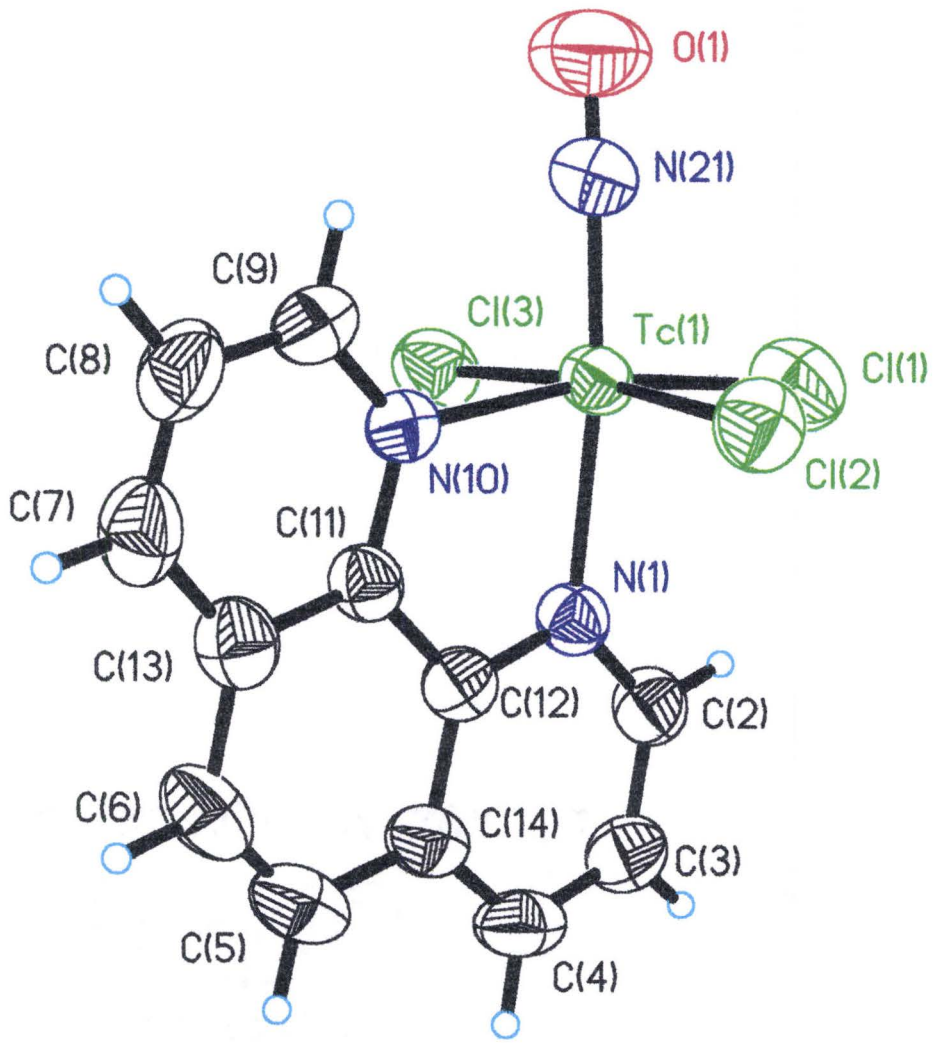

Figure 3.1: Structure of *mer*-[Tc(NO)Cl_3phen] (**4a**) drawn with 50% probability displacement ellipsoids.

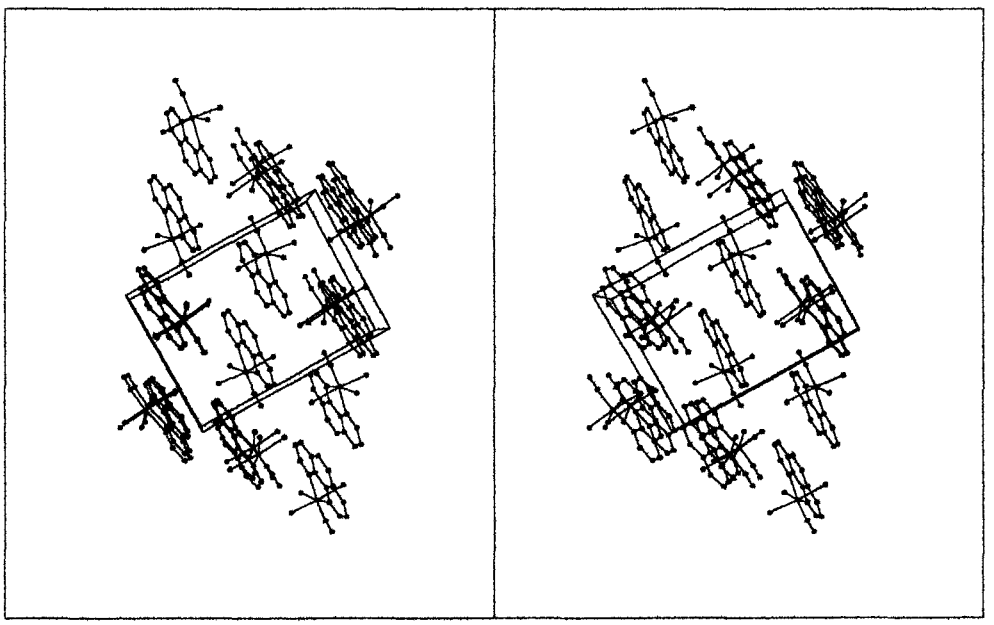

Figure 3.2: A stereoview of the packing of *mer*-[Tc(NO)Cl_3phen] (**4a**) within the unit cell. Hydrogen atoms have been omitted for clarity.

Table 3.4: Summary of the crystal data, collection and refinement conditions for **4b**.

Crystal Data		
Identification code	dg11a	
Empirical formula	$C_{25}H_{19}Cl_3N_6OTc$	
Formula weight	531.30	
Temperature	210(2) K	
Wavelength	0.71073 A	
Crystal system	Triclinic	
Space group	P-1	
Unit cell dimensions	a = 9.848(3) A	α = 108.62(2) deg.
	b = 10.798(2) A	β = 105.39(2) deg.
	c = 12.504(4) A	γ = 92.43(2) deg.
Volume, Z	1203.0(6) A^3, 2	
Density (calculated)	1.467 Mg/m^3	
Crystal colour, habit	Red-brown	
Absorption coefficient	0.840 mm^-1	
F(000)	532	
Crystal size	.10 x .15 x .28 mm	
Data Collection		
Theta range for data collection	1.80 to 26.43 deg.	
Limiting indices	-12<=h<=12, -13<=k<=13, -15<=l<=15	
Reflections collected	11899	
Independent reflections	4553 [R(int) = 0.2614]	
Absorption correction	None	
Refinement		
Refinement method	Full-matrix least-squares on F^2	
Data / restraints / parameters	4553 / 0 / 303	
Goodness-of-fit on F^2	1.178	
Final R indices [I>2sigma(I)]	R1 = 0.0829, wR2 = 0.2081	
R indices (all data)	R1 = 0.1351, wR2 = 0.2337	
Extinction coefficient	0.005(3)	
Largest diff. peak and hole	2.006 and -2.134 e.A^-3	

Table 3.5: Atomic coordinates (x 10^4) and equivalent isotropic displacement parameters (A^2 x 10^3) for **4b**. U(eq) is defined as one third of the trace of the orthogonalized Uij tensor.

	x	y	z	U(eq)
Tc	5045(1)	7689(1)	7464(1)	33(1)
Cl(1)	7039(2)	8223(2)	9180(2)	42(1)
Cl(2)	4663(4)	9882(4)	7806(3)	84(1)
Cl(3)	2903(3)	6901(2)	5891(2)	47(1)
N(21)	5128(8)	5664(6)	7291(6)	36(2)
C(22)	5780(10)	4818(8)	6654(7)	42(2)
C(23)	5788(11)	3530(8)	6632(8)	45(3)
C(24)	5109(11)	3090(9)	7304(8)	51(3)
C(25)	3676(10)	3611(8)	8730(8)	41(2)
C(26)	3049(10)	4492(9)	9392(7)	45(3)
C(27)	2410(10)	6793(10)	10048(8)	49(3)
C(28)	2497(10)	8031(9)	9972(7)	41(2)
C(29)	3256(10)	8323(8)	9274(7)	41(2)
N(210)	3840(8)	7423(7)	8602(6)	37(2)
C(211)	3768(10)	6170(7)	8664(7)	35(2)
C(212)	3077(9)	5797(8)	9383(7)	35(2)
C(213)	4455(9)	5233(7)	7962(7)	34(2)
C(214)	4404(9)	3970(8)	7988(7)	36(2)
N(1)	9287(9)	4307(8)	8325(8)	49(2)
C(2)	9104(11)	5521(9)	8366(10)	51(3)
C(3)	9494(11)	6129(10)	7632(10)	58(3)
C(4)	10115(11)	5390(11)	6807(9)	53(3)
C(5)	11044(12)	3296(12)	5945(8)	59(3)
C(6)	11236(11)	2076(11)	5880(8)	54(3)
C(7)	10983(12)	243(10)	6582(9)	55(3)
C(8)	10518(13)	-282(10)	7307(10)	63(3)
C(9)	9815(13)	523(11)	8049(12)	68(4)
N(10)	9647(10)	1702(8)	8164(8)	56(2)
C(11)	10069(10)	2215(9)	7420(8)	47(3)
C(12)	10768(11)	1491(10)	6616(9)	54(3)
C(13)	9878(9)	3558(9)	7509(8)	42(2)
C(14)	10313(10)	4116(10)	6720(8)	45(2)
N(1)	6305(10)	7659(8)	6375(8)	0(2)
C(32)	5000	10000	5000	96(6)
N(31)	6360(16)	10202(16)	5232(14)	121(5)
O	6634(15)	7591(14)	6169(12)	66(5)

Table 3.6: Bond lengths (Å) and angles (°) for **4b**.

Tc-N(1)	2.067(9)	Tc-N(21)	2.134(7)
Tc-N(210)	2.155(6)	Tc-Cl(2)	2.333(4)
Tc-Cl(3)	2.371(3)	Tc-Cl(1)	2.381(3)
N(21)-C(22)	1.319(9)	N(21)-C(213)	1.371(9)
C(22)-C(23)	1.383(12)	C(23)-C(24)	1.379(13)
C(24)-C(214)	1.404(11)	C(25)-C(26)	1.338(12)
C(25)-C(214)	1.443(11)	C(26)-C(212)	1.412(13)
C(27)-C(28)	1.371(14)	C(27)-C(212)	1.435(12)
C(28)-C(29)	1.386(11)	C(29)-N(210)	1.327(10)
N(210)-C(211)	1.380(11)	C(211)-C(212)	1.401(11)
C(211)-C(213)	1.435(10)	C(213)-C(214)	1.374(12)
N(1)-C(2)	1.317(12)	N(1)-C(13)	1.365(11)
C(2)-C(3)	1.404(14)	C(3)-C(4)	1.388(14)
C(4)-C(14)	1.37(2)	C(5)-C(6)	1.32(2)
C(5)-C(14)	1.455(13)	C(6)-C(12)	1.42(2)
C(7)-C(12)	1.36(2)	C(7)-C(8)	1.37(2)
C(8)-C(9)	1.404(14)	C(9)-N(10)	1.258(14)
N(10)-C(11)	1.364(11)	C(11)-C(12)	1.417(12)
C(11)-C(13)	1.444(14)	C(13)-C(14)	1.448(12)
N(1)-O	0.46(2)	C(32)-N(31)#1	1.29(2)
C(32)-N(31)	1.29(2)		

N(1)-Tc-N(21)	93.5(3)	N(1)-Tc-N(210)	170.9(3)
N(21)-Tc-N(210)	77.6(2)	N(1)-Tc-Cl(2)	95.8(3)
N(21)-Tc-Cl(2)	170.5(2)	N(210)-Tc-Cl(2)	93.1(2)
N(1)-Tc-Cl(3)	94.4(3)	N(21)-Tc-Cl(3)	85.3(2)
N(210)-Tc-Cl(3)	87.1(2)	Cl(2)-Tc-Cl(3)	92.26(11)
N(1)-Tc-Cl(1)	92.9(3)	N(21)-Tc-Cl(1)	87.5(2)
N(210)-Tc-Cl(1)	84.7(2)	Cl(2)-Tc-Cl(1)	93.64(11)
Cl(3)-Tc-Cl(1)	170.09(8)	C(22)-N(21)-C(213)	117.6(7)
C(22)-N(21)-Tc	127.7(5)	C(213)-N(21)-Tc	114.6(5)
N(21)-C(22)-C(23)	122.6(7)	C(24)-C(23)-C(22)	120.1(8)
C(23)-C(24)-C(214)	118.6(8)	C(26)-C(25)-C(214)	120.8(8)
C(25)-C(26)-C(212)	121.0(7)	C(28)-C(27)-C(212)	119.8(7)
C(27)-C(28)-C(29)	119.8(8)	N(210)-C(29)-C(28)	122.7(8)
C(29)-N(210)-C(211)	118.5(7)	C(29)-N(210)-Tc	127.9(6)
C(211)-N(210)-Tc	113.5(5)	N(210)-C(211)-C(212)	122.9(7)
N(210)-C(211)-C(213)	117.2(7)	C(212)-C(211)-C(213)	119.9(7)

C(211)-C(212)-C(26)	119.4(7)	C(211)-C(212)-C(27)	116.2(8)
C(26)-C(212)-C(27)	124.5(7)	N(21)-C(213)-C(214)	123.7(7)
N(21)-C(213)-C(211)	117.0(7)	C(214)-C(213)-C(211)	119.3(7)
C(213)-C(214)-C(24)	117.5(7)	C(213)-C(214)-C(25)	119.6(7)
C(24)-C(214)-C(25)	122.8(8)	C(2)-N(1)-C(13)	119.0(8)
N(1)-C(2)-C(3)	124.7(9)	C(4)-C(3)-C(2)	117.2(10)
C(14)-C(4)-C(3)	120.3(9)	C(6)-C(5)-C(14)	123.6(9)
C(5)-C(6)-C(12)	120.8(9)	C(12)-C(7)-C(8)	120.1(9)
C(7)-C(8)-C(9)	116.5(11)	N(10)-C(9)-C(8)	126.4(11)
C(9)-N(10)-C(11)	117.1(9)	N(10)-C(11)-C(12)	121.6(10)
N(10)-C(11)-C(13)	119.0(8)	C(12)-C(11)-C(13)	119.3(9)
C(7)-C(12)-C(11)	118.0(9)	C(7)-C(12)-C(6)	121.9(9)
C(11)-C(12)-C(6)	120.0(11)	N(1)-C(13)-C(14)	119.6(9)
N(1)-C(13)-C(11)	120.7(8)	C(14)-C(13)-C(11)	119.7(8)
C(4)-C(14)-C(13)	119.2(8)	C(4)-C(14)-C(5)	124.4(9)
C(13)-C(14)-C(5)	116.3(9)	O-N(1)-Tc	168(3)
N(31)#1-C(32)-N(31)	180.000(3)		

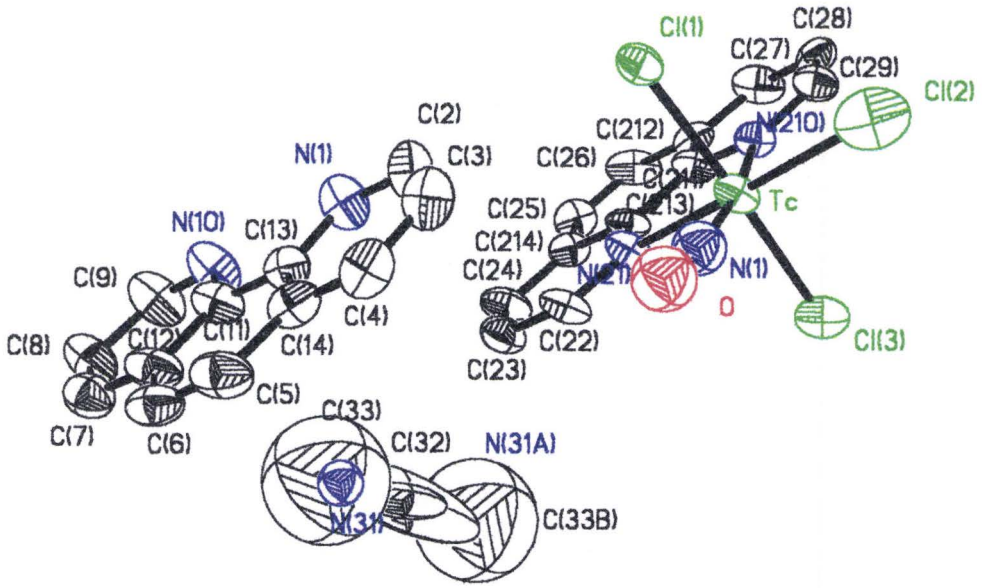

Figure 3.3: Structure of *mer*-[Tc(NO)Cl_3phen]·(phen)·(MeCN) (**4b**) drawn with 50% probability displacement ellipsoids.

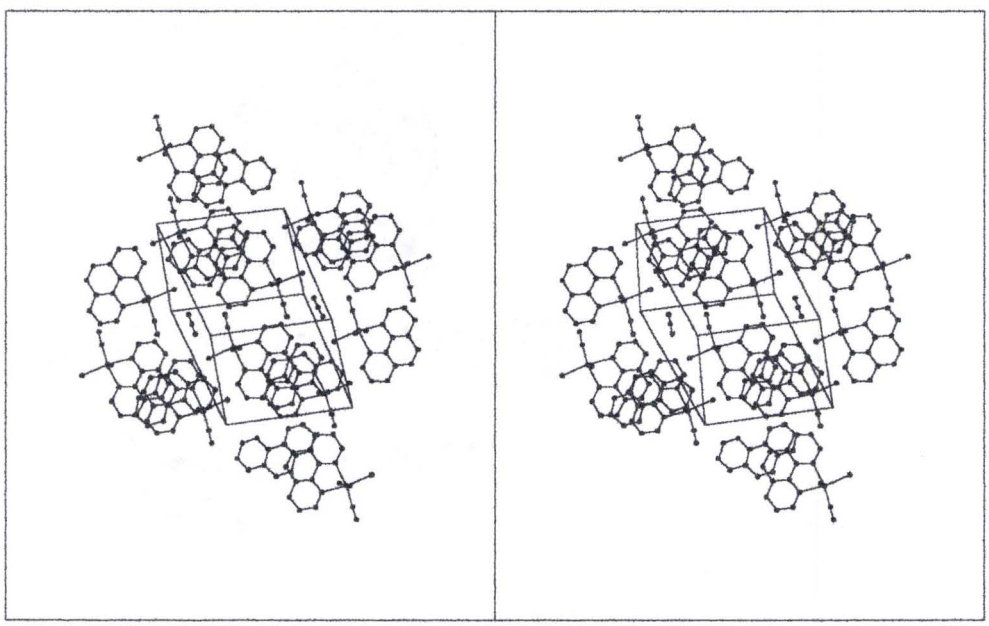

Figure 3.4: A stereoview of the packing of *mer*-[Tc(NO)Cl_3phen]·(phen)·(MeCN) (**4b**) within the unit cell. Hydrogen atoms have been omitted for clarity.

Tc-N bond is 1.797(4) Å in length which is quite a long Tc-N bond length. Selected technetium nitrosyl complexes are listed in Table 3.7 with their bond lengths and angles (where available) as well as nitrosyl stretching frequencies.

With competition for the dπ orbitals from the nitrosyl and phenanthroline group it appears there is less electron density available for backbonding from the metal to the π^* antibonding orbital of the nitrosyl. This results in a weaker Tc-N bond than is usually seen in other Tc(II) nitrosyl systems and a stronger N-O bond since less electron density is being put into an antibonding orbital. This can be compared to $[Tc^{(II)}(NO)(acac)Cl_3]^-$ (Table 3.7) where the oxygen atoms are considered to be π donating ligands rather than π accepting ones and thus only the nitrosyl is competing for electron density from the dπ orbitals. This results in a much stronger Tc-N bond and a weaker nitrosyl bond.

There is a *trans* influence associated with the nitrosyl ligand. The Tc-N_{trans} bond for **4a** is 0.030(6) Å (2.165(3) - 2.135(3)) shorter than the Tc-N_{cis} bond. That for **4b** is 0.021(13) (Å 2.120(5) - 2.146(5)) shorter but is not statistically significant with the large estimated standard deviations (esd's) of the bond lengths. The average Tc-Cl distances are 2.353 Å for **4a** and 2.362 for **4b** which are normal distances.

An interesting feature of **4b** is the co-crystallization of phenanthroline ligand with the metal complex. It was first thought that the phenanthroline was protonated and the metal was in a lower oxidation state as $[Tc^{(I)}(NO)(phen)Cl_3]^-$, but the infrared spectra of these complexes looked similar (only a 3-4 cm^{-1} difference in the NO stretch) and this compound was paramagnetic giving a 10 line EPR spectrum identical to **4a** indicating the metal was in the Tc(II) oxidation state (Section 3.6). This would make **4b** neutral and as

such does not require a cation to balance the charge. Since **4a** was recrystallized from acetonitrile (after being reacted in methanol solvent) the co-crystallization was most likely induced by adding double the usual amount of phenanthroline to the reaction mixture (10 equivalents were added compared to 5 that were normally added).

Table 3.7: Selected technetium nitrosyl complexes with bond lengths, angles, and infrared stretching frequencies (where available). Compounds in bold indicate the present work.

Tc-NO Compound	NO (Å)	Tc-NO (Å)	<Tc-N-O	ν_{NO} (cm^{-1})	Ref.
$[Tc^{(III)}(NO)(tmbt)_3]$	1.150(7)	1.767(6)	176.8(6)	1798	33
$[Tc^{(II)}(NO)(phen)Cl_3]$	**1.107(5)**	**1.797(4)**	**168.3(5)**	**1801**	
$[Tc^{(II)}(NO)(phen)Cl_3]\cdot phen\cdot MeCN$	-	-	-	**1798**	
†**$[Tc^{(II)}(NO)(bipy)Cl_3]$**	-	-	-	**1787**	
$[Tc^{(II)}(NO)(NH_3)_4(H_2O)]^{3+}$	-	-	-	1815	23
$[Tc^{(II)}(NO)(NCS)_5]^{3-}$	-	-	-	1785	19
$[Tc^{(II)}(NO)(Ph_3P)_2Cl_3]$	-	-	-	1805	30
$[Tc^{(II)}(NO)Cl_4(MeOH]^-$	1.17(2)	1.69(1)	175.5(10)	1805	40
‡$[Tc^{(II)}(NO)(acac)Cl_3]^-$ N_3O_3	1.20(4)	1.74(3)	159(3)	1770	31
N_4O_4	1.16(5)	1.71(3)	152(5)		
$[Tc^{(I)}(NO)(bipy)_2(MeCN)]^{2+}$	**1.162(13)**	**1.739(13)**	**176.4(12)**	**1744**	
$[Tc^{(I)}(NO)(phen)_2(NH_3)]^{2+}$	1.16(1)	1.74(1)	171.9(8)	1712	25
$[Tc^{(I)}(NO)(NH_3)_4(H_2O)]^{2+}$	1.203(6)	1.716	178.7(2)	1690	39
$[Tc^{(I)}(NO)py_3Cl_2]$	1.192(5)	1.781(5)	176.8(7)	1688	26
$[Tc^{(I)}(NO)(NCS)_5]^{3-}$	-	-	-	1690	19
$[Tc^{(I)}(NO)(dppe)_2(Cl)]^+$	-	-	-	1708	15
†$[Tc^{(I)}(NO)(diars)_2(Cl)]^+$	-	-	-	1720	32

† the disorder of the nitrosyl in the crystal structure prevents the accurate determination of these bond lengths and angles.

‡ the nitrosyl has a 2 fold site disorder in which both N_3O_3 and N_4O_4 are refined at half occupancy.

3.3 X-ray Crystal Structure Determination of *mer*-trichloronitrosyl-2, 2'-bipyridyltechnetium(II): (5)

Compound **5** was prepared by the addition of five equivalents of 2,2'-bipyridyl to [TBA][$Tc(NO)Cl_4$] in acetonitrile with recrystallization of the product from acetonitrile and petroleum ether (50-110 °C) (Section 3.7).

The x-ray crystallographic data, atomic positional parameters and important interatomic distances for **5** are summarized in Tables 3.8 - 3.10. A perspective view of **5** is shown in Figure 3.5 and a packing diagram is shown in Figure 3.6.

The structural characterization of **5** demonstrated that the meridonial isomer was synthesized rather than the facial isomer. The nitrosyl was somewhat disordered at full occupancy, enough that the bond lengths and angles could not be determined accurately.

There is a *trans* influence associated with the nitrosyl ligand. The Tc-N_{trans} bond for **5** is 0.026(10) Å (2.146(5) - 2.120(5)) longer than the Tc-N_{cis}. This is interesting how two similar compounds have different *trans* influences. This might be related to the out-of-plane displacement of the Tc atom and the rigidity that a phenanthroline molecule displays compared to the more flexible bipyridyl. The average Tc-Cl distances are 2.354 Å which are normal bond lengths.

Table 3.8: Summary of the crystal data, collection and refinement conditions for **5**.

Crystal Data		
Identification code	dg4	
Empirical formula	$C_{10}H_8Cl_3N_3OTc$	
Formula weight	390.54	
Temperature	300(2) K	
Wavelength	0.71073 A	
Crystal system	Monoclinic	
Space group	Pn	
Unit cell dimensions	a = 8.18710(10) A	α = 90 deg.
	b = 6.76260(10) A	β = 104.8730(10) deg.
	c = 12.5890(2) A	γ = 90 deg.
Volume, Z	673.65(2) A^3, 2	
Density (calculated)	1.925 Mg/m^3	
Crystal colour, habit	dark green-black	
Absorption coefficient	1.652 mm^-1	
F(000)	382	
Crystal size	.03 x .16 x .18 mm	
Data Collection		
Theta range for data collection	2.69 to 26.43 deg.	
Limiting indices	-10<=h<=10, -8<=k<=8, -15<=l<=15	
Reflections collected	6841	
Independent reflections	2659 [R(int) = 0.0540]	
Absorption correction	None	
Refinement		
Refinement method	Full-matrix least-squares on F^2	
Data / restraints / parameters	2659 / 2 / 163	
Goodness-of-fit on F^2	1.018	
Final R indices [I>2sigma(I)]	R1 = 0.0391, wR2 = 0.0964	
R indices (all data)	R1 = 0.0419, wR2 = 0.0983	
Absolute structure parameter	0.05(6)	
Largest diff. peak and hole	1.099 and -1.036 e.A^-3	

Table 3.9: Atomic coordinates (x 10^4) and equivalent isotropic displacement parameters (A^2 x 10^3) for **5**. U (eq) is defined as one third of the trace of the orthogonalized Uij tensor.

	x	y	z	U(eq)
Tc	2683(1)	2872(1)	9509(1)	28(1)
N(1)	4893(6)	4482(7)	9479(4)	31(1)
C(2)	5387(9)	6191(10)	10055(6)	42(1)
C(3)	6828(10)	7168(10)	10004(8)	52(2)
C(4)	7813(12)	6412(11)	9370(10)	63(3)
C(5)	7347(9)	4659(10)	8787(7)	48(2)
C(6)	5876(7)	3727(8)	8868(5)	34(1)
C(7)	5267(8)	1856(9)	8288(5)	33(1)
C(8)	6129(10)	891(10)	7620(6)	45(2)
C(9)	5469(10)	-851(10)	7112(6)	49(2)
C(10)	3949(10)	-1561(10)	7262(6)	45(2)
C(11)	3165(8)	-552(9)	7950(5)	38(1)
N(12)	3795(6)	1154(7)	8443(4)	32(1)
Cl(1)	392(2)	704(3)	9322(2)	56(1)
Cl(2)	1295(2)	4619(2)	7910(1)	43(1)
Cl(3)	4358(2)	994(3)	10966(1)	45(1)
O	1674(9)	5455(12)	10920(7)	73(2)
N(3)	1974(9)	4608(12)	10466(6)	49(2)

Table 3.10: Bond lengths (Å) and angles (°) for **5**.

Tc-N(3)	1.878(9)	Tc-N(1)	2.120(5)
Tc-N(12)	2.146(5)	Tc-Cl(1)	2.345(2)
Tc-Cl(2)	2.358(2)	Tc-Cl(3)	2.360(2)
N(1)-C(6)	1.348(8)	N(1)-C(2)	1.368(8)
C(2)-C(3)	1.368(11)	C(3)-C(4)	1.371(13)
C(4)-C(5)	1.395(11)	C(5)-C(6)	1.387(9)
C(6)-C(7)	1.482(8)	C(7)-N(12)	1.356(7)
C(7)-C(8)	1.391(9)	C(8)-C(9)	1.383(10)
C(9)-C(10)	1.391(10)	C(10)-C(11)	1.384(9)
C(11)-N(12)	1.348(8)	O-N(3)	0.887(9)
N(3)-Tc-N(1)	95.5(2)	N(3)-Tc-N(12)	172.0(3)
N(1)-Tc-N(12)	76.5(2)	N(3)-Tc-Cl(1)	94.8(2)
N(1)-Tc-Cl(1)	169.67(14)	N(12)-Tc-Cl(1)	93.19(14)
N(3)-Tc-Cl(2)	94.2(2)	N(1)-Tc-Cl(2)	87.40(14)
N(12)-Tc-Cl(2)	85.8(2)	Cl(1)-Tc-Cl(2)	91.72(7)
N(3)-Tc-Cl(3)	92.9(2)	N(1)-Tc-Cl(3)	87.80(14)
N(12)-Tc-Cl(3)	86.54(14)	Cl(1)-Tc-Cl(3)	91.80(7)
Cl(2)-Tc-Cl(3)	171.73(6)	C(6)-N(1)-C(2)	118.9(5)
C(6)-N(1)-Tc	116.9(4)	C(2)-N(1)-Tc	124.2(4)
C(3)-C(2)-N(1)	121.6(7)		
C(2)-C(3)-C(4)	119.4(7)		
C(3)-C(4)-C(5)	120.1(8)		
C(6)-C(5)-C(4)	118.2(8)		
N(1)-C(6)-C(5)	121.8(6)		
N(1)-C(6)-C(7)	115.5(5)		
C(5)-C(6)-C(7)	122.7(6)		
N(12)-C(7)-C(8)	122.1(6)		
N(12)-C(7)-C(6)	115.2(5)		
C(8)-C(7)-C(6)	122.7(6)		
C(9)-C(8)-C(7)	118.7(7)		
C(8)-C(9)-C(10)	119.3(7)		
C(11)-C(10)-C(9)	119.3(6)		
N(12)-C(11)-C(10)	121.8(6)		
C(11)-N(12)-C(7)	118.8(5)		
C(11)-N(12)-Tc	125.3(4)		
C(7)-N(12)-Tc	115.9(4)		
O-N(3)-Tc	177.8(9)		

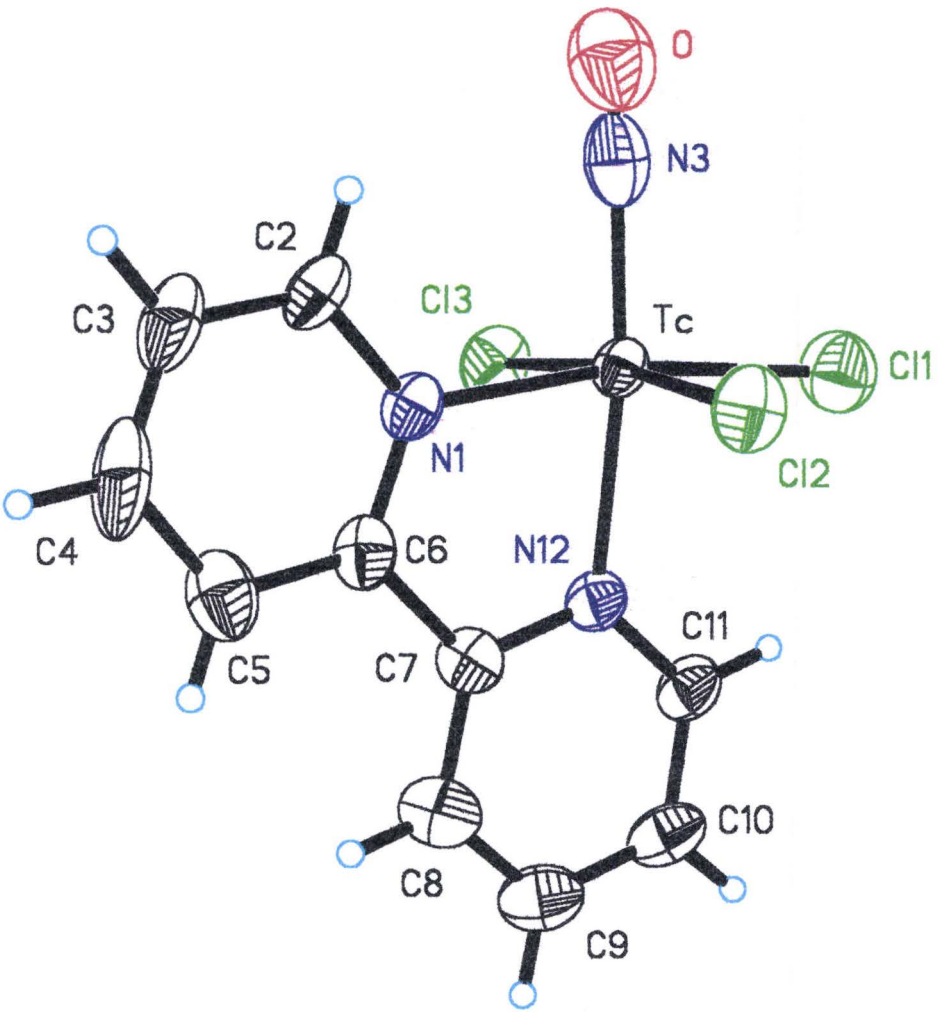

Figure 3.5: Structure of *mer*-[Tc(NO)Cl_3bipy] (**5**) drawn with 50% probability displacement ellipsoids.

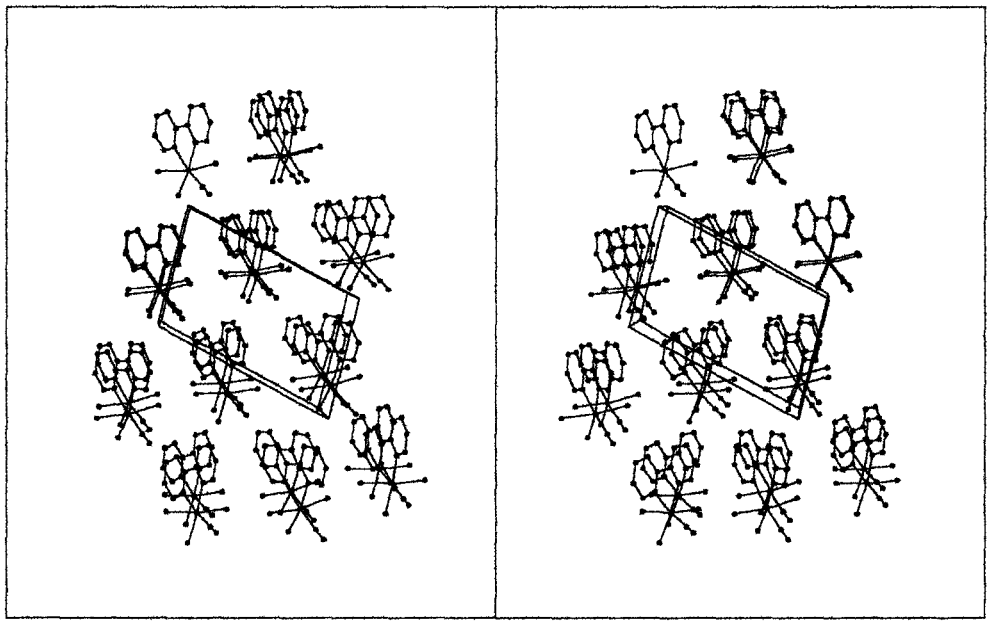

Figure 3.6: A stereoview of the packing of *mer*-[$Tc(NO)Cl_3$bipy] (**5**) within the unit cell. Hydrogen atoms have been omitted for clarity.

3.4 X-ray Crystal Structure Determination of *cis*-acetonitrilebis(2, 2'-bipyridyl)technetium(I) tetrafluoroborate: (6)

Compound **6** was prepared by the addition of $AgBF_4$ to an acetonitrile solution of $Tc(NO)Cl_3(bipy)$, followed by filtration of precipitated AgCl and addition of five equivalents of 2,2'-bipyridyl. The reaction was then refluxed and crystals formed after vapour diffusion of petroleum ether (50-110 °C) into the acetonitrile reaction mixture. (Section 3.7).

The x-ray crystallographic data, atomic positional parameters and important interatomic distances for **6** are summarized in Tables 3.11 - 3.13. A perspective view of **6** is shown in Figure 3.7 and a packing diagram is shown in Figure 3.8.

The structural characterization of **6** revealed that two bipyridyl ligands had bonded to technetium and acetonitrile had replaced the last chloride in a *cis* orientation with the nitrosyl. The two BF_4^- counterions indicated that the metal complex had an overall charge of 2+ and thus the metal was in the Tc(I) oxidation state.

The crystal used to determine the structure was small and did not diffract to high angles. This is one reason why the residuals are high. Another factor contributing to the high residuals are the disordered BF_4^- anions. This is common for a tetrahedral anion. One of the anions could be modeled fairly well with two distinct BF_4^- units refined at half occupancy while the other anion seemed to be in at least three orientations.

The nitrosyl does not exhibit disorder as seen in **4b** and **5**. The nitrosyl has a typical bond length of 1.162(13) Å and the Tc-N-O angle is 176.4(12)° indicating that it is a linearly bonded nitrosyl and is formally considered as a NO^+ ligand. Tc-NO bond is

Table 3.11: Summary of the crystal data, collection and refinement conditions for **6**.

Crystal Data		
Identification code	dg9a	
Empirical formula	$C_{22}H_{19}B_2F_8N_6OTc$	
Formula weight	655.05	
Temperature	300(2) K	
Wavelength	0.71073 A	
Crystal system	Monoclinic	
Space group	P2(1)/c	
Unit cell dimensions	a = 13.0545(4) A	α = 90 deg.
	b = 17.63960(10) A	β = 100.487(2) deg.
	c = 11.5493(4) A	γ = 90 deg.
Volume, Z	2615.10(12) A^3, 4	
Density (calculated)	1.664 Mg/m^3	
Crystal colour, habit	red, plate	
Absorption coefficient	0.636 mm^-1	
F(000)	1304	
Crystal size	.005 x .04 x .12 mm	
Data Collection		
Theta range for data collection	1.59 to 26.47 deg.	
Limiting indices	-15<=h<=16, -22<=k<=22, -14<=l<=14	
Reflections collected	21050	
Independent reflections	5067 [R(int) = 0.3067]	
Absorption correction	None	
Refinement		
Refinement method	Full-matrix least-squares on F^2	
Data / restraints / parameters	5067 / 0 / 346	
Goodness-of-fit on F^2	1.055	
Final R indices [I>2sigma(I)]	R1 = 0.1267, wR2 = 0.1859	
R indices (all data)	R1 = 0.2861, wR2 = 0.2508	
Largest diff. peak and hole	0.860 and -0.586 e.A^-3	

Table 3.12: Atomic coordinates (x 10^4) and equivalent isotropic displacement parameters (A^2 x 10^3) for **6**. U(eq) is defined as one third of the trace of the orthogonalized Uij tensor.

	x	y	z	U(eq)
Tc(1)	12428(1)	14758(1)	12838(1)	43(1)
N(1)	12200(9)	14440(7)	14194(11)	55(4)
O	11993(9)	14240(7)	15081(10)	84(4)
N(21)	12036(9)	13723(7)	12030(11)	53(4)
C(22)	11872(12)	13145(11)	11635(15)	72(5)
C(23)	11705(25)	12382(13)	11112(22)	119(10)
N(31)	12488(8)	15205(7)	11116(9)	43(3)
C(32)	13285(12)	15139(9)	10539(12)	57(4)
C(33)	13309(14)	15469(9)	9481(13)	66(5)
C(34)	12479(15)	15889(9)	8963(14)	69(5)
C(312)	11646(12)	15612(8)	10628(12)	43(4)
C(35)	11635(12)	15972(8)	9527(12)	50(4)
C(311)	10780(12)	15616(8)	11241(14)	51(4)
C(36)	9861(14)	16008(10)	10886(16)	79(6)
C(37)	9061(15)	15951(11)	11486(18)	87(6)
C(38)	9183(14)	15517(10)	12495(18)	77(6)
C(39)	10123(13)	15136(10)	12864(14)	65(5)
N(310)	10910(8)	15200(7)	12246(10)	46(3)
N(41)	14076(9)	14558(6)	13145(9)	40(3)
C(42)	14495(14)	13855(10)	13088(13)	64(5)
C(43)	15578(15)	13799(11)	13264(13)	66(5)
C(44)	16206(14)	14448(14)	13503(14)	75(6)
C(45)	15721(13)	15118(11)	13551(13)	62(5)
C(46)	14575(13)	16597(10)	13806(13)	63(5)
C(47)	13979(18)	17195(11)	14019(15)	81(6)
C(48)	12931(19)	17117(10)	13979(15)	81(6)
C(49)	12480(13)	16418(9)	13677(13)	59(5)
N(410)	13031(9)	15819(7)	13456(10)	45(3)
C(411)	14077(15)	15908(10)	13541(13)	58(5)
C(412)	14663(11)	15197(11)	13402(11)	52(4)
B(1)	8806(85)	13274(63)	13712(96)	139(22)
F(11)	9900(24)	13277(18)	13465(31)	136(3)
F(12)	8684(23)	13955(19)	14074(27)	136(3)
F(13)	9305(27)	12870(23)	15050(32)	136(3)
F(14)	7995(25)	13225(19)	13597(28)	136(3)
B(1A)	9419(81)	13173(67)	14073(100)	139(22)
F(11A)	9492(28)	13125(19)	12957(27)	136(3)
F(12A)	9249(23)	13885(19)	14575(26)	136(3)
F(13A)	9231(27)	12620(21)	14642(35)	136(3)
F(14A)	8206(26)	12826(19)	13332(28)	136(3)
B(2)	6101(59)	16562(39)	11043(69)	102(14)
F(21)	6670(24)	16078(16)	11716(28)	136(3)

F(22)	5167(22)	16960(19)	11329(26)	136(3)
F(23)	6691(23)	17358(18)	10948(26)	136(3)
F(24)	5772(24)	16453(17)	9913(27)	136(3)
B(2A)	6269(61)	16836(44)	11188(70)	102(14)
F(21A)	6731(25)	16414(18)	12015(30)	136(3)
F(22A)	5319(23)	16167(17)	10721(27)	136(3)
F(23A)	5742(26)	17239(18)	11630(27)	136(3)
F(24A)	6567(23)	16787(18)	10180(28)	136(3)

Table 3.13: Bond lengths (Å) and angles (°) for **6**.

Tc(1)-N(1)	1.739(13)	Tc(1)-N(21)	2.072(13)
Tc(1)-N(410)	2.103(12)	Tc(1)-N(310)	2.124(11)
Tc(1)-N(41)	2.145(12)	Tc(1)-N(31)	2.155(10)
N(1)-O	1.162(13)	N(21)-C(22)	1.12(2)
C(22)-C(23)	1.48(3)	N(31)-C(32)	1.34(2)
N(31)-C(312)	1.35(2)	C(32)-C(33)	1.36(2)
C(33)-C(34)	1.36(2)	C(34)-C(35)	1.39(2)
C(312)-C(35)	1.42(2)	C(312)-C(311)	1.44(2)
C(311)-N(310)	1.36(2)	C(311)-C(36)	1.38(2)
C(36)-C(37)	1.36(2)	C(37)-C(38)	1.38(2)
C(38)-C(39)	1.40(2)	C(39)-N(310)	1.36(2)
N(41)-C(42)	1.36(2)	N(41)-C(412)	1.37(2)
C(42)-C(43)	1.40(2)	C(43)-C(44)	1.41(2)
C(44)-C(45)	1.35(2)	C(45)-C(412)	1.37(2)
C(46)-C(47)	1.36(2)	C(46)-C(411)	1.38(2)
C(47)-C(48)	1.37(2)	C(48)-C(49)	1.38(2)
C(49)-N(410)	1.33(2)	N(410)-C(411)	1.36(2)
C(411)-C(412)	1.49(2)	B(1)-F(11)	1.51(12)
B(1)-F(14)	1.05(11)	B(1)-F(13)	1.72(10)
B(1)-F(12)	1.29(11)	B(1A)-F(11A)	1.31(12)
B(1A)-F(13A)	1.23(10)	B(1A)-F(12A)	1.42(12)
B(1A)-F(14A)	1.77(11)	F(11A)-F(12A)	2.37(5)
B(2)-F(21)	1.29(7)	B(2)-F(23)	1.61(8)
B(2)-F(22)	1.50(8)	B(2)-F(24)	1.31(7)
B(2A)-F(23A)	1.17(7)	B(2A)-F(21A)	1.27(8)
B(2A)-F(24A)	1.30(8)	B(2A)-F(22A)	1.73(8)
N(1)-Tc(1)-N(21)	93.0(5)	N(1)-Tc(1)-N(410)	95.5(5)
N(21)-Tc(1)-N(410)	169.5(5)	N(1)-Tc(1)-N(310)	96.1(5)
N(21)-Tc(1)-N(310)	92.2(5)	N(410)-Tc(1)-N(310)	93.0(5)
N(1)-Tc(1)-N(41)	97.5(5)	N(21)-Tc(1)-N(41)	95.0(5)
N(410)-Tc(1)-N(41)	77.8(5)	N(310)-Tc(1)-N(41)	164.3(4)
N(1)-Tc(1)-N(31)	171.9(5)	N(21)-Tc(1)-N(31)	87.4(5)
N(410)-Tc(1)-N(31)	85.0(4)	N(310)-Tc(1)-N(31)	75.9(4)
N(41)-Tc(1)-N(31)	90.5(4)	O-N(1)-Tc(1)	176.4(12)
C(22)-N(21)-Tc(1)	176.0(13)	N(21)-C(22)-C(23)	178(2)
C(32)-N(31)-C(312)	119.2(12)	C(32)-N(31)-Tc(1)	126.1(10)
C(312)-N(31)-Tc(1)	114.7(9)	N(31)-C(32)-C(33)	124(2)
C(32)-C(33)-C(34)	119(2)	C(35)-C(34)-C(33)	119(2)

N(31)-C(312)-C(35)	119.2(1)	N(31)-C(312)-C(311)	116.8(13)
C(35)-C(312)-C(311)	124(2)	C(34)-C(35)-C(312)	120(2)
N(310)-C(311)-C(36)	120(2)	N(310)-C(311)-C(312)	115.6(13)
C(36)-C(311)-C(312)	125(2)	C(37)-C(36)-C(311)	121(2)
C(36)-C(37)-C(38)	119(2)	C(37)-C(38)-C(39)	119(2)
N(310)-C(39)-C(38)	120(2)	C(39)-N(310)-C(311)	120.4(14)
C(39)-N(310)-Tc(1)	123.4(11)	C(311)-N(310)-Tc(1)	116.0(10)
C(42)-N(41)-C(412)	123(2)	C(42)-N(41)-Tc(1)	122.7(11)
C(412)-N(41)-Tc(1)	114.0(10)	N(41)-C(42)-C(43)	118(2)
C(42)-C(43)-C(44)	121(2)	C(45)-C(44)-C(43)	117(2)
C(44)-C(45)-C(412)	124(2)	C(47)-C(46)-C(411)	117(2)
C(46)-C(47)-C(48)	121(2)	C(47)-C(48)-C(49)	118(2)
N(410)-C(49)-C(48)	123(2)	C(49)-N(410)-C(411)	117.7(14)
C(49)-N(410)-Tc(1)	126.2(11)	C(411)-N(410)-Tc(1)	115.9(11)
N(410)-C(411)-C(46)	123(2)	N(410)-C(411)-C(412)	115(2)
C(46)-C(411)-C(412)	122(2)	C(45)-C(412)-N(41)	117(2)
C(45)-C(412)-C(411)	127(2)	N(41)-C(412)-C(411)	116.1(13)
F(11)-B(1)-F(14)	162(10)	F(11)-B(1)-F(13)	87(5)
F(14)-B(1)-F(13)	107(8)	F(11)-B(1)-F(12)	104(8)
F(14)-B(1)-F(12)	86(9)	F(13)-B(1)-F(12)	98(7)
F(11A)-B(1A)-F(13A)	122(10)	F(11A)-B(1A)-F(12A)	120(8)
F(13A)-B(1A)-F(12A)	115(10)	F(11A)-B(1A)-F(14A)	74(5)
F(13A)-B(1A)-F(14A)	75(6)	F(12A)-B(1A)-F(14A)	108(6)
B(1A)-F(11A)-F(12A)	31(5)	B(1A)-F(12A)-F(11A)	29(4)
F(21)-B(2)-F(23)	113(5)	F(21)-B(2)-F(22)	125(6)
F(23)-B(2)-F(22)	91(4)	F(21)-B(2)-F(24)	123(6)
F(23)-B(2)-F(24)	98(5)	F(22)-B(2)-F(24)	99(5)
F(23A)-B(2A)-F(21A)	105(7)	F(23A)-B(2A)-F(24A)	137(8)
F(21A)-B(2A)-F(24A)	117(7)	F(23A)-B(2A)-F(22A)	96(5)
F(21A)-B(2A)-F(22A)	93(5)	F(24A)-B(2A)-F(22A)	89(5)

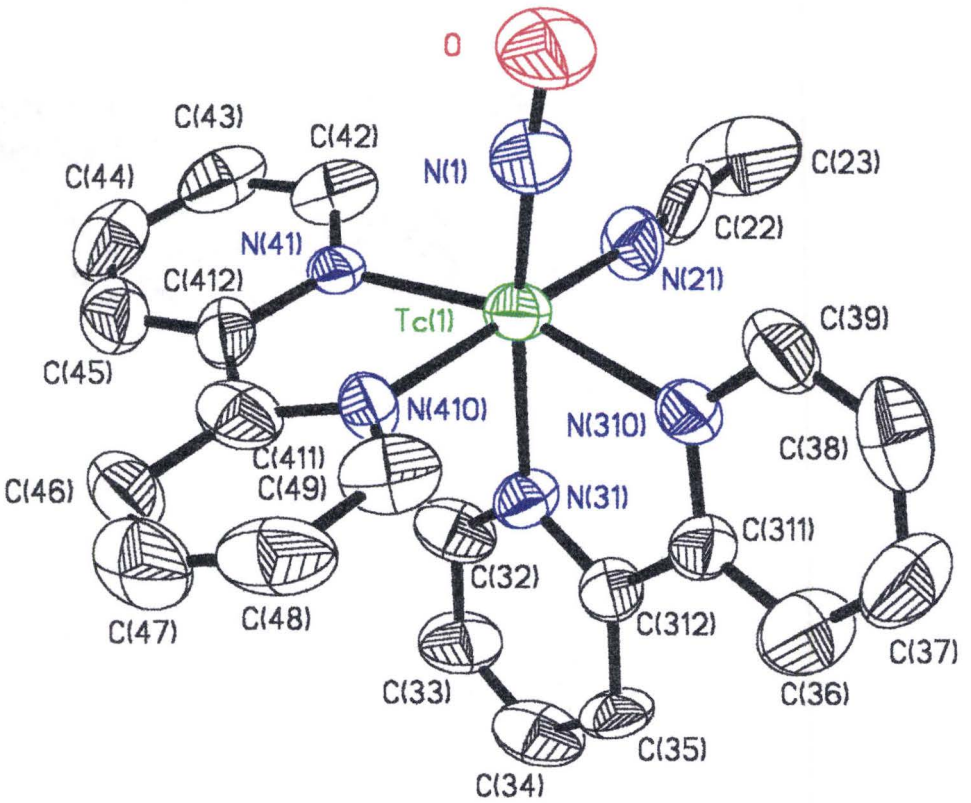

Figure 3.7: Structure of *cis*-$[Tc(NO)(bipy)_2(MeCN)]^{2+}$ cation (**6**) drawn with 50% probability displacement ellipsoids. Hydrogen atoms have been omitted for clarity.

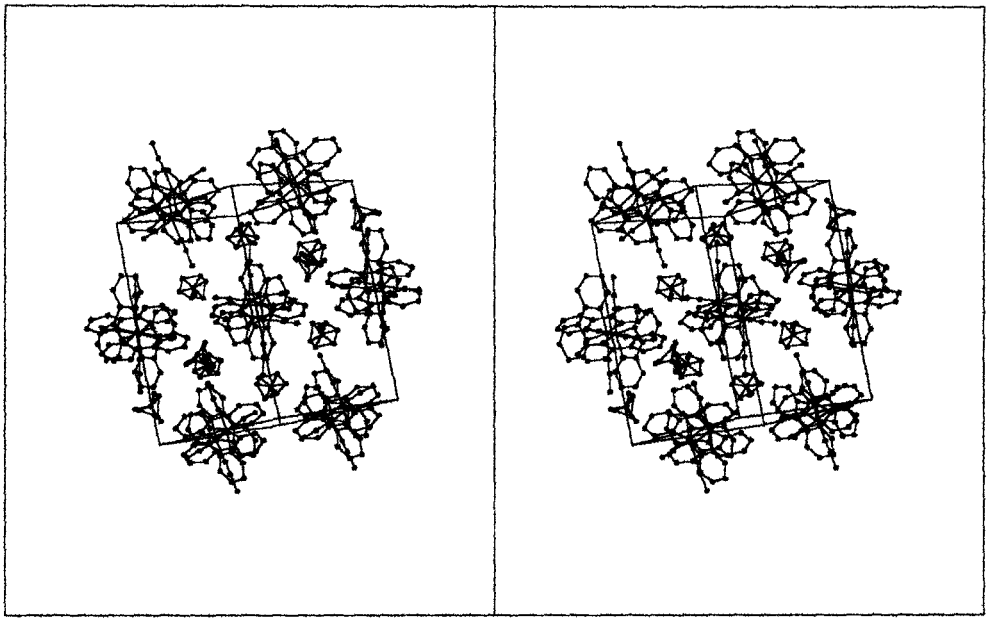

Figure 3.8: A stereoview of the packing of *cis*-$[Tc(NO)(bipy)_2(MeCN)][BF_4]_2$ (**6**) within the unit cell. Hydrogen atoms have been omitted for clarity.

relatively short at 1.739(13) Å in length. The competition for the dπ orbitals from the nitrosyl and phenanthroline are present here as well. This can be compared to $[Tc^{(I)}(NO)(NH_3)_4(H_2O)]^{2+}$ where there is no competition for backdonation of electron density from the ammine ligands and the average $Tc\text{-}_{NH3}$ distance is 1.716 Å. The average $Tc\text{-}N_{bipy}$ bond length is 2.132 Å. The nitrogen atom *trans* to the acetonitrile ligand has the shortest Tc-N bond length of 2.103(12) Å while that which is *trans* to the nitrosyl appears to be slightly elongated with a Tc-N bond length of 2.155(10) Å.

All these values compare well to the structure of $[Tc^{(I)}(NO)(phen)_2(NH_3)]^{2+}$ except that the Tc-N-O angle for **6** is closer to linearity at 176.4(12)° compared to 171.9(8)°. The average $Tc\text{-}N_{phen}$ bond length of 2.124 Å is also similar to the $Tc\text{-}N_{bipy}$ in **6**.

3.5 Discussion of Synthesis and Crystal Structures

With an extra electron belonging to the technetium in the Tc(I) complex of $[Tc^{(I)}(NO)(bipy)_2(MeCN)]^{2+}$, (**6**), there is more electron density that is available for backbonding to the ligands compared to similar Tc(II) complexes. This is most evident in the $[Tc^{(I)}\text{-}NO]^{2+}$ bond distance of 1.739(13) Å for **6** compared to the Tc(II) complex $[Tc^{(II)}(NO)(phen)Cl_3]$, (**4a**), where the $[Tc^{(II)}\text{-}NO]^{3+}$ bond distance is approximately 0.05 Å longer at 1.797(6) Å. As a result of less backdonation, the NO bond is stronger and shorter for the Tc(II) complexes as well. It appears that the nitrosyl bond length can be somewhat correlated to the infrared stretching frequencies to determine the oxidation state as seen in Table 3.1. For complexes with nitrogen and phosphorus donors the $[Tc^{(II)}\text{-}NO]^{3+}$ core has a nitrosyl stretching frequency that ranges from 1770-1815 cm^{-1} whereas for the $[Tc^{(I)}\text{-}NO]^{2+}$ complexes this range is from 1690-1744 cm^{-1}.

One of the benefits of having the acetonitrile ligated in **6** is that this is easily displaced by other ligands and therefore can be used as a precursor to other compounds. This is unlike $[Tc^{(I)}(NO)(phen)_2(NH_3)]^{2+}$ where the ammine ligand cannot be easily displaced. Similarly, the chlorides of **4a** and **5** can be displaced to form other compounds as was shown for the synthesis of **6**.

There has been difficulty in synthesizing $[Tc^{(I)}(NO)(phen)_2Cl]^+$ and $[Tc^{(I)}(NO)(bipy)_2Cl]^+$ to this point. In methanol, the reaction turns purple-brown in colour and the dark green compound, **4a** or **5** can be formed from phenanthroline and bipyridyl, respectively. When these precipitates are filtered the filtrates are purple in colour and often a small amount of red crystals form from these solutions. A unit cell for a hexagonally shaped red crystal of the phenanthroline complex was determined but the crystal was too small to determine the structure (Section 3.7). The purple compound has not crystallized as of yet, after trials with a number of solvent conditions and counterions. For the phenanthroline complexes, a bright yellow compound is precipitated from solution when the reaction is too concentrated. This has been recrystallized to form x-ray quality crystals which are awaiting structure determination. Compound **4a** is also formed as is the purple compound when the recrystallization of the yellow compound takes place. Perhaps these compounds are ones that contain two phenanthrolines or bipyridyls ligated to the metal. Compounds **4a** and **6** form red coloured solutions in acetonitrile with heat (72 h.) or after time (1 week.). X-ray quality red crystals have formed from the solution in the NMR tube and these are also awaiting structure determination.

The solvent dependency of these reactions is interesting. In acetonitrile, only one phenanthroline or bipyridyl ligand can complex the metal, whereas is methanol,

it appears that at least one ligand can, and two ligands might be able to complex the metal (possibly the purple or yellow compound). In dichloromethane, a small amount of a red/purple coloured material precipitates after stirring overnight, but after filtration the filtrate produces only **4a** or **5**.

In a related example, it was found that in acetonitrile only $[Tc^{(VI)}NCl_3bipy]$ forms from $[Tc^{(VI)}NCl_4]^-$ whereas in methanol two bipyridyl ligands complex the metal in $[Tc^{(V)}(N)(bipy)_2Cl]^+$.[57]

Given the different *trans*-influences observed for **4a**, **5**, and **6**, it is difficult to assess the *trans*-influence for all technetium nitrosyl compounds with certainty. For examples with $[Tc^{(I)}\text{-}NO]^{2+}$ cores, it appears that the bond *trans* to the nitrosyl are lengthened by 0.05-0.1 Å. With the $[Tc^{(II)}\text{-}NO]^{3+}$ core, there are insufficient data to comment at this point.

3.6 EPR of Tc(II) Nitrosyl Complexes

Technetium possesses six oxidation states which are or may potentially be paramagnetic (Tc^0, Tc^{II}, Tc^{III}, Tc^{IV}, Tc^V, Tc^{VI}).[58] Only the Tc^0, Tc^{II} (d^5-low spin), and Tc^{VI} oxidation states have an electronic configuration with only one unpaired electron (S = 1/2) which allows for the detection of well resolved EPR spectra at convenient temperatures. Very low temperatures (~0-10 °K) are required to observe EPR signals for the Tc^{III}, Tc^{IV}, and Tc^V oxidation states because of the short spin lattice relaxation times of these multiple spin systems. As of yet, there have been no reported EPR spectra for the Tc^0 oxidation state thus leaving complexes involving the Tc^{II} (d^5-low spin) and Tc^{VI} oxidation states as the most studied systems.

EPR can not be used to obtain a complete structural characterization of an unknown complex. However, it can provide useful information about a compound such as the determination of the oxidation state and often insight to the composition of the coordination sphere can be given for paramagnetic metal complexes.

Ambient temperature EPR spectra for technetium complexes typically consist of a well resolved 10-line pattern that is due to the interaction of the unpaired electron with the nuclear spin of the ^{99}Tc nucleus ($I = 9/2$). Frozen solution EPR spectra results in ^{99}Tc multiplets being observed for each of the parallel and perpendicular parts of the spectrum. Ligand hyperfine interactions (superhyperfine coupling) have been observed for one technetium nitrosyl complex, $[Tc^{II}(NO)Cl_3(Me_2PhP)_2]$.[29] The frozen solution spectrum contained well resolved triplets (at the outer extremes of the spectrum) due to the superhyperfine coupling of the two ^{31}P nuclei ($I = 1/2$) while the room-temperature spectrum displayed very poorly resolved triplets.

EPR spectra were obtained for compounds **3**, **4a**, and **5** in dichloromethane solvent and are shown in Figures 3.9 - 3.11 with the corresponding <g> and <a> values. The EPR spectra confirmed that these complexes were all paramagnetic, owing to the d^5 low-spin electronic configuration for the $Tc^{(II)}$ oxidation state. No superhyperfine interactions are observed between the unpaired electron and the nitrogen atoms of the nitrosyl or phenanthroline ligands, or for the chlorine ligands. The literature EPR values for $[Tc^{(II)}(NO)Cl_4]^-$ in acetone are reported as <g> = 2.12 and <a> = 157.6 G.[59] These values are similar to those obtained in the present work (<g> = 2.115 and <a> = 161.8 G) and the small difference may be related to the change of solvent from acetone to dichloromethane.

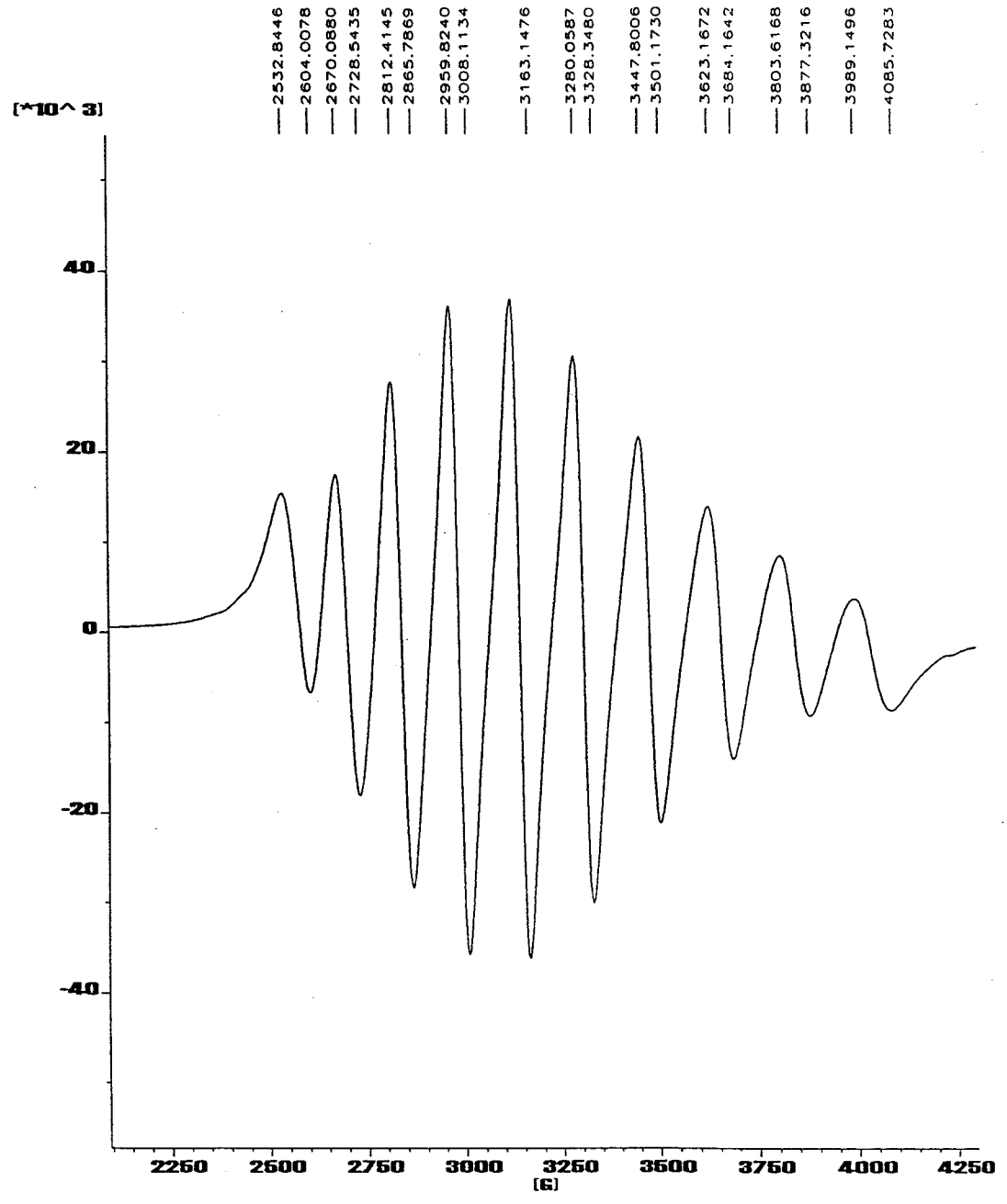

Figure 3.9: Room temperature EPR spectrum of **3** in dichloromethane with <g> = 2.115 and <a> = 161.8 G.

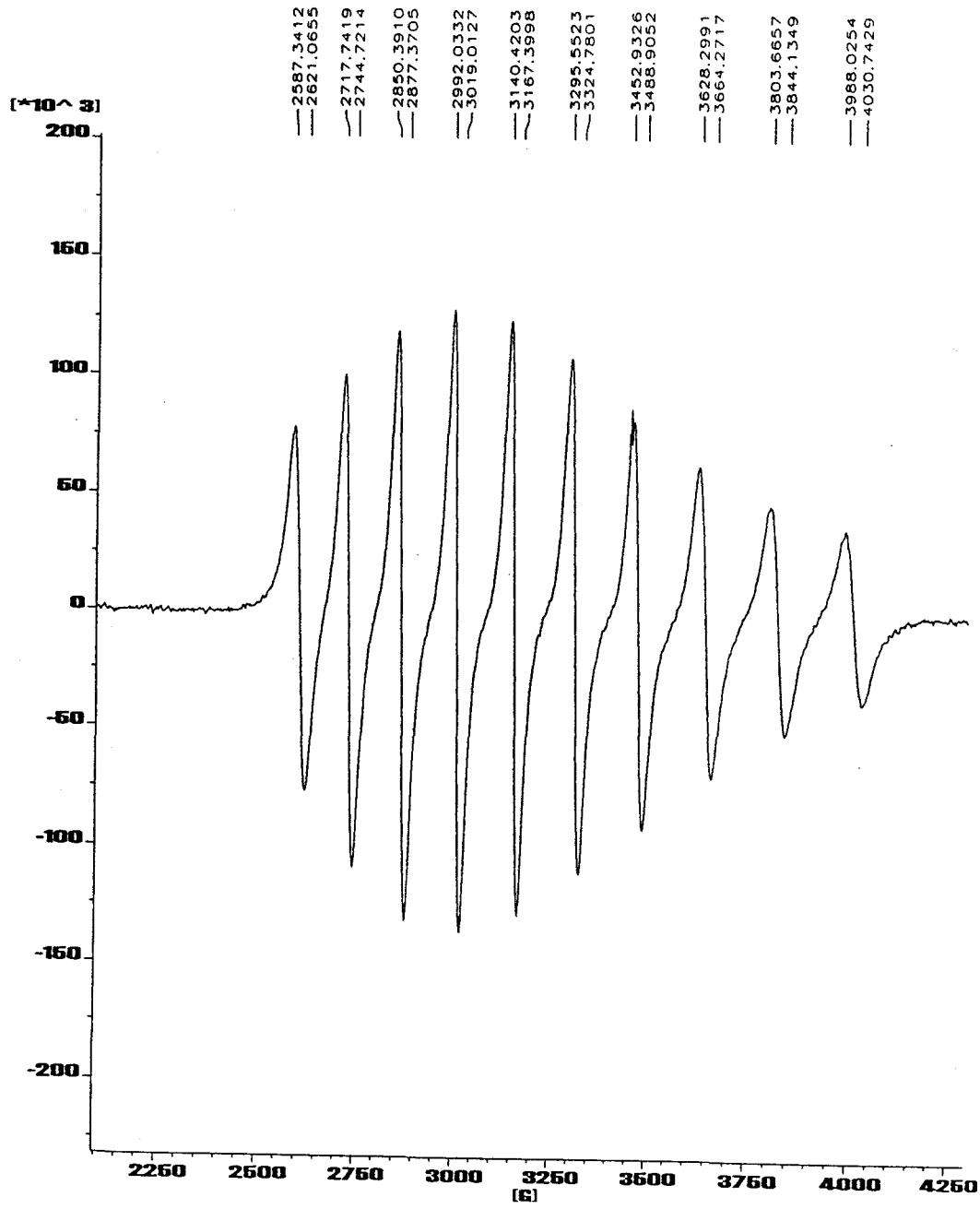

Figure 3.10: Room temperature EPR spectrum of **4a** (or **4b**) in dichloromethane with <g> = 2.106 and <a> = 155.6 G.

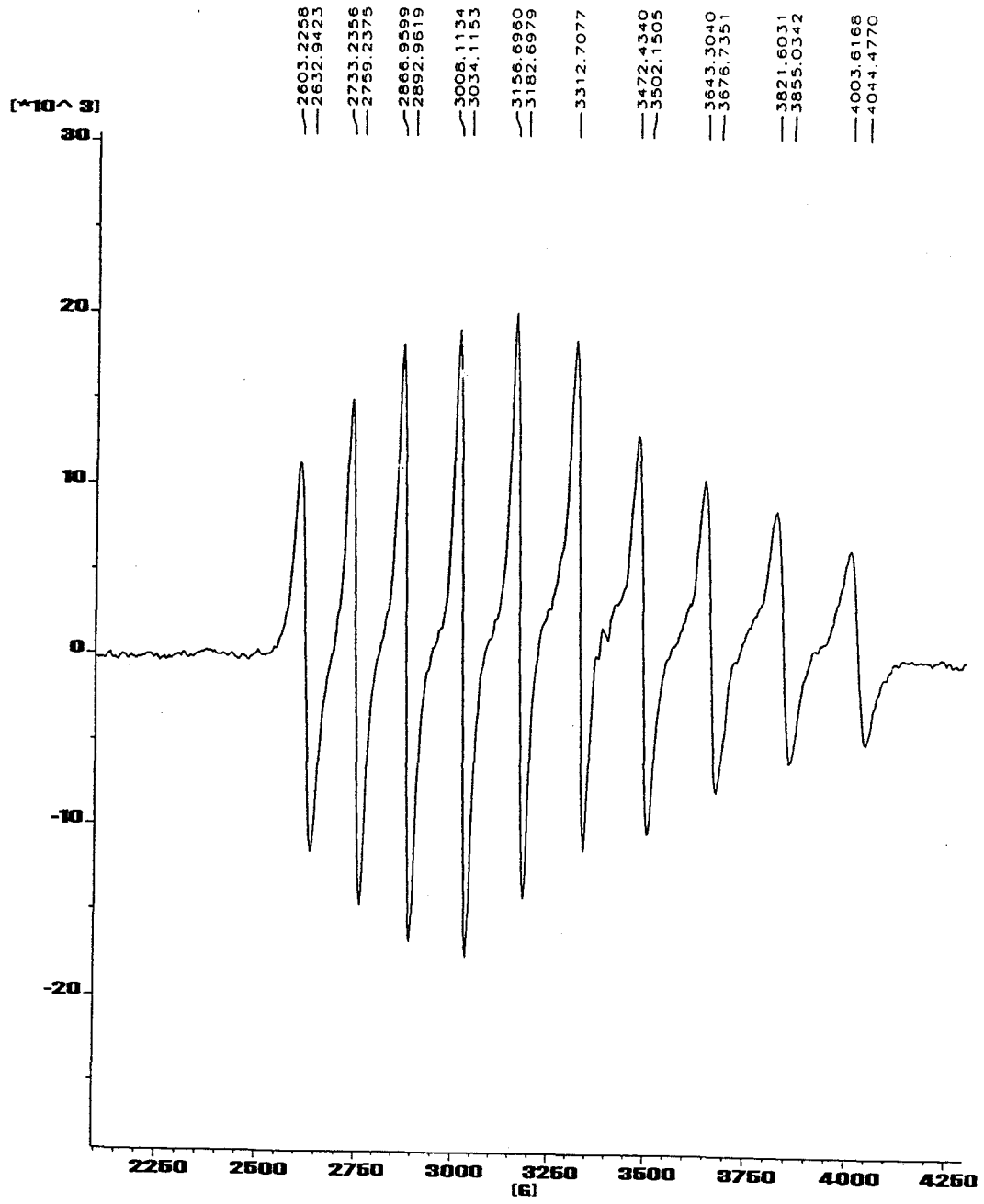

Figure 3.11: Room temperature EPR spectrum of **5** in dichloromethane with <g> = 2.104 and <a> = 155.6 G.

ligands have on either the hyperfine coupling constants (hfcc) or the g-values. Since $[Tc^{(II)}(NO)Cl_4]^-$ is five-coordinate and axially symmetric, it may not be appropriate to compare it to the six-coordinate axially unsymmetric complexes of *mer*-$[Tc^{(II)}(NO)Cl_3phen]$ (**4a**) and *mer*-$[Tc^{(II)}(NO)Cl_3bipy]$ (**5**). A more suitable comparison would be to the analogous *mer*-$[Tc^{(II)}(NO)Cl_3acac]^-$ anion. The room-temperature EPR spectrum of this complex in ethanol displays the characteristic 10-line pattern with <g> = 2.12 and <a> = 135 G.[60] The g-values and hfcc's for the phenanthroline complex (**4a**) are <g> = 2.016 and <a> = 155.6 G and those for the bipyridyl complex (**5**) are <g> = 2.104 and <a> = 155.6 G, which are almost identical. The g-values for **3**, **4a**, **5**, and *mer*-$[Tc^{(II)}(NO)Cl_3acac]^-$ are all fairly similar. The hfcc's for **4a** and **5** are much larger than those for *mer*-$[Tc^{(II)}(NO)Cl_3acac]^-$. Possibly the presence of π-acid ligands results in larger hfcc values in these complexes. The phosphine complexes $[Tc^{(II)}(NO)Cl_3(Me_2PhP)_2]$ and $[Tc^{(II)}(NO)Cl_3(Ph_3P)_2]$ have room-temperature EPR values reported as <g> = 2.052 and <a> = 125.6 G for the former complex[29] and <g> = ~2.0 and <a> = ~130 G for the latter complex.[61] While the g-values are only slightly less for the phosphorous complexes, the hfcc's are much smaller compared to the phenanthroline and bipyridyl complexes, which again, may be related to the latter complexes being better π-acid ligands. As discussed above, triplets are observed in the frozen solution spectrum of $[Tc^{(II)}(NO)Cl_3(Me_2PhP)_2]$ and these suggest mutually *trans* phosphine ligands. This does not have the same connectivity to the technetium atom as in **4a**, **5**, or *mer*-$[Tc^{(II)}(NO)Cl_3acac]^-$ where one atom of the bidentate ligand is *trans* to the nitrosyl. However, it is not known how this difference in connectivity affects the hfcc's.

Frozen solution EPR spectra were obtained for compounds **3** and **4a**. Their spectra are shown in Figures 3.12 - 3.13. No superhyperfine interactions are observed between the unpaired electron and the nitrogen atoms of the nitrosyl or phenanthroline ligands, or for the chlorine ligands. In the frozen solution spectra, anisotropic values are obtained for the parallel and perpendicular parts of the spectrum, however, they become complex and simulations are required to fully interpret the spectrum which are currently under investigation.

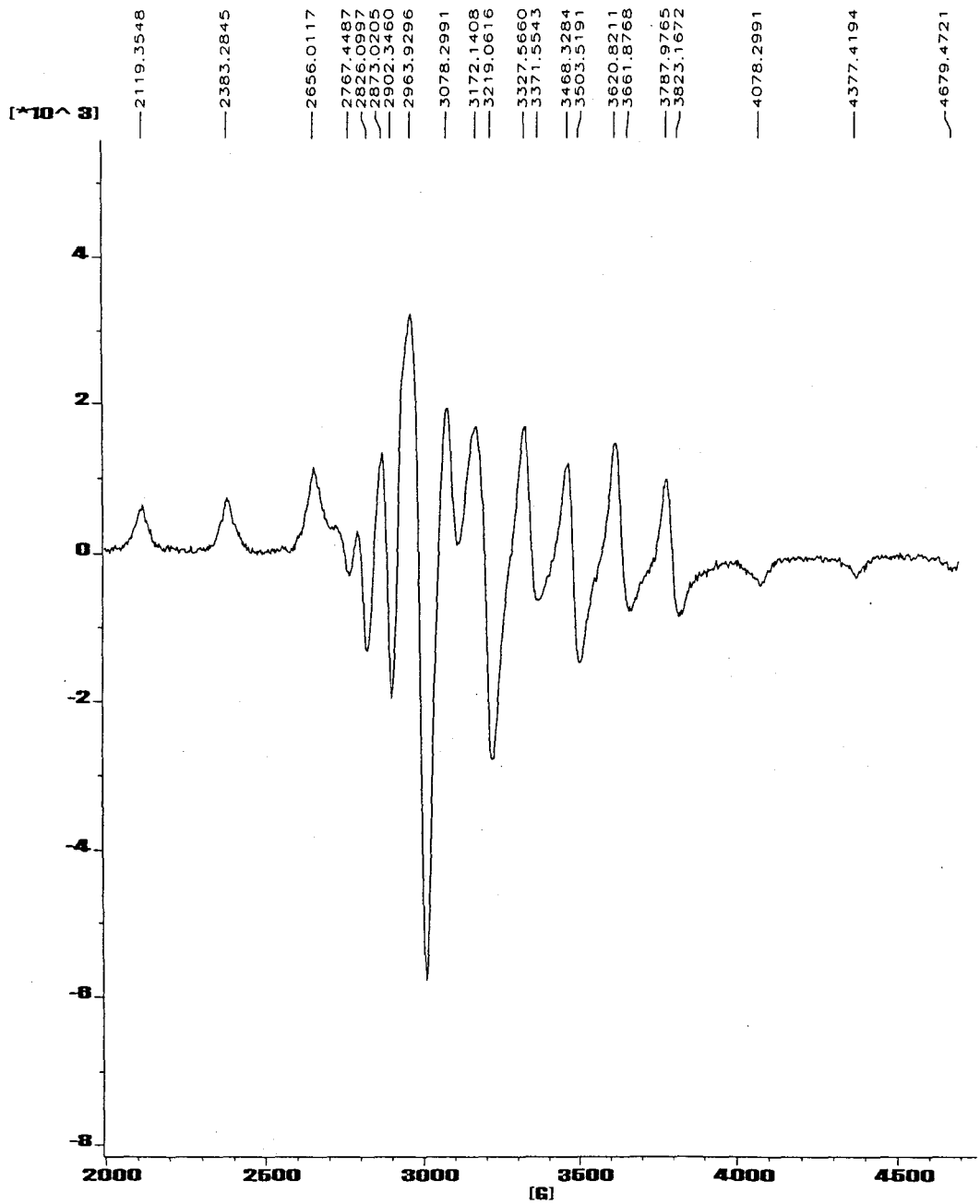

Figure 3.12: Frozen solution (150 °K) EPR spectrum of **3** in dichloromethane.

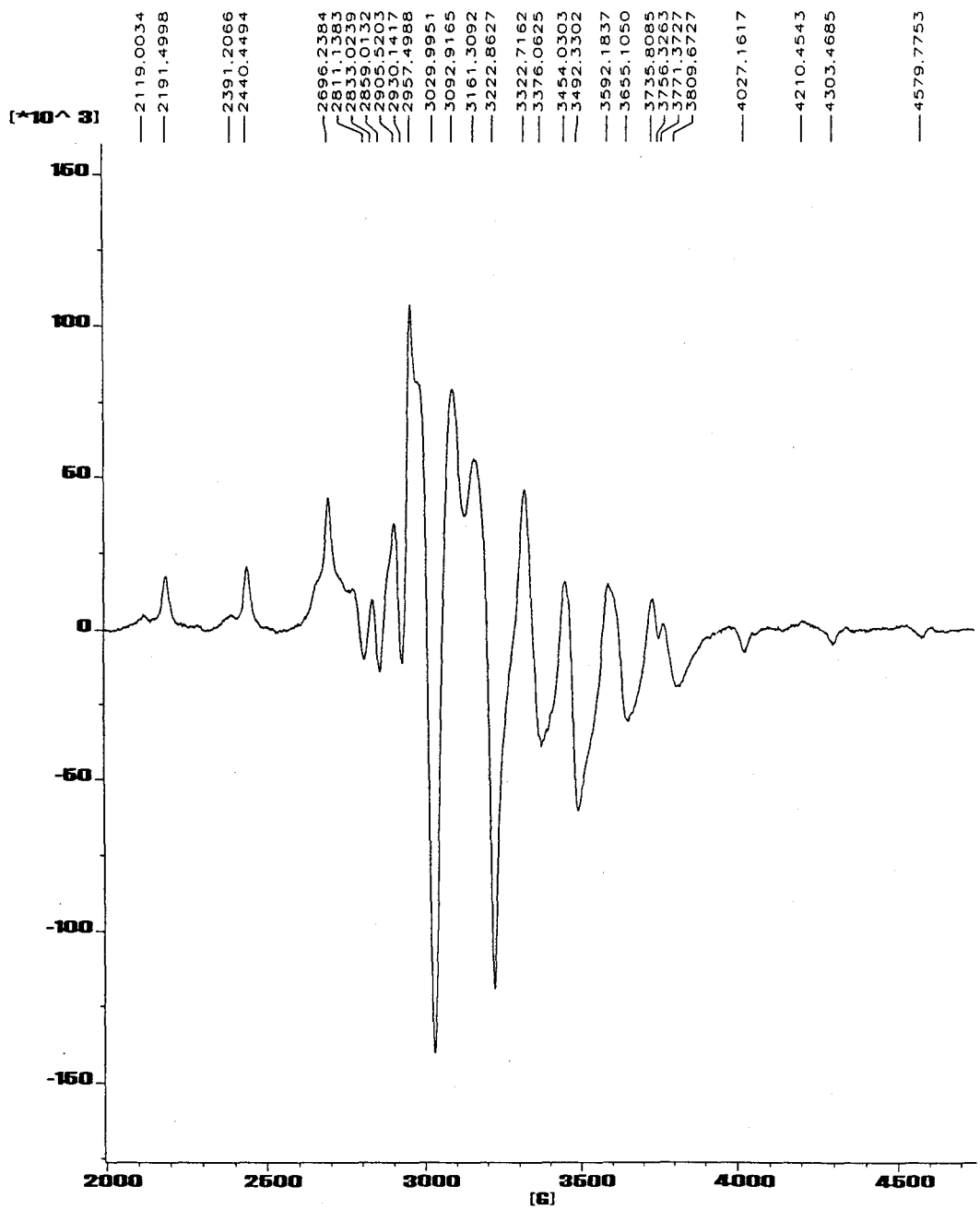

Figure 3.13: Frozen solution (150 °K) EPR spectrum of **4a** (or **4b**) in dichloromethane.

3.7 Experimental Section

Preparation of tetrabutylammonium tetrachloronitrosyltechnetate(II): 3

Two methods were used to prepare [TBA][Tc(NO)Cl_4]. The first method was a modification of the procedure developed by Hildreth.[32] Typically, 163 mg (0.900 mmol) of ammonium pertechnetate was dissolved in 20 mL water in an open 100 mL beaker equipped with a magnetic stir bar. To this solution was added 30 mL conc. HCl and the reaction mixture immediately changed from colourless to yellow. The beaker was heated on the hot plate at ~ 90°C for 30 minutes and the solution was a yellow colour tinged with green. This solution was diluted with 20 mL water and 3.13 g (45 mmol, 50 equiv.) of solid hydroxylamine hydrochloride was added. The solution was heated at 90 °C and it began to change to a green colour after a few minutes. Heating was continued for 30 min. and the grass-green solution was cooled to room temperature. A 75% solution (3g, 108 mmol, in 4mL of water) of [TBA][Cl] hydrate was added and the [TBA][Tc(NO)Cl_4] was extracted into dichloromethane (DCM) (5 x 20 mL). The water layer remained a light green colour. The organic layers were combined and the solvent removed by evaporation under reduced pressure (Buchi rotovapor) at room temperature. The nitrosyl technetate was recrystallized from a minimum amount of methanol and diethyl ether giving 223.6 mg (82% yield) of grass-green coloured crystals. In general, **3** was either recrystallized or left as a semi-crystalline material in a viscous solution of methanol that was dried before use. Complete drying of compound **3** produced a yellowish coloured material.

The second method was a modification of the procedure developed by Cheah *et al.*[41] Typically, 49.8 mg (0.100 mmol) of [TBA][$TcOCl_4$] was added to a 10 mL two-necked round bottom flask with stir bar and the vessel was sealed with septa and purged

with nitrogen. Dry methanol (5 mL) was added via syringe and a green solution formed. Before use in a reaction, hydroxylamine hydrochloride was ground, spread on a petri dish, and left in a vacuum desiccator with phosphorous pentoxide as a desiccant, or heated with a blow dryer under vacuum for approximately 6 hours. The dried $NH_2OH{\cdot}HCl$ was quickly added to the flask as the solid (1.1 equivalents, 7.7 mg) in the outgoing nitrogen flow neck. The reaction mixture changed to a brown colour shortly after addition and was stirred at room temperature overnight (approximately 12 hours), when the solution became a grass-green colour. Yields are reported to be quantitative[101] and were taken as such. The methanol solution was typically used in further reactions directly, or was recrystallized after reducing the methanol volume with nitrogen.

Compound **3** showed:

IR (KBr pellet; cm^{-1}): ν_{NO} = 1793, $\nu_{Tc\text{-}Cl}$ = 306; literature value[15]: ν_{NO} = 1805, $\nu_{Tc\text{-}Cl}$ = 326

ESMS (negative ion): 269, 271, 273, 275 (4 Cl pattern); $[TcCl_4]^-$ 239, 241, 243, 245 (4Cl pattern); $[Tc(NO)Cl_3]^-$ 234, 236, 238 (3 Cl pattern); $[Tc(NO)Cl_2]^-$ 199, 201 (2 Cl pattern)

Preparation of *mer*-trichloronitrosyl-1,10-phenanthrolinetechnetium(II): 4a

The method used was a modification of the procedure developed by Hildreth.[32] To a 15 mL ground glass Erlenmeyer flask with magnetic stir bar was added 110.2 mg (0.215 mmol) of **3** and 2 mL of methanol. A reflux condenser with a septum sealing the top was added and the system purged with nitrogen for 15 minutes while stirring. Five equivalents (1.073 mmol, 212.7 mg) of phenanthroline monohydrate in 4mL methanol were then added, and the initial green coloured solution changed to a brownish colour upon addition. A small amount of yellow precipitate formed and was removed by

filtration through a pipette containing glass wool. The solution was heated at reflux for 10 hours in a 80° C oil bath after which the solution became a dark brown/purple colour. A few drops of the reaction mixture were dried and ground into a KBr pellet. Infrared showed only one strong nitrosyl stretching frequency at 1801 cm^{-1}. The solution was cooled and petroleum ether (50-110°C) then vapour diffused into the methanol solution at room temperature. Poor quality, dark brown-purple crystals and an amorphous precipitate were obtained from the brown-purple mother liquor after standing undisturbed for a few days. The crystals were collected by filtration on a fine porosity frit, washed with 2 mL cold methanol and dried *in vacuo* to give 32 mg (36% yield) of **4a**. Much cleaning and cutting of these crystals was required to obtain a single crystal suitable for x-ray diffraction.

Compound **4a** showed:

IR (KBr pellet; cm^{-1}): ν_{NO} =1801 (vs); $\nu_{Tc\text{-}Cl}$=339 (w); 1630 (vw, br); 1516 (w); 1429 (w); 850 (m); 719 (m)

ESMS (negative ion): 414, 416, 418 (3 Cl pattern) $[Tc(NO)Cl_3(phen)]^-$; 234, 236, 238 (3 Cl pattern) $[Tc(NO)Cl_3]^-$

The filtrate of **4a** was a purple colour and frequently small amounts of red precipitate formed when this was cooled. When left to evaporate small amounts of dark purple amorphous precipitate and bright red hexagonal crystals formed. These crystals were found to have a hexagonal unit cell a = 13.1744, b = 13.1744, c = 21.1093; α = 90.000, β = 90.000, γ = 120.000, but were too small to be able to determine the structure. The dark purple solid had a very strong infra-red stretching frequency of 1789 cm^{-1} and

was very soluble in methanol, water, and acetonitrile and insoluble in acetone. The purple compound could not be recrystallized despite many solvent systems and anions added.

It was later found that better x-ray quality single crystals of **4a** could be grown by evaporating the methanol solvent with a stream of nitrogen, redissolving the residue into acetonitrile, filtering through a pipette filled with glass wool and vapour diffusing petroleum ether (50-110 °C) into the solution at room temperature. These crystals were a dark green-black colour and changed from green to brown colour in polarized light. TLC (cellulose) of the reaction with a 10:1 mixture of MEK:MeOH showed (UV) phenanthroline, a dark spot for $Tc(NO)Cl_3phen$, no $[TBA][Tc(NO)Cl_4]$ starting material, and a dark residue left on the bottom of the plate presumed to be either undissolved $Tc(NO)Cl_3phen$ or possibly $[Tc(NO)(phen)_2Cl]^+$. Compound **4** was sparingly soluble in acetonitrile, dichloromethane and formed a green solution with these solvents.

Preparation of **4a** *in dilute dichloromethane:*

With more dilute reaction conditions than above, 104.3 mg (0.203 mmol) of **3** was dissolved in 10 mL of dichloromethane which was reacted with 10 equivalents of phenanthroline (anhydrous, 366.2 mg, 2.03 mmol) that was injected in 4 mL dichloromethane and the reaction proceeded immediately to form a purple colour. The reaction mixture was heated at reflux for 12 hours in a 50 °C oil bath, after which a small amount of red-purple precipitate formed. This was removed by filtration The red-purple coloured precipitate adhered to the frit but was washed with warm methanol to form a purple coloured solution, or warm water to form a pink-red coloured solution. The filtrate was a dark green colour and this reaction mixture was let stand for 3 days

whereupon dark green-black crystals formed. These were collected by filtration on a fine porousity frit, washed with 2 mL dichloromethane and dried *in vacuo* to give 9.0 mg (11% yield) of **4a**.

If in the reaction the reagents are at too high a concentration (~0.1 M for [TBA][$Tc(NO)Cl_4$] and ~0.3 M for the phenanthroline solution added) much of semi-crystalline, bright yellow compound precipitates (in methanol, acetonitrile or dichloromethane) within a few minutes after phenanthroline is added. This material had a very strong nitrosyl stretching frequency of 1771 cm^{-1}. Once completely dry the compound was very insoluble in dichloromethane, methanol and acetonitrile. Addition of water immediately formed a black precipitate (presumably TcO_2). After 2 weeks in acetonitrile the sample turned orange. Similarly, upon refluxing for 72 hours in acetonitrile the yellow compound turned orange. Attempts to recrystallize this led to a dark purple coloured compound. If the yellow compound was refluxed for 12 hours (with stirring under nitrogen) the solution turns yellow. X-ray quality crystals are obtained by slow evaporation of acetonitrile in an open container but some amorphous dark purple solid forms as do crystals of what appears to be the shape and colour of $Tc(NO)Cl_3$phen. Vapour diffusion methods only caused a red solution to form and after time this changed to a dark purple colour.

Preparation of *mer*-trichloronitrosyl-1,10-phenanthrolinetechnetate(I)·(phen)·(MeCN): 4b

To a 15 mL ground glass Erlenmeyer flask equipped with a magnetic stir bar was added 180.9 mg (0.352 mmol) of **3**. The flask was purged with nitrogen for 15 minutes and 3 mL of dry acetonitrile was added via syringe. Ten equivalents of phenanthroline

(anhydrous, 634 mg, 3.53 mmol) in 4 mL of dry acetonitrile was then added dropwise via a syringe and the initial green coloured solution changed to a brown coloured solution and a large amount of yellow precipitate formed. This was stirred for 10 minutes, then the solution was cooled on ice and filtered. The filtrate was washed with 2 x 1 mL of acetonitrile which produced 48.2 mg of semi-crystalline yellow solid after drying *in vacuo*. The brownish coloured filtrate was returned to a 15 mL Erlenmeyer flask where it was heated at reflux in a 90 °C oil bath for 24 hours after which the colour of the solution remained unchanged from brown. The solution was cooled and petroleum ether (50-110°C) then vapour diffused into the methanol solution at room temperature. Crystals formed after 24 hours but the vial was left standing undisturbed for 5 days before removing the mother liquor with a pipette. This revealed excellent x-ray quality, parallelepiped shaped dark brown-red crystals that extinguished from red to yellow in polarized light. The crystals were washed of excess phenanthroline with cold dichloromethane (2 x 1 mL) collected by filtration on a fine porosity frit, washed with 2 mL cold dichloromethane and dried *in vacuo* to give 21.7 mg (10 % yield) of **4b**.

Compound **4b** showed:

IR (KBr pellet, cm^{-1}) ν_{NO}=1798; 1635(vw, br); 1516 (w); 1505 (w); 1425 (w); 1384 (w); 850 (m); 736 (w); 720 (m)

Preparation of *mer*-trichloronitrosyl-2,2-bipyridinetechnetium(II): 5

The method used was a modification of the procedure developed by Hildreth.[32] To a 15 mL ground glass Erlenmeyer flask with stir bar was added 58.0 mg (0.113 mmol) of **3** and 2 mL of dry acetonitrile. A reflux condenser with a septum sealing the top was

added and the system purged with nitrogen for 15 minutes while stirring. Five equivalents (0.565 mmol, 112 mg) of 2,2'-bipyridine in 4mL acetonitrile was then added and the initial green coloured solution immediately changed to a brownish coloured solution. The solution was heated at reflux for 10 hours in a 80° C oil bath after which the solution became a brown/purple colour. After cooling to room temperature, petroleum ether (50-110 °C) was vapour diffused into the solution and after standing undisturbed for one week at room temperature, excellent x-ray quality, green-black triangular crystals of **5** were formed. The mother liquor was removed by pipette and the crystals in the vial were washed with 2 mL of cold acetonitrile and dried *in vacuo* (18 mg, 41% yield).

Compound **5** showed:

IR (KBr pellet, cm^{-1}) ν_{NO}=1787; ν_{Tc-Cl}=311; 1634 (w, br); 1601 (w); 1495 (vw); 1469 (w); 1443 (w); 1384 (w); 1315 (w); 1032 (w, br); 1022 (w, br); 769 (m); 726 (vw).

^1H NMR showed a very broad signal at 7.15 ppm.

ESMS (negative ion): 390, 392, 394 (3 Cl pattern) $[Tc(NO)Cl_3(bipy)]^-$; 234, 236, 238 (3 Cl pattern) $[Tc(NO)Cl_3]^-$

EI: 390, 392, 394 (close to a 3 Cl pattern) $[Tc(NO)Cl_3(bipy)]$; 360, 362, 364 (3 Cl pattern) $[TcCl_3(bipy)]$; 325, 327, 329 (2 Cl pattern) $[TcCl_2(bipy)]$; 290, 292 (1 Cl pattern) [TcCl(bipy)]

Even with ultrasonication, the crystals of **5** are very sparingly soluble (<1 mg/mL) in acetonitrile, acetone, and dichloromethane and insoluble in methanol and benzene. After sitting in acetonitrile for one week the solution changed from green to orange which

was likely indicative of the solvent coordination to the metal, since a green colour remained in dichloromethane solution. The ^{1}H NMR shows a large peak at 2.129 ppm (shoulder at 2.112 ppm) in CD_3CN with the peaks around 7-9 ppm no longer observable.

Preparation of *cis*-acetonitrile-bis(2,2'-bipyridine)nitrosyltechnetium(I) tetrafluoroborate: 6

This compound can be prepared from either **4a** or **3** in a similar fashion. The preparation from **4a** is preferred since only one red coloured product is obtained with this procedure with all other products being white crystals that are not radioactive. Preparations from **3** resulted in similar shaped crystals being formed but these were mixed in with a brownish oil. Both procedures are included below.

*Preparation from **4a**:*

To a 25 mL ground glass Erlenmeyer flask equipped with a magnetic stir bar was added 20.2 mg (0.0486 mmol) of recrystallized **4a**. The flask was purged with nitrogen for 15 minutes and 15 mL of dry acetonitrile was added via syringe. To this solution was added (dropwise via a syringe) a 3 mL solution containing 37.9 mg (0.243 mmol, 5 equivalents) 2,2'-bipyridine. The solution changed from a green to an orange colour after one minute at room temperature with stirring. Stirring was continued for 10 minutes and the colour remained orange. Five equivalents (0.243 mmol, 47.3 mg) of $AgBF_4$ in 5 mL dry acetonitrile was added dropwise to the solution. A white precipitate started forming upon addition of $AgBF_4$ which became denser in volume. This was stirred for 10 minutes and the precipitate was removed by filtration through a pipette containing glass wool. The remaining orange solution was heated at reflux for 10 hours in a 80° C oil bath after which the solution became a red-pink colour. The volume was reduced to ~5 mL with a

stream of nitrogen and a precipitate formed. This was removed by filtration through a pipette containing glass wool the filtrate was separated into four vials where petroleum ether (50-110 °C) was vapour diffused into the acetonitrile solvent. This produced red plate-like crystals mixed with some bipyridyl and $AgBF_4$ crystals.

Compound **6** showed:

IR (KBr pellet, cm^{-1}) ν_{NO} = 1744 (s); 1650 (w, br); 1635 (w, br); 1606 (w, br); 1384 (m); 1123 (w); 1083 (m); 1033 (w); 776 (w); 733 (w); 668 (w)

*Preparation from **3**:*

To a 25 mL ground glass Erlenmeyer flask equipped with a magnetic stir bar was added 73.4 mg of recrystallized **3**. The flask was purged with nitrogen for 15 minutes and 10 mL of dry acetonitrile was added via syringe. To this solution was added (dropwise via a syringe) a 5 mL solution containing 258 mg (1.43 mmol, 10 equivalents) phenanthroline hydrate. The solution changed from a green to an orange colour after one minute at room temperature with stirring. Stirring was continued for 10 minutes and the colour remained orange. Four equivalents (0.572 mmol, 111 mg) of $AgBF_4$ in 5 mL dry acetonitrile was added dropwise to the solution. A white precipitate started forming upon addition and the solution became very thick and would not stir. An additional 5 mL of acetonitrile was added and the solution was swirled for a few minutes. After cooling on ice, the precipitate was filtered in a fine porosity frit and washed with 2 mL of acetonitrile. The filtrate was a dark orange colour at this point. More $AgBF_4$ in acetonitrile (~0.5 equivalents, 15 mg in 1mL) was added to the filtrate until no more precipitate appeared. The fresh precipitate was removed by filtration in the same frit and

washed again with 2 mL of cold acetonitrile. The remaining precipitate was a light yellow colour and weighed 390 mg (probably a mixture of AgCl, [TBA][BF_4] and some phenanthroline). The filtrate (~25 mL) was collected, the volume was decreased to ~15 mL with a stream of nitrogen, and then the whole refluxed in a 90 °C oil bath for 24 hours. The solution remained unchanged as a dark orange colour. The volume was reduced to ~3 mL with a stream of nitrogen and a precipitate formed. This was removed by filtration with a fine porosity frit and petroleum ether (50-110 °C) was vapour diffused into the acetonitrile filtrate. After one week with no crystal formation, the cap of the vial was unscrewed. Red crystals had formed but were coated with a brown oil. The infrared spectrum displayed a similar nitrosyl stretching frequency of 1744 cm^{-1}.

CHAPTER 4

CONCLUSIONS AND FUTURE WORK

Reactions of O-substituted hydroxylamines with $[TcOCl_4]^-$ in methanol produce the $[Tc(NO)Cl_4]^-$ anion. There are two likely ways in which this reaction mechanism proceeds. One plausible pathway includes a chloride attack of the α-carbon of the O-substituted hydroxylamine producing the corresponding chloroalkane, however, such a species was not found in the proton NMR spectra of the reaction mixtures recorded in the present work. The other pathway has the oxo group attacking the α-carbon forming the corresponding alcohol. There was NMR evidence found for the presence of alcohols in these reactions, as well as one undetermined species which may be an O-substituted hydroxylamine bound intermediate in equilibrium with the final product, $[Tc(NO)Cl_4]^-$. In an attempt to confirm this mechanism, O-18 labeled $[TcOCl_4]^-$ was synthesized and NMR, IR, and ESMS spectra were used to monitor the reaction. ESMS evidence shows that the O-18 label is not incorporated into $[Tc(NO)Cl_4]^-$, however, at the present time, there is no conclusive evidence for the O-18 being incorporated into the alcohol either. Future work includes the distillation of methanol solvent from the labeled O-benzylhydroxylamine reaction which would leave labeled benzyl alcohol that could be analyzed by mass spectroscopy. Similarly, more elaborate separations may be needed such as GC-MS analysis of the product. Other methods that would be useful in following the reaction include frozen solution EPR spectroscopy that could be used to identify the formation of known products such as $[Tc(NO)Cl_4]^-$, as well as other paramagnetic intermediates or products that are present. UV-VIS experiments would also aid in identifying products and intermediates. The use of tandem mass spectrometry to investigate the mass range of 268-278 and 236-240 would also give insight into the

composition of these species. Related work would include the reaction of N-substituted hydroxylamines with $[TcOCl_4]^-$ to determine the product(s) and/or mechanism of this reaction.

The substitution reactions of $[Tc(NO)Cl_4]^-$ with phenanthroline and bipyridyl ligands produced $[Tc^{(II)}(NO)Cl_3phen]$ (**4a**) and $[Tc^{(II)}(NO)Cl_3bipy]$ (**5**), respectively. The crystal structures of these complexes showed that the meridonial isomer is produced with one nitrogen atom of the bidentate ligand *trans* to the nitrosyl moiety. The EPR spectra of these compounds confirm the Tc(II) oxidation state of the metal. Compounds **4a** and **5** are precursors to other inorganic complexes since the remaining chlorine ligands can also be displaced, as was the case in the synthesis of $[Tc^{(I)}(NO)(bipy)_2(MeCN)]^{2+}$, where the displacement of all of the chlorine ligands were induced by the addition of a silver salt. The acetonitrile ligand also has the potential of being displaced to form other new and interesting compounds. Future work includes developing an efficient synthesis to the $[Tc^{(II)}(NO)(phen)_2Cl]$ and $[Tc^{(II)}(NO)(bipy)_2Cl]$. Possibly the yellow or purple/red compounds that are often seen in these reactions are in fact the forementioned complexes. Crystals of a yellow and purple/red phenanthroline complex are awaiting x-ray structure determinations.

REFERENCES

1. Baldas, J. *Adv. Inorg. Chem.* **1994**, *41*, 1.

2. Noddack, W.; Tack, I.; Berg, O. *Naturwissenschaften* **1925**, *13*, 571.

3. Zvyagintsev, O.E. *Nature* **1926**, *118*, 226.

4. Perrier, C.; Segré, E. *Nature* **1937**, *140*, 193.

5. Kenna, B.T.; Kuroda, J. *Inorg. Nucl. Chem.* **1961**, *23*, 142.

6. Menill, P.W. *Science* **1952**, *115*, 484.

7. Schwochau, K. *Radiochim. Acta.* **1983**, *32*, 139.

8. Coursey, B.M.; Gibson, J.A.B.; Heitzmann, M.W.; Leak, J.C. *Int. J. Appl. Radiat. Isot.* **1984**, *35*, 1103.

9. Parker, G.W., Martin, W. *Oak Ridge National Laboratory Declassified Report* ORNL-1116, **1952**, p. 26.

10. Kotegov, K.V.; Pavlov, O.N.; Shvedov, *Adv. Inorg. Chem. Radiochem.*, **1968**, *11*, 1.

11. Richards, P.; Tucker, W.D.; Srivastava, S.C. *Int. J. Appl. Radiat. Isot.*, **1982**, *33*, 793.

12. Schwochau, K. *Angew. Chem. Int. Ed. Engl.* **1994**, *33*, 2258.

13. Sprawls Jr., P. Physical Principles of Medical Imaging, Aspen Publishers, Rockville, Maryland, **1987**, Chapter 2.

14. Abrams, M.J.; Davison, A.; Jones, A.G.; Costello, C.E.; Pang, H. *Inorg. Chem.* **1983**, *22*, 2798.

15. Latham, I.A.; Thornback, J.R.; Newman, J.L. *U.S. Patent* 5,081,232, **1992**.

16. Raynor, J.B. *Inorg. Chim. Acta* **1972**, *6*, 347.

17. Richter-Addo, G.B.; Legzdins, P. Metal Nitrosyls, Oxford University Press, New York, **1992**, Chapter 1.

18. Kurzina, A.F.; Oblova, A.A.; Spitsyn, V.I. *Russ. J. Inorg. Chem.* **1972**, *17*, 2630.

19. Orvig, C.; Davison, A.; Jones, A.G. *J. Labelled Compounds and Radiopharm.* **1981**, *18*, 148.

20. Kirmse, R.; Stach, J.; Abram, U.; Marov, I.N. *Z. Anorg. Allg. Chem.* **1984**, *518*, 210.

21. Kirmse, R.; Stach, J.; Abram, U. *Polyhedron* **1985**, *4*, 1275.

22. Kirmse, R.; Abram, U. *Z. Anorg. Allg. Chem.* **1989**, *573*, 63.

23. Armstrong, A.A.; Taube, H. *Inorg. Chem.*, **1976**, *15*, 1904.

24. Yang, G.C.; Heitzmann, M.W.; Ford, L.A.; Benson, W.R. *Inorg. Chem.* **1982**, *21*, 3242.

25. Lu, J.; Clarke, M.J. *J. Chem. Soc. Dalton Trans.*, **1992**, 1243-8.

26. Blanchard, S.S.; Nicholson, T.; Davison, A.; Davis, W.; Jones, A.G. *Inorg. Chim. Acta*, **1996**, *244*, 121.

27. Abram, U.; Kirmse, R. *J. Radioanal. And Nucl. Chem.* **1988**, *122*, 311.

28. Blanchard, S.S.; Nicholson, T.; Davison, A.; Davis, W.; Jones, A.G. *Inorg. Chim. Acta*, **1997**, *254*, 225.

29. Kirmse, R.; Lorenz, B.; Schmidt, K. *Polyhedron* **1983,** *2*, 935.

30. Pearlstein, R.M.; Davis, W.M.; Jones, A.G.; Davison, A. *Inorg. Chem.* **1989**, *28*, 3332.

31. Brown, D.S.; Newman, J.L.; Thornback, J.R. *Acta Cryst.* **1988**, *C44*, 973-5.

32. Hildreth, J.L.; Ph.D. Thesis, Loughborough University of Technology, **1992.**

33. de Vries, N.; Cook, J.; Davison, A.; Nicholson, T.; Jones, A.G. *Inorg. Chem.* **1990**, *29*, 1062.

34. Sabherwal, I. H.; Burg, A.B. *J. Chem. Soc. Chem. Comm.* **1970**, 1001.

35. Zang, V.; van Eldik, R. *Inorg. Chem.* **1990**, *29*, 4462.

36. Sarkar, S.; Subramanian, P. *Inorg. Chim. Acta* **1979**, *35*, L357.

37. Eakins, J.D.; Humphreys, D.G.; Mellish, C.E. *J. Chem. Soc.*, **1963**, 6012.

39. Radonovich, L.J.; Hoard, J.L. *J. Phys. Chem.* **1984**, *88*, 6711.

40. Brown, D.S.; Newman, J.L.; Thornback, J.R.; Davison, A. *Acta Cryst.*; **1987**, *C43*, 1692-4.

41. Cheah, C.T.; Newman, J.L.; Nowotnik, D.P.; Thornback, J.R. *Nucl. Med. Biol.* **1987**, *14*, 573.

42. Pine, S.H. Organic Chemistry, 5th ed., McGraw-Hill, Toronto, **1987**, p. 42.

43. Abram, U.; Wollert, R. *Radiochim. Acta* **1993**, *63*, 149.

44. Aldrich Catalogue Handbook of Fine Chemicals, Milwaukee, **1996-7**, p. 151.

45. Giguere, P.A., Liu, J.D. *Can. J. Chem.* **1952**, *30*, 948.

46. Xapumohoe, R.; Capyxahoe, M.A.; Sapahoeckuu, N.S.; Nkamoe, X.Y. *Optika I Spektroskopiya*, **1965**, *19*, 460.

47. Hansen, P.E. *Prog. NMR Spectrosc.* **1988**, *20*, 207.

48. Hansen, P.E. *Annu. Rep. NMR Spectrosc.* **1983**, *15*, 105.

49. Vederas, J.C. *J. Am. Chem. Soc.* **1980**, *102*, 374.

50. Davison, A. in Technetium in Chemistry and Nuclear Medicine, ed.'s Deutsch, E.; Nicolini, M.; Wagner Jr., H.N., Cortina International, Verona, **1983**, p.4.

51. Peacock, R.D.; The Chemistry of Technetium and Rhenium, Elsevier, London, **1966**, p. 32.

52. Keller, C.; Kanellakopulos, B. *Radiochim. Acta* **1963**, 1, 107.

53. Muller, A.; Krebs, B. *Z. Naturforsch.* **1965**, *20a*, 967.

54. Davison, A.; Orvig, C.; Trop, H.S.; Sohn, M.; DePamphilis, B.V.; Jones, A.G. *Inorg. Chem.* **1980**, *19*, 1988.

55. Cotton, F.A.; Davison, A.; Day, V.W.; Gage, L.D.; Trop, H.S. *Inorg. Chem.* **1979**, *18*, 3024.

56. Received as a gift from Dr. Raman Chirakal, McMaster University Hospital.

57. Lorenz, B.; Kranke, P.; Schmidt, K.; Kirmse, R.; Hubener, R.; Abram, U. *Z. anorg. allg. Chem.* **1994**, *620*, 921.

58. Abram, U.; Kirmse, R. *Radiochim. Acta* **1993**, *63*, 139.

59. Kirmse, R.; Abram, U. *Z. anorg. Allg. Chem.* **1989**, *573*, 63.

60. Brown, D.S.; Newman, J.L.; Thornback, J.R.; Pearlstein, R.M.; Davison, A; Lawson, A. *Inorg. Chim. Acta* **1988**, *150*, 193.

61. Pearlstein, R.M.; Davis, W.M.; Jones, A.G.; Davison, A. *Inorg. Chem.* **1989**, *28*, 3332.

Appendix I

Experimental Methods

Analytical TLC was performed on silica gel 60-F_{254} (Merck) plates with detection by long wavelength ultraviolet light unless specified otherwise. All commercial reagents were used as supplied. Solvents were distilled, under nitrogen, from calcium hydride. Nitrogen was dried by passing it through anhydrous calcium sulphate. All reactions were protected from light and carried out under a slow flow of nitrogen unless stated otherwise. Solvents were evaporated with a rotary evaporator (Buchi Rotovapor - 20 mmHg).

Selected NMR spectra were recorded on a Bruker Avance DRX-500 spectrometer. Proton spectra were acquired at 500.130 MHz with a 5 mm broadband inverse probe with triple axis gradient capability. Spectra were obtained in 8 scans in 32 K data points over a 4.006 kHz spectral width (4.096 a acquisition time). Sample temperature was maintained at 30 °C by a Bruker Eurotherm variable temperature unit. Gaussian multiplication (line broadening: -1.5 Hz, Gaussian broadening: 0.2) was used to process the free induction decay (FID) which was zero-filled to 64 K before Fourier transformation. Coupling constants (J) are reported in Hz.

Carbon-13 NMR spectra were recorded at 125.758 MHz with a 5 mm broadband inverse probe with triple axis gradient capability. The spectra were acquired over a 28.986 kHz spectral width in 32K data points (0.557 s acquisition time). The ^{13}C pulse width was 4.0 μs (30° flip angle). A relaxation delay of 0.5 s was used. Exponential

multiplication (line broadening: 4.0 Hz) was used to process the FID which was zero-filled to 64K before Fourier transformation.

Compounds studied by NMR were dissolved in the appropriate deuterated solvents (Isotec, Inc.) to a concentration of approximately 15.0 mg mL^{-1} whenever possible. Chemical shifts are reported in ppm relative to TMS. The residual solvent signals were used as internal references for the ^{1}H and ^{13}C spectra, respectively.

All other NMR spectra were recorded on a Bruker AC-200 spectrometer. Proton spectra were acquired at 200.133 MHz with a 5 mm dual frequency probe. Spectra were obtained in 8 scans in 16K data points over a 2.403 KHz spectral width (3.408 s acquisition time). Spectra were acquired at ambient temperature. The free induction decay (FID) was processed with exponential multiplication (line broadening: 0.1 Hz) and was zero-filled to 32K before Fourier transformation.

Carbon-13 NMR spectra were recorded at 50.323 MHz with the 5 mm QNP probe. The spectra were acquired over a 12.195 kHz spectral width in 16K data points (0.672 s acquisition time). The ^{13}C pulse width was 1.5μs (42° flip angle). A 0.5 s relaxation delay was used. The FIDs were processed with exponential multiplication (line broadening: 3.0 Hz) and zero-filled to 32K before Fourier transformation.

Infrared spectra were recorded on a Bio Rad FTS-40 Fourier transform spectrometer. Solid samples were prepared as KBR pellets in the region of 4000-400 cm^{1}. The far-IR region was observed from 400-250 cm^{-1} as KBr pellets.

Electrospray ionization mass spectrometry was performed with 50/50 CH_3CN/H_2O as the mobile phase at a flow rate of 15 μL per minute, with the use of a

Brownlee Microgradient syringe pump. Samples were dissolved in 50/50 CH_3CN/H_2O with no base added in negative mode, or often one drop of 0.1% TFA for samples that were to be analyzed in the positive mode. Typically, 10 μL of the completely dissolved sample was injected as a very dilute solution with a Hamilton Co. 25 μL syringe. Full scan ESMS experiments were performed with a Fisons Platform quadrupole instrument.

EPR was run on selected paramagnetic samples with the Bruker EMX EPR Spectrometer. Samples were dissolved in dichloromethane in a quartz EPR tube. Typically only 1-3 scans were needed for a good signal to noise ratio. The modulation frequency was set to 100 kHz and the modulation amplitude was set to 5.000 G. The microwave frequency was in the range of 9.45 GHz and a low attenuation setting from 0-2 was typically chosen (power = ~160 mW). The conversion and time constant were typically set to 81.920 ms and 40.960 ms, respectively. The resolution was 1024 points over ~4000 G for solution samples. Certain regions of the spectra for the low temperature samples were expanded by using 2048 points and decreasing the modulation amplitude to 0.1-0.3 G, while also increasing the number of scans.

Experimental Description of the Crystal Structure Determinations Carried Out Using The CCD Area Detector

X-ray crystallographic data for **4a, 4b, 5,** and **6** were collected from a single crystal sample, which was mounted on a glass fiber. For low temperature acquisition of data, **4b** was mounted on a glass fiber that was glued to a brass pin for insertion into the goniometer head. Data were collected using a P4 Siemens diffractometer, equipped with

a Siemens SMART IK Charge-Coupled Device (CCD) Area Detector (using the program SMART **[a]**) and a rotating anode using graphite-monochromated Mo-Kα radiation (λ = 0.71073 Å). The crystal-to-detector distance was 3.991 cm, and the data collection was carried out in 512 x 512 pixel mode, utilizing 2 x 2 pixel binning. The initial unit cell parameters were determined by a least-squares fit of the angular settings of the strong reflections **[b]**, collected by a 4.5 degree scan in 15 frames over three different parts of reciprocal space (45 frames total). One complete hemisphere of data was collected, to better than 0.8 Å resolution. Upon completion of the data collection, the first 50 frames were recollected in order to improve the decay corrections analysis. Processing was carried out by use of the program SAINT **[c]**, which applied Lorentz and polarization corrections to three -dimensionally integrated diffraction spots. The program SADABS **[d]** was utilized for the scaling of diffraction data, the application of a decay correction, and an empirical absorption correction based on redundant reflections. The structures for **4a** and **5** were solved by using the direct methods procedure and those for **4b** and **6** were solved by using the Patterson method procedure both of which are in the Siemens SHELXTL program library **[e]**, and refined by full-matrix least squares methods with anisotropic thermal parameters for all non-hydrogen atoms. The hydrogen atoms were generated at calculated positions, with thermal parameters based on the carbons to which they are attached.

[a] SMART (1996), Release 4.05; Siemens Energy And Automation Inc., Madison, WI 53719
[b] To determine the number of reflections, consult the .p4p file associated with the data set.
[c] SAINT (1996), Release 4.05; Siemens Energy And Automation Inc., Madison, WI 53719
[d] Sheldrick, G.M. SADABS (Siemens Area Detector Absorption Corrections) (1996).
[e] Sheldrick, G.M. Siemens SHELXTL (1994), Version 5.03; Siemens Crystallographic